

Assessment of Seat Comfort by Virtual Simulation

Author

Hesam Shahbazi Gahrouei

Supervisor

Prof. Maria Pia Cavatorta

A Thesis in the Field of Mechanical Engineering
for the Degree of Master of Science

Politecnico di Torino

July 2018

Abstract

Next to an increase in the number of car users, comfort has become a major aspect by which car manufacturers can distinguish their products from their competitors. At today, the assessment of seating comfort is largely based on subjective measures. A disadvantage of such measures is that the relationship with design parameters is often unclear. Furthermore, prototype development and testing are both time consuming and costly.

In this respect, virtual testing tools represent promising solutions to support early automotive tests and, ultimately, reduce development times and associated costs. Moreover, virtual testing tools allow to investigate parameters that are hard to measure, such as the intervertebral disc pressure or the pressure distribution in the human soft tissues of the buttocks, and put them in relation with (dis)comfort and physical complaints.

For prediction of seating comfort by virtual testing, in addition to a detailed seat model, a highly sophisticated model of the occupant and objective parameters are necessary. In the simulation work of this thesis, the human model CASIMIR, presented by Pankoke (2003), was used. CASIMIR represents a dynamic, anatomical predictive finite element model of a man in a sitting posture (Siefert et al., 2006) and it is currently available for the ABAQUS code. The most significant characteristics of the CASIMIR model in seat comfort analysis are: a detailed model of the lumbar spine, including frequency-dependent damping properties of the intervertebral discs, a detailed model of the relevant abdominal and dorsal musculature, together with a detailed skeletal model. Regarding the objective parameters, the mean and maximum pressure, the load percentage and contact area are the

parameters, which are mostly reported in the literature to relate to (dis)comfort, and are therefore used in this thesis.

The comfort factor that relate to the automobile seat is generally explored in the literature by the following indicators: height, adjustment, position, properties of upholstered seat such as width, length and shape, foam softness and aesthetics. Some works have been conducted to show association between seat dimensions, seat shape, seat material and interface pressure but little is known about the influence of the properties of the seat and their interactions on the (dis)comfort perception of drivers. Moreover, a strong optimization of seat properties in order to fulfill comfort criteria is not established in literature.

This thesis tries to enlighten the interactions of different parameters in order to achieve optimum seat design based on the comfort criterion proposed by Mergl in 2006. In the first step, the validity of the model was investigated through the level of correlation between experimental pressure maps and numerical results. The test group consisted of six male subjects with anthropometric data close to 50th percentile (a man with average anthropometric values). The pressure maps were obtained through the Xsensor pressure mat during static seating of the subjects. The comparison between experimental objective parameters related to (dis)comfort and numerical output data showed a good correlation.

In the second phase of the thesis, the numerical model was then used to evaluate the sensitivity of static seat comfort to some input variables, i.e. the stiffness of cushion and backrest foams and some geometry parameters of the seat cushion and backrest such as length of cushion, concavity and convexity of seat surfaces and angle of bolsters. In order to perform the sensitivity analysis, a reduced factorial technique was used. Sensitivity

analysis of the DOE technique showed a direct relation between maximum interaction pressure and shape of seat cushion, as well as stiffening of materials in soft parts of the seat. Thereafter, the results of DOE run were used to create an approximation of the response variable over the design space, in order to implement the multi-objective optimization based on comfort criteria.

Dedication

For my father & mother, whose affection, love, encouragement and prays of day and night make me able to get such success and honor, along with those who gave me up.

For those who answer the call for help with no expectation of personal gain.

Acknowledgments

The preparation of this thesis was done at Centro Ricerche Fiat (CRF). The author extends his thanks to Innovation & Methodologies team at Vehicle Virtual Analysis department and especially Mr. Mauro Olivero for their valuable contributions to this effort.

Table of Contents

Dedication	vi
Acknowledgments	vii
List of Tables	x
List of Figures	xi
Chapter 1. Introduction	1
Chapter 2. Seat Comfort and Discomfort	5
Human Characteristics and Their Effects on Interface Pressure.....	8
Ethnicity.....	9
Age	10
Gender	11
Secular trends	11
Anthropometric variables and interface pressure	12
Seat Characteristics and Their Influence on Interface Pressure.....	16
Context Characteristics and Their Influence on Interface Pressure	18
Subjective measures vs. Virtual assessment.....	19
Chapter 3. Virtual Simulation	22
Finite Element Analysis (FEA)	23
Finite Element discretization	25
Element displacement functions	26
Linear Finite Element	29

Non-Linear Finite Element	30
Implicit solution method vs. Explicit	33
Virtual Simulation of Seat Comfort.....	38
Seat modelling.....	40
Material properties.....	45
Human FE model CASIMIR	54
Chapter 4. Numerical vs. Experimental Study	62
Numerical Study	63
Experimental study	68
Correlation.....	74
Chapter 5. Virtual Optimization	86
Design of Experiment – DOE.....	90
Results	96
Response Surface Model - RSM.....	99
Virtual Optimization	104
Conclusion and Recommendations.....	111
Appendix 1. STEP definition in foam characterization.....	114
[Bibliography/References/Works Cited.]	117

List of Tables

Table 1. Causes of seating discomfort.	6
Table 2. Experimental test subjects	68
Table 3. PX100:36.36.02 characteristics	69
Table 4. Zoning of the body map	74
Table 5. Discomfort guidelines (“green” strong relation, “blue” acceptable relation, “orange” weak relation, “-“ no relation); (10/11 buttocks, 13/14 middle of thigh, 16/17 front of thigh, 12/15 sideways, 1/2 shoulder, 4 upper back, 6 lower back, 8 coccyx, 7/9 lateral iliac crest).....	88
Table 6. DOE characteristics.....	94
Table 7. RSM and DOE characteristics	101
Table 8. Mean absolute error and R-squared comparison for different RSM techniques.....	103
Table 9. Characteristics of Multi-Objective Genetic Algorithm	104

List of Figures

Figure 1. XchangE vehicle concept	2
Figure 2a. Theoretical model of sitting comfort and discomfort	7
Figure 2b. Conceptual model of sitting comfort and discomfort	8
Figure 3. Stature distribution of different male populations: the Netherlands, North America and Japan (dimensions obtained from DINED)	10
Figure 4. Schedule for comfort prediction by virtual testing	21
Figure 5. The basic procedure for general FEM analysis	24
Figure 6. Various types of elements	25
Figure 7. Model of seat structure	41
Figure 8. FE model of height adjustment mechanism	42
Figure 9. Kinematic coupling of structural parts	43
Figure 10. Model of cushion and backrest foam with tetrahedron elements	44
Figure 11. Discretization of foam specimen	46
Figure 12. Comparison of stress-strain-curve for tested foam materials	50
Figure 13. Comparison of Experimental and Numerical results for seat-cushion-foam ...	51
Figure 14. Comparison of Experimental and Numerical results for seat-backrest-foam ..	52
Figure 15. Effect of order of formulation on numerical simulation for seat-cushion- foam	53
Figure 16. Effect of order of formulation on numerical simulation for seat-backrest- foam	53

Figure 17. Phenomenological models of a man in the sitting posture	55
Figure 18. Anatomical models of the compliant thigh with pelvis and femur	56
Figure 19. CASIMIR model for man of the 50th percentile	58
Figure 20. Detailed model of abdominal muscles (left) and lumbar spine (right)	59
Figure 21. CASIMIR family—f05—m50—m95 (left to right)	61
Figure 22. CASIMIR posture definition	64
Figure 23. Positioning of CASIMIR with respect to seat.....	65
Figure 24. STEP definition	66
Figure 25. Pressure distributions of backrest (left) and cushion (right).....	67
Figure 26. PX100:36.36.02 pressure mat.....	70
Figure 27. Experimental body pressure distribution (BPD)	71
Figure 28. Symmetric body pressure distribution (BPD)	73
Figure 29. Body map (Hartung 2006).....	75
Figure 30. Virtual Xsensor.....	76
Figure 31. Flow-chart of virtual Xsensor creation (left) and numerical BPD (right).....	77
Figure 32. Comparison of experimental mean BPD and subjects' BPD	78
Figure 33. Maximum pressure spider graph for the cushion	80
Figure 34. Mean pressure spider graph for the cushion.....	81
Figure 35. Load percentage spider graph for the cushion.....	82
Figure 36. Maximum pressure spider graph for the backrest.....	83
Figure 37. Mean pressure spider graph for the backrest.....	84
Figure 38. Load percentage spider graph for the backrest.....	85
Figure 39. workflow at modeFRONTIER for sensitivity analysis	93

Figure 40. Different cushions' material used for DOE analysis and virtual optimization	95
Figure 41. Correlation matrix obtained by DOE analysis.....	98
Figure 42. modeFRONTIER workflow used for RSM implementation.....	102
Figure 43. Weight of each objective function.....	105
Figure 44. Comparison between virtual optimal cases and corresponding FEM	108
Figure 45. Optimal seat (b) compared to the nominal seat (a).....	109
Figure 46. Cushion (a) and backrest (b) cross-sections of optimal seat.....	110

Chapter 1.

Introduction

Until teleportation becomes reality, individuals rely upon different methods for transportation from one place to another, such as aircraft, trains, and cars. The numbers of car users are increasing. For example, the sales volume of automobiles shows continuous growth in which car sales volumes of the FCA Group have been increased almost 35% the past four years, delivering around 5 million vehicles in 2017 (Statista website).

Next to an increase in the number of car users, the diversity of car drivers and passengers increases as well. Although it is expected to slow down to an average of 8% a year between 2011 and 2020, China's automotive sector grew at an average rate of 24% a year between 2005 and 2011 (McKinsey & Co. 2012). Hence, in the automotive industry, the diversity in drivers and passengers increases.

Rather than cultural diversity of car users, the world population in itself is changing as well. In spite of the fact that the trend of increasing height has been gradually slowing or stopping in many populations (Godina 2008), there is a strong tendency towards increasing weight and obesity in many European countries and the USA (Komlos and Baur 2004). In the last twenty years, the number of people in the USA who are considered "obese" has doubled. Another trend is the ageing of the population: the proportion of people 60 years and over is predicted to increase to as much as 21% by 2050 (Ilmarinen 2005).

Furthermore, development of autonomous driving cars also introduces a larger variation in activities that car users perform while traveling. Currently, active safety features such as lane change warning, autonomous cruise control, and collision avoidance increasingly find their way into passenger cars (Litman 2015). Additionally, many major automotive manufacturers, including Volkswagen, BMW, Volvo, Toyota and Mercedes Benz, are testing driverless car systems as of 2013. The XchangeE concept by Rinspeed, presented at the Geneva Motor Show in 2014, shows how the interior of an autonomous vehicle could be designed (see Figure 1). In a self-driving car, the driver becomes a passenger and as a result, is able to perform other activities while being driven towards the destination. Current vehicle interiors do not facilitate this yet and thus, this could be an opportunity for car manufacturers.



Figure 1. XchangeE vehicle concept

Thus, although the first studies on seat comfort and activities appeared already 50 years ago (Branton and Grayson 1967) the driver population, technological developments

and travel habits have changed, resulting in other activities and a different context. Unfortunately for the driver, the comfort rate is still one of the major problems.

To attract passengers and drivers, seats should allow car users to feel fit after a few hours traveling without experiencing discomfort. Discomfort is a predictor of musculoskeletal pain (Hamberg-van Reenen et al. 2008), and also seems inversely related to productivity (e.g., Hozeski and Rohles 1987). However, every year, passengers are traveling in restricted postures, not being able to perform the activities they want and risking health problems such as back pain (Helander and Quance 1990; Burdorf et al. 1993) and neck pain (Ariëns et al. 2000; 2001).

Comfortable seats can attract drivers. The seat is an important feature of every vehicle interior, as it is the interface with the driver for the whole journey. According to Zhang et al. (1996), comfort and discomfort are two independent factors associated with different underlying factors. Discomfort is associated with feelings of pain, soreness, numbness and stiffness, and is caused by physical constraints in the design. On the other hand, comfort is associated with feelings of relaxation and well-being, and can be influenced by, for example, the aesthetic impression. Thus, reducing discomfort will not necessarily increase comfort, but in order to accomplish a high level of comfort, the level of discomfort should be low (Helander and Zhang 1997).

Building on the model by Helander and Zhang (1997), the theoretical model of comfort and discomfort and its underlying factors by De Looze et al. (2003) distinguishes three levels: human, seat and context level. For instance, at context level, the physical environment has an influence on sitting discomfort, whereas at seat level, aesthetic design

can influence sitting comfort. At human level, physical capacity as well as expectations and emotions play a role in the perception of sitting discomfort and comfort, respectively.

However, little is known yet about the influence of drivers' anthropometry, the posture and movement, and the properties of the seat, on the comfort and discomfort perception of passengers.

The aim of this thesis is to provide knowledge on how to optimize comfortability of driver seats, taking into account the seat properties as the most important factor in the theoretical model of comfort and discomfort. In order to accomplish this goal, first, a literature review has been conducted on the current state of knowledge, to investigate the effect of human, seat and context characteristics on comfort and discomfort. Next, the seat pressure distribution evaluated by numerical simulation has been correlated by experimental pressure maps. Finally, the ideal pressure distribution defined by Mergl (2006) has been used as the best objective measure for discomfort in order to implement a virtual optimization.

Chapter 2.

Seat Comfort and Discomfort

The Cambridge Advanced Learner's Dictionary defines comfort as pleasant feeling of being relaxed and free from pain. Comfort is a generic and subjective feeling that is tough to quantify, know related to human physiological homeostasis and psychological sound presence (Shen et al. 1997).

In spite of abundant research studies in automotive seating, many questions still remain about what really contributes to seating comfort. As stated by Corlett (1989): Though Hertzberg (1958) defined comfort as the absence of discomfort, here is no universally known effective definition of discomfort. Furthermore, there is no approved dependable technique for measuring the feeling of discomfort or comfort. While driving the occupant comfort hang on different features and the environment. As the customer who makes the final determination and customer evaluations are based on their opinions having experienced the seat (Runkle 1994), the seat comfort will be a subjective concern.

According to Zhang, Helander, and Drury (1996), comfort and discomfort are two independent factors associated with different underlying factors. Discomfort is associated with feelings of pain, soreness, numbness and stiffness, and is caused by physical constraints in the design. Discomfort feelings, as described by Helander and Zhang (1997), is affected by biomechanical aspects and fatigue. The causes of different discomfort are listed in Table 1.

Table 1. Causes of seating discomfort.

Human Experience mode	Biomechanical		Seat/environment
	Physiology causes	Engineering causes	Source
Pain	Circulation occlusion	Pressure	Cushion stiffness
Pain	Ischemia	Pressure	Cushion stiffness
Pain	Nerve occlusion	Pressure	Seat contour
Discomfort	-	Vibration	Vehicle ride
Perspiration	Heat	Material Breathability	Vinyl upholstery
Perception	Visual/auditory/tactile	Design/vibration	Vehicle cost

Comfort, on the other hand, is associated with feelings of relaxation and well-being, and can be influenced by, for example, the aesthetic impression of a product or environment. Thus, reducing the level of experienced discomfort will not necessarily increase the level of comfort, but in order to accomplish a high level of comfort, the level of discomfort needs to be low (Helander and Zhang 1997).

Building upon the model by Helander and Zhang (1997), the theoretical model of comfort and discomfort and its underlying factors by De Looze, Kuijt-Evers, and Van Dieën (2003) distinguishes three levels: human, seat and context levels (see Figure 2a). For instance, at context level, the physical environment has an influence on sitting discomfort, whereas at seat level, aesthetic design can also influence sitting comfort. Although the models of Helander and Zhang (1997) and De Looze, Kuijt-Evers, and Van Dieën (2003) contribute to the understanding of the concepts ‘comfort’ and ‘discomfort’, none of these is able to predict either comfort or discomfort.

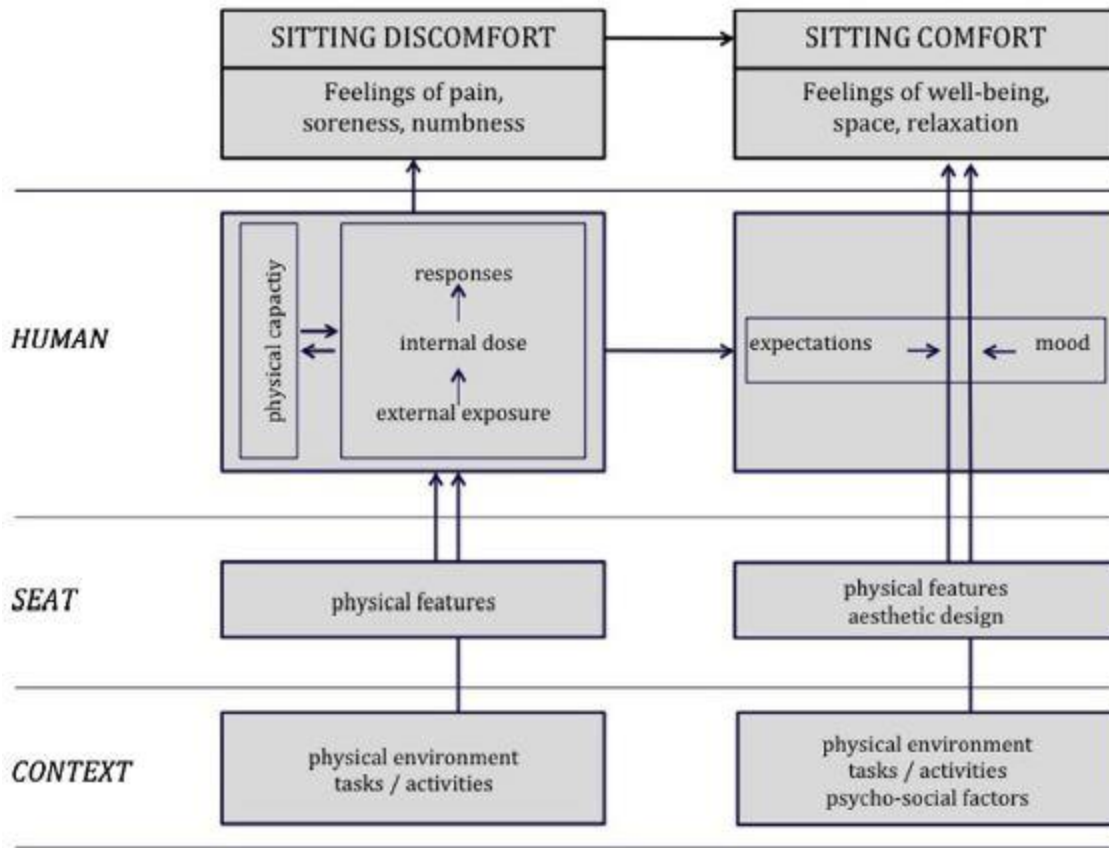


Figure 2a. Theoretical model of sitting comfort and discomfort

Based on the theory of Helander and Zhang (1997); who consider discomfort and comfort as two separate entities, with discomfort having a dominant effect (Figure 2b), the relationship between human, seat and context characteristics (left) and the perception of comfort and discomfort (right) can be explained by three mediating variables: posture, pressure and movement (middle). For example, body posture is not only determined by a passenger’s anthropometry (human), but also by the seat characteristics (e.g. reclined backrest angle) and context (the performed activity, such as reading or working on laptop). In the following sections, human, seat and context characteristics and their influence on the

interface pressure as the objective parameter of current thesis are described based on literature.

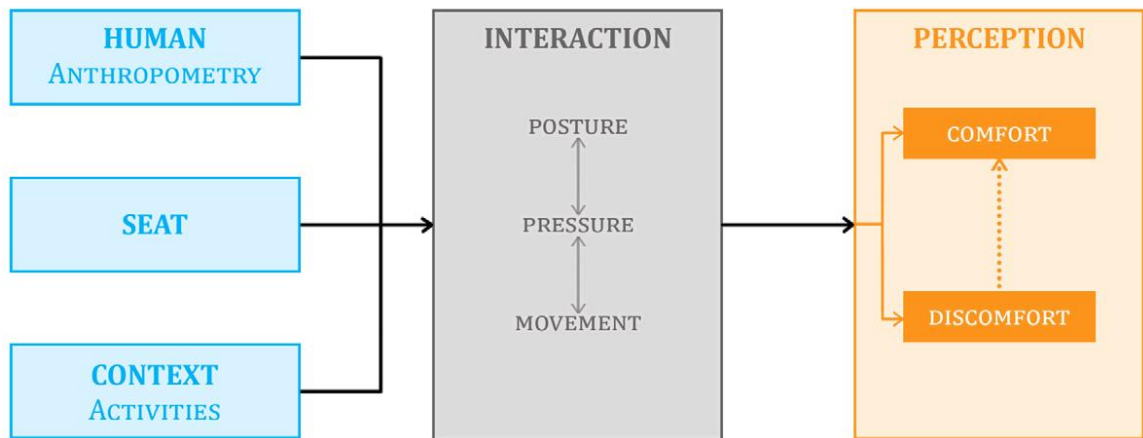


Figure 2b. Conceptual model of sitting comfort and discomfort

Human Characteristics and Their Effects on Interface Pressure

Human characteristics include a number of characteristics, such as age, nationality, gender and body dimensions. In this thesis, the focus is on anthropometric variables, such as stature and weight. However, it is important to keep in mind that anthropometric variables are related to age, nationality and gender, and is also subject to secular trends.

Anthropometry is the scientific study of measurements of the human body. When designing passenger seats, anthropometric data are a valuable source of information to determine seat dimensions, but also to evaluate seats. It is important to note, however, that the average passenger does not exist, and that it is very uncommon for a person to have multiple body dimensions that are average. A tall person in stature might not have the

largest measurement for other body dimensions as well. Consequently, there is also no 5th or 95th percentile passenger. The level of correlation between different body dimensions varies; for example, the correlation coefficient between stature and popliteal height is 0.82 (with 0 = no relationship and 1 = a perfect positive relationship), while the correlation between stature and hip breadth is considerably less with 0.37 (Kroemer 1989).

Anthropometric variability is mostly related with ethnicity, gender and age (Jürgens et al. 1990). However, anthropometric characteristics also change over time, but not always at the same rate. Molenbroek (1994), for example, found that stature in the Netherlands increased between 1965 and 1980 more rapidly, but that the growth rate decreased between 1980 and 1992.

Ethnicity

The majority of body dimensions follows a normal distribution. However, the normal curve looks different for different populations. A 95th percentile male from the Netherlands is taller than the 95th percentile males from Japan or North America, as can be seen in Figure 3. In fact, the 95th percentile male from Japan corresponds with a 50th percentile male from the Netherlands.

In addition, populations do not only differ in overall body size, but also in ratio (measure of body proportions). For example, Japanese torsos are proportionally longer than their legs, as compared to most other populations (Kennedy 1976), while the Turkish population has relatively small arms compared to Western European populations (Ali and Arslan 2009).

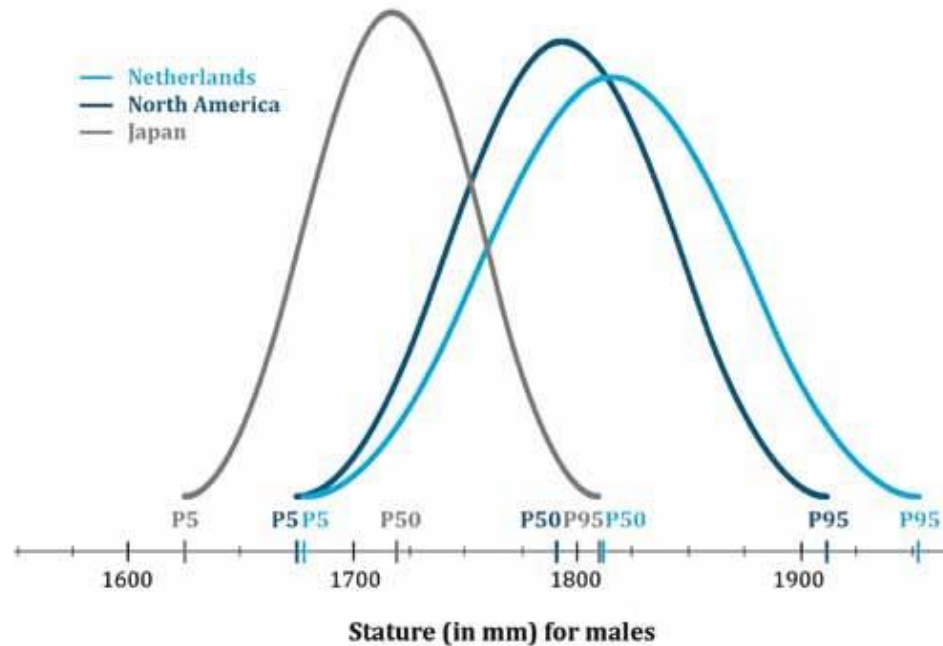


Figure 3. Stature distribution of different male populations: the Netherlands, North America and Japan (dimensions obtained from DINED)

Age

According to Perissinotto et al. (2002), specific anthropometric reference data are needed for elderly populations, because the anthropometric standards from adult populations may not be appropriate due to changes in body composition that occur during ageing. For example, stature decreases with age, most likely due to shrinkage that occurs in the intervertebral discs of the spine. This starts at around 40 years of age, and is very rapid between age 50 and 60 (Ali and Arslan 2009). Weight, however, increases steadily until the age of 50-55 years, after which it starts to decrease (Ali and Arslan 2009).

Furthermore, the mobility of passengers decreases with age, which is especially relevant for the in- and egress in aircraft seats. For example, a study by Lijmbach et al.

(2014) shows that elderly people need more time before sitting down and use more hand and foot movements compared to students.

Ortman et al. (2014) state that the US will experience considerable growth in its older population between 2012 and 2050, where in 2050, the population aged 65 and over will have almost doubled to 83.7 million.

Gender

The average stature of a Dutch male between 20 and 30 years old is 1848 mm, which is 161 mm taller than the average Dutch female (1687 mm). A seat that is designed for the 5th to 95th percentile male would therefore fit 90% of men, but less than 40% of women, since the stature of 5th percentile male, 1716 mm, corresponds with a 66.7th percentile female. Seats should be designed for a population of male and female passengers.

Furthermore, the body proportions differ for males and females. For example, the average hip breadth sitting is approaching the average shoulder breadth (bideltoid) for Dutch females (402 vs. 422 mm), whereas this difference is 82 mm in Dutch males (388 vs. 470 mm).

Secular trends

Changes in life styles, nutrition and ethnic composition of populations lead to changes in the distribution of body dimensions (Pheasant and Haslegrave 2006), which is why regular updating of anthropometric data collections is necessary.

Although the trend of increasing height has been gradually slowing or stopping in many populations (Godina 2008), there is a strong tendency towards increasing weight and obesity in many European countries and the USA (Komlos and Baur 2004). In the last twenty years, the number of people in the USA who are considered “obese” has doubled. Matton et al. (2007) also found an increase in weight, stature and BMI in Flemish adolescents between 1969 and 2005, while physical fitness declined.

For products with a relative short lifetime, this might not be relevant, but for vehicles such as aircrafts and trains, the development time is long, as well as the expected lifetime, and designers have to anticipate on changing body dimensions. For example, the hip width of the P95 Dutch male has increased from 408 mm in 1982 to 440 mm in 2004 (DINED 2004).

Anthropometric variables and interface pressure

Literature (Vos et al. 2006, Hostens et al. 2001, Jackson et al. 2009, Kyung and Nussbaum 2008, Paul et al. 2012, Moes 2007, Gyi and Porter 1999, Park et al. 2013, Kyung and Nussbaum 2013) reported a correlation between anthropometry and pressure. Different variables of pressure were studied, such as contact area, sitting force, mean pressure, peak pressure, pressure factor (the combination of peak and mean pressure) and pressure gradient. Anthropometric variables were stature, weight, gender, age, BMI, RPI, percentage of subcutaneous fat and ectomorphic index. Below, the correlations are described for each pressure variable.

Some studies found effects of anthropometric variables on contact area. For vehicle occupant seats, Paul, Daniell, and Fraysse (2012) found a correlation between weight and contact area on the seat pan (r ranges from $r = 0.432$ to $r = 0.845$), and between weight and

contact area on the backrest ($r = 0.432$ to $r = 0.741$) for different car seats. Differences between car seats were explained by different body postures. According to Paul, Daniell, and Fraysse (2012), body mass and hip circumference were the best anthropometric indicators for the seat pan contact area. Kyung and Nussbaum (2008) also found effects of stature on pressure variables related to the contact area in the driver's seat of cars. The contact area at the right thigh (due to the asymmetric driving posture) and that at the upper back was significantly larger for taller persons. Vos et al. (2006) found correlations between several anthropometric variables and the seat pan contact area in office chairs: BMI and contact area ($r = 0.62$), weight and contact area ($r = 0.61$), RPI and contact area ($r = 0.50$) and stature and contact area ($r = 0.48$). According to Moes (2007), who studied pressure in upright sitting without back support, there is also a correlation between the percentage of subcutaneous fat and the contact area of the seat pan. Vincent, Bhise, and Mallick (2012) found that the contact area in different seat regions (e.g. front half of the seat pan) could be predicted relatively well on the basis of cushion hardness and hip width, gender, weight and stature. When comparing older and younger drivers, Kyung and Nussbaum (2013) found that the average contact area at the right buttock was larger for the older drivers, which could be explained by different driving postures. To summarize, the highest correlation coefficients were found, in more than one study, for body mass with contact area, followed by stature with contact area. Furthermore, correlations were found for hip breadth, hip circumference, BMI and percentage of subcutaneous fat with contact area.

Effects of anthropometric variables on mean pressure have been investigated by several works. For agricultural machinery, Hostens et al. (2001) found a linear increase in

mean pressure with BMI ($r = 0.88$) for sitting on seats with the feet unsupported. Gyi and Porter (1999) studied the correlation between anthropometry and pressure variables while driving a car. They found that the highest average pressure was in thin and tall males (with highest RPI), and found a positive correlation between weight and thigh pressure (no correlation coefficients reported). Furthermore, hip breadth was one of the independent variables that explains mean pressure in a multiple regression (Gyi and Porter 1999). Vincent, Bhise, and Mallick (2012) found that weight, stature and buttock–popliteal length were the best predictors of average pressures. Additionally, Moes (2007) found that gender was the best predictor of average pressure (mult. $r = 0.75$), with the average pressure being lower for females than for males, and explains this by the lower mass in combination with a larger contact area for women. Lower mass, in turn, is correlated with a lower sitting force (Moes 2007; Paul, Daniell, and Fraysse 2012). Furthermore, Kyung and Nussbaum (2013) found that the average contact pressure at the lower back was higher for younger drivers compared to older drivers.

The effect of anthropometric variables on peak or maximum pressure was described in some studies. Hostens et al. (2001) found no correlation between BMI and maximum pressure, just as Jackson et al. (2009), who studied the effects of anthropometric variables on peak pressure of glider pilot seats. They did not find a relationship between weight, stature or BMI and peak pressure. This can be explained by the small variation in anthropometrics of the subjects, as all of them were UK glider pilots (Jackson et al. 2009). Moes (2007) found that the ectomorphic index (which is one of the indexes of the somatotype classification) was the only explaining variable of maximum pressure (mult. $r = 0.73$). Although the maximum pressure could not be predicted as good as the average

pressure, weight, stature and buttock–popliteal length were, again, the best predictors (Vincent, Bhise, and Mallick 2012). In addition, Kyung and Nussbaum (2013) found significant effects of age on average peak pressure ratio at the upper back, which was higher for younger drivers.

A number of studies also included less common pressure variables, such as circular pressure gradient, transverse pressure gradient (Moes 2007) and pressure factor (a combination of pressure variables, derived from a principle compound analysis) (Vos et al. 2006). Moes (2007) found that the ectomorphic index and stature were the explaining variables for the transverse pressure gradient (mult. $r = 0.90$), and that the ectomorphic index was the only explaining variable for the circular pressure gradient (mult. $r = 0.80$). Vos et al. (2006) found correlations between BMI and pressure factor ($r = 0.31$), weight and pressure factor ($r = 0.44$) and stature and pressure factor ($r = 0.38$). Park et al. (2013) did not find significant effects of car driver's gender on pressure distribution of upper body parts (i.e. back and lumbar).

In conclusion, several studies report correlations between anthropometric variables and different variables of pressure. Age was found to influence posture and, therefore, pressure distribution. Most commonly studied pressure variables were contact area, average pressure and peak pressure. A larger contact area can be explained by higher weight and greater stature. A higher average pressure can be explained by a higher weight. However, gender seems to affect this relationship, as the contact area for women is larger (due to larger hip breadth). Besides weight and stature, buttock–popliteal length was found to be a predictor of average and maximum pressures. Peak pressure is best explained by the score on the ectomorphic index of the somatotype classification.

Seat Characteristics and Their Influence on Interface Pressure

Seat characteristics can be divided into seat dimensions, shape of the seat and material of the seat cushions based on literature (Kyung et al. 2008, Fazlollahtabar 2010, Grujicic et al. 2009, Reed et al. 1994, Kolich 2004, Ebe et al. 2001, Kolich 2003 and Mircheski 2014). Their associations with the contact pressure are described in the below.

The study by Ebe and Griffin (2009) has pointed out that low foam hardness is more comfortable than high stiffness, but the relation between stiffness and comfort in the seat have not been linear. This indicates that the comfort rate is affected by two indicators: the feeling of being accommodated while seating and the feeling of the foam hardness.

For Reed, Schneider and Ricci (1994), the project parameters of automobile seats focused on comfort are divided into three categories interacting among themselves, such as, for example: a change on the back curvature (support) will affect the distribution of pressure (sensation) and also change the length of the effective cushioning (adjustment). The three categories described in this study are: 1) Adjustment parameters, established through the anthropometrics of the population of passengers and it includes measures such as the length of the seat cushion. 2) Parameters of sensation reported from the physical contact between the occupant and the seat. These are a combination of subjective and objective measurements, such as, for example, the distribution of pressure and the upholstery features. 3) Parameters of support, affecting the occupier's posture and include the seat shape to its settings.

Kyung and Nussbaum (2008) found significant effects of different seats on pressure variables, such as average pressure on buttock and thigh, peak pressure on buttock and

thigh and contact area on buttock and thigh. This may be due to the different dimensions of the tested seats, but may also be caused by different shapes and cushion materials.

According to Reed et al. (2000), cushion length is an important determinant of thigh support. A cushion that is too long can put pressure on the posterior portion of the occupant's legs near the knee. Pressure in this area will lead to local discomfort and restrict blood flow to the legs. This finding is supported by Mergl (2006), who defined the ideal pressure distribution for car driver's seats. He showed that comfort is rated high when there is an ideal pressure distribution under the legs and buttocks, namely 24.5–28.5% of the total load for both left and right buttocks, less than 14% of the total load for the thighs and less than 3% of the total load for the front of the thighs. The shape of the seat pan can contribute to this ideal pressure distribution.

Additionally, Hostens et al. (2001) found that a smaller backrest inclination angle leads to higher sub-maximum pressures on the seat pan and smaller sub-maximum pressures on the backrest. However, Park et al. (2013) did not find significant effects of car driver's seat height (determined by occupant package layout) on pressure distribution of lower body parts (i.e. buttock and thighs).

According to Chen et al. (2007), different shapes of cushions lead to different pressure distributions. Carcone and Keir (2007) studied the effects of anthropometry (individual size and stature) on backrest preference, but found no significant effects.

Andreoni et al. (2002) analysed pressure and comfort in a larger number of seats with different shapes and foam stiffness, and defined correlations with the shape of the human body at the interface measured by the imprinted surface. Using this method, it was possible to find an optimum shape and stiffness of the foam. Noro et al. (2012) found a

larger contact area and lower average pressure for a prototype of surgical seat that followed the buttock–sacral contour of the human body compared to a conventional surgical seat. In a comparison of nine different office chairs, Zemp, Taylor, and Lorenzetti (2016) concluded that material properties and shape of the cushions strongly influence pressure distribution measurements. Therefore, they suggest chair-specific sensor calibration before analyzing and comparing different chairs.

Although none of the studies calculated correlations between seat characteristics and interface pressure, their results do show associations between seat dimensions, seat shape, seat material and interface pressure; however, the exact relationships are unclear.

Context Characteristics and Their Influence on Interface Pressure

According to De Looze et al. (2003), it is generally agreed that comfort is a reaction to the environment. A product is not comfortable by itself, but how the comfort of a product is experienced depends on the way in which the user interacts with a product (Hekkert and Schifferstein 2011). This interaction between a human and a product always takes place within a specific context. Thus, the comfort experience is influenced by the context in which the human-product interaction takes place (Desmet and Hekkert 2007). This context can vary from physical circumstances, such as lighting conditions or temperature of the room, to a broader cultural and social situation that influences how people experience products (Hekkert and Schifferstein 2011).

The context characteristics that are considered most important for the design of comfortable passengers' seats are the activities that passengers perform and the duration of the journey. In the case of driver, due to the fact that drivers perform driving tasks, their activities are more restricted with respect to passenger. Hence, investigation of different

activities as the context characteristics on the body posture and comfort/discomfort perception is somehow meaningless. Exposure duration plays a role in the perception of comfort and discomfort. For instance, Bazley et al. (2015) found declining physical comfort levels throughout the day in offices. Other studies report an increase in discomfort over time (Porter et al. 2003; Jackson 2009; Sember 1994; Na et al. 2005; Le et al. 2014), concluding that it takes between 30 and 45 minutes before discomfort occurs. Additionally, there is a relationship between discomfort over time in combination with seat pressure dose: the longer the duration, the greater the discomfort (Noro et al. 2005).

Mastrigt (2015) studied the differences in posture of passengers reading a book, using a laptop and using a tablet device while sitting in the back seat of a driving car. This study has illustrated how much the body posture of car passengers is restricted by the car interior and the performed activity. Especially working on a laptop seems to restrict variation in body posture.

No studies were found that describe the direct association between performed activities and interface pressure. Earlier, it was concluded that posture is dependent on the task or activity, and that posture is associated with interface pressure. This is probably the reason that no studies were found that describe a direct relationship between activities and interface pressure.

Subjective measures vs. Virtual assessment

Until now the assessment of seating comfort is largely based on subjective measures: when a prototype of a new seat has been developed, a limited number of people is asked for their opinion about this new seat. A disadvantage of such measures is that the relationship with design parameters is often unclear. Furthermore, these subjective comfort

measures can only be assessed once a prototype has been made. Prototype development and testing are both time consuming and costly, while short time to market and low costs are critical for the automotive industry.

The above described economic problem introduce a need for efficient methods and tools which support early automotive tests and, ultimately, reduce development times and associated costs. Virtual testing can be regarded as a partial solution for the above mentioned problems. In the early stages of the design process, a new design can be tested for its degree of comfort by computer simulations, which would reduce the amount of prototypes needed to introduce a new seat design. Moreover, virtual testing tools allow investigations of parameters that are hard to measure, such as intervertebral disc pressure or pressures in the human soft tissues of the buttocks, in relation with (dis)comfort and physical complaints.

For prediction of seating comfort by virtual testing, objective parameters are required. The discrepancy between the subjective feeling of comfort and the prediction of the comfort level of new designs by virtual testing needs to be resolved by relationships between that subjective feeling and objective parameters (Figure 4). These relationships between objective parameters and comfort can be obtained from volunteer experiments in which the volunteers are asked for their subjective sensation of comfort and at the same time objective parameters are measured (first step). These objective parameters can be predicted by virtual testing tools (second step).

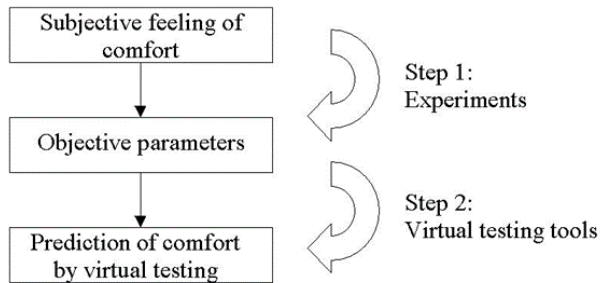


Figure 4. Schedule for comfort prediction by virtual testing

There are a number of objective parameters relating to the subjective parameter of (dis)comfort in automotive conditions. The contact interaction between the human body and the seat is one of the factors influencing the sensation of (dis)comfort for a subject. Measurement of pressure distributions is a means to express the stresses acting at the contact interface between the human and the seat. Seat pressure distribution seems to be the objective parameter relating to (dis)comfort in quasi-static conditions. Most studies investigating this relation found a statistically significant relation. Average pressure, maximum pressure, load percentage, the size and symmetry of the contact area are the parameters mostly reported in literature to relate to (dis)comfort. The studies that were not able to establish a relation, clearly described that they investigated discomfort as subjective rating. Probably, the measured pressures were too low to cause any discomfort feeling. It can be concluded seat pressure distributions is most clearly related to (dis)comfort thus, it is used in the current thesis.

Chapter 3.

Virtual Simulation

In many industrial branches the development process of new products is changing from the experimental testing methods to the digital prototyping method. Considering the fact that, using hardware prototypes results in very time and money consuming, the numerical simulation obtains a more and more decisive role due to the time and efficiency aspects. This procedure can be observed especially in the automotive industry. There the market always disposes the OEM to reduce the time and cost invested on a new product. Corresponding approaches can be observed in the construction and the commercial vehicle branches accordingly.

Hence, remarkable advantages of Virtual Simulation such as digital development phase application, reduction of required hardware prototypes, investigation of innovative concepts / materials and evaluation on not measureable quantities comes it into product development department of each company. This process of virtual development started more than two decades ago.

As the evolution of the numerical simulation tools was happening simultaneously, the solution of complex problem is possible today. Despite its long history, the finite element method continues to be the predominant strategy employed by engineers to conduct structural analysis.

Finite Element Analysis (FEA)

The finite element method is a general discretization method for the solution of partial derivative differential equations and, consequently, it finds its application in many other fields beyond structural static and dynamic analysis. The FEM is based on the subdivision of the structure into finite elements, i.e., into parts whose dimensions are not vanishingly small. Generally speaking, finite element analysis is comprised of pre-processing, solution and post-processing phases. Usually, in pre-processing step, we carry out a modeling of an actual structure. After a modeling work, we execute the discretization and mesh generation. Then, we enter the material properties and the boundary conditions. Secondly, in solving step, by using the information inputting in previous pre-processing step, solver operates the FEM analysis as a major one. Finally, in post-processing step, by using the various tools, we check several results of the solved model from the pre-processor and the solver, after the finite element analysis is completed.

As stated, the finite element method is a numerical procedure for obtaining solutions to boundary-value problems. The principle of the method is to replace an entire continuous domain by a number of subdomains in which the unknown function is represented by simple interpolation functions with unknown coefficients. Thus, the original boundary-value problem with an infinite number of degrees of freedom is converted into a problem with a finite number of degrees of freedom, or in other words, the solution of the whole system is approximated by a finite number of unknown coefficients. Therefore, a finite element analysis of a boundary-value problem should include the following basic steps (Figure 5):

- Discretization or subdivision of the domain

- Selection of the interpolation functions (to provide an approximation of the unknown solution within an element)
- Formulation of the system of equations
- Solution of the system of equations (Once we have solved the system of equations, we can then compute the desired parameters and display the result in form of curves, plots, or color pictures, which are more meaningful and interpretable.)

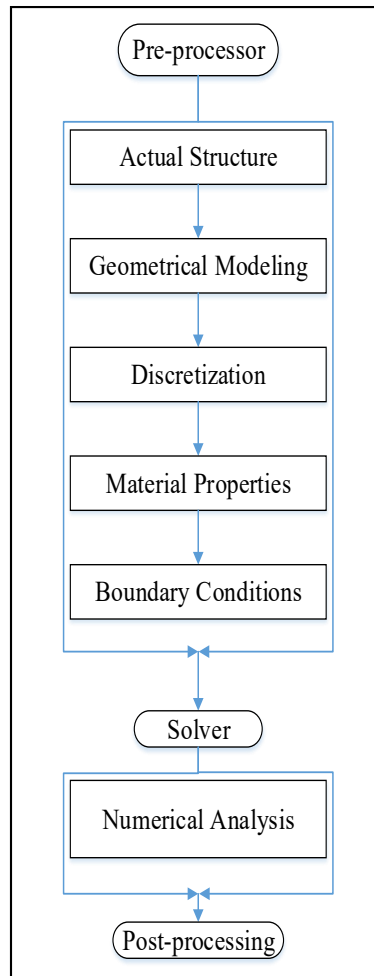


Figure 5. The basic procedure for general FEM analysis

Finite Element discretization

The finite element method is a general discretization method for the solution of partial derivative differential equations and, consequently, it finds its application in many other fields beyond structural static and dynamic analysis. The FEM is based on the subdivision of the structure into finite elements, i.e., into parts whose dimensions are not vanishingly small. Many different element formulations have been developed, depending on their shape and characteristics: beam elements, shell elements, plate elements, solid elements, and many others. In figure 6 elements family and order of interpolation for most common and usable elements is displayed.

Examples of various types of elements









	Element Name	Element Shape	
		First Order	Second Order
1D Elements Line Element	Spring, Damper Beam, Truss		
2D Elements Surface Element	Shell, Plane2D		
3D Elements Volume element	Hexahedral		
	Tetrahedral		

Figure 6. Various types of elements

A structure can be built by assembling elements of the same or different types, as dictated by the nature of the problem and by the capabilities of the computer code used.

Element displacement functions

After the discretization of the elements, the displacement functions must be defined for finite elements. The displacement is written as a vector of order 3 in the tridimensional space (sometimes of higher order, if rotations are also considered), and the equation expressing the displacement of the points inside each element is

$$u(x, y, z, t) = N(x, y, z)q(t)$$

where q is a vector where the n generalized coordinates of the element are listed and N is the matrix containing the *shape functions*. There are as many rows in N as in u and as many columns as the number n of degrees of freedom (Genta 2009).

Usually the degrees of freedom of the elements are the displacements at given points, referred to as *nodes*. In this case, previous equation reduces to the simpler form,

$$\begin{Bmatrix} u_x(x, y, z, t) \\ u_y(x, y, z, t) \\ u_z(x, y, z, t) \end{Bmatrix} = \begin{bmatrix} N(x, y, z) & 0 & 0 \\ 0 & N(x, y, z) & 0 \\ 0 & 0 & N(x, y, z) \end{bmatrix} \begin{Bmatrix} q_x(t) \\ q_y(t) \\ q_z(t) \end{Bmatrix}$$

where the displacements in each direction are functions of the nodal displacements in the same direction only. In this case matrix N has only one row and as many columns as the number of nodes of the element. Above equation has been written for a three-dimensional element; a similar formulation can also be easily obtained for one- or two-dimensional elements.

Each element is essentially the model of a small deformable solid. The behavior of the element is studied using an assumed-modes approach. A limited number, usually small, of degrees of freedom is then substituted to the infinity of degrees of freedom of each element. Inside each element, the displacement $u(x, y, z)$ of the point of coordinates x, y, z

is approximated by the linear combination of a number n of arbitrarily assumed functions, the shape functions.

The shape functions are, as already stated, arbitrary. The freedom in the choice of such functions is, however, limited, because they must satisfy several conditions. A first requirement is a simple mathematical formulation: A set of polynomials in the space coordinates is thus usually assumed.

The results of the analysis converge toward the exact solution of the differential equations constituting the continuous model discretized by the FEM, with decreasing element size (i.e., with increasing number of elements) if the shape functions

- are continuous and differentiable up to the required order, which depends on the type of element;
- are able to describe rigid-body motions of the element leading to vanishing elastic potential energy;
- lead to a constant strain field when the overall deformation of the element dictates so; and
- lead to a deflected shape of each element that matches the shape of the neighboring elements.

The last condition means that when the nodes of two neighboring elements displace in a compatible way, all the interfaces between the elements must displace in a compatible way.

Another condition, not always satisfied, is that the shape functions are isotropic, i.e., do not show geometrical properties that depend on the orientation of the reference frame.

Sometimes not all these conditions are completely met; in particular, there are elements that fail to completely satisfy the matching of the deflected shapes of neighboring elements.

The nodes are usually located at the vertices or on the sides of the elements and are common to two or more of them, but points that are internal to an element may also be used.

The strains can be expressed as functions of the derivatives of the displacements with respect to space coordinates. In general, it is possible to write a relationship of the type

$$\epsilon(x, y, z, t) = B(x, y, z)q(t)$$

where ϵ is a column matrix in which the various elements of the strain tensor are listed (it is commonly referred to as a *strain vector* but it is such only in the sense that it is a column matrix) and B is a matrix containing appropriate derivatives of the shape functions. B has as many rows as the number of components of the strain vector and as many columns as the number of degrees of freedom of the element.

If the element is free from initial stresses and strains and the behavior of the material is linear, the stresses are obtained from the strains as

$$\sigma(x, y, z, t) = E \epsilon = E(x, y, z)B(x, y, z)q(t)$$

where E is the stiffness matrix of the material. It is a symmetric square matrix whose elements can theoretically be functions of the space coordinates but are usually constant within the element. The potential energy of the element can be expressed as

$$U = \frac{1}{2} \int \epsilon^T \sigma dV = \frac{1}{2} q^T \left(\int B^T E B dV \right) q$$

The integral in above equation is the stiffness matrix of the element

$$K = \int B^T E B dV$$

Because the shape functions do not depend on time, the generalized velocities can be expressed as

$$\dot{u}(x, y, z, t) = N(x, y, z) \dot{q}(t)$$

In the case where all generalized coordinates are related to displacements, the kinetic energy and the mass matrix of the element can be expressed as

$$T = \frac{1}{2} \int \rho \dot{u}^T \dot{u} dV = \frac{1}{2} \dot{q}^T \left(\int \rho N^T N dV \right) \dot{q},$$

$$M = \int \rho N^T N dV$$

Linear Finite Element

If some generalized displacements are rotations, last equation must be modified to introduce the moments of inertia, but its basic structure remains the same.

Once it is assumed that the displacements of the finite element model are infinitesimally small and that the material is linearly elastic. In addition, it is assumed that the boundary conditions remain unchanged during the application of loading on the finite element model. With these assumptions, the finite element equilibrium equation was derived for *static analysis* as presented in below. The equation corresponds to *linear*

analysis of a structural problem because the displacement response $\{u\}$ is a linear function of the applied force vector $\{F\}$. This means that if the forces are increased with a constant factor, the corresponding displacements will be increased with the same factor.

$$\{F\} = [K]\{u\}$$

where $\{F\}$ is the assembled vector of the whole structure global nodal forces, $[K]$ is the whole structure assembled global stiffness matrix, and $\{u\}$ is the assembled vector of the whole structure global unknown nodal degrees of freedom or displacements. It should be noted that static linear equation must be modified to account for the boundary conditions or support constraints.

Solving static linear equation will result in the evaluation of the unknown nodal degrees of freedom or generalized displacements. The equation can be solved using Matrix Inversion Method i.e.

$$\{F\} = [K]\{u\} \quad \rightarrow \quad \{u\} = [K]^{-1}\{F\}$$

Non-Linear Finite Element

Nonlinearities can arise from large-displacement effects, material nonlinearity, and/or boundary nonlinearities such as contact and friction and must be accounted for. The basic problem in a general nonlinear analysis is to find the state of equilibrium of a body corresponding to the applied loads. Assuming that the externally applied loads are described as a function of time, the equilibrium conditions of a system of finite elements representing the body under consideration can be expressed as

$$R^t - F^t = 0$$

where the vector F^t lists the externally applied nodal point forces in the configuration at time t and the vector R^t lists the nodal point forces that correspond to the element stresses in this configuration. The relation must express the equilibrium of the

system in the current deformed geometry taking due account of all nonlinearities. Also, in a dynamic analysis, the vector F^t would include the inertia and damping forces.

Considering the solution of the nonlinear response, we recognize that the equilibrium relation must be satisfied throughout the complete history of load application; i.e., the time variable t may take on any value from zero to the maximum time of interest. In a static analysis without time effects other than the definition of the load level, time is only a convenient variable which denotes different intensities of load applications and correspondingly different configurations. However, in a dynamic analysis and in static analysis with material time effects, the time variable is an actual variable to be properly included in the modeling of the actual physical situation. Based on these considerations, we realize that the use of the time variable to describe the load application and history of solution represents a very general approach and corresponds to our earlier assertion that a "dynamic analysis is basically a static analysis including inertia effects."

As for the analysis results to be calculated, in many solutions only the stresses and displacements reached at specific load levels or at specific times are required. In some nonlinear static analyses, the equilibrium configurations corresponding to these load levels can be calculated without also solving for other equilibrium configurations. However, when the analysis includes path-dependent nonlinear geometric or material conditions, or time-dependent phenomena, the equilibrium relations need to be solved for the complete time range of interest. This response calculation is effectively carried out using a step-by-step incremental solution, which reduces to a one-step analysis if in a static time-independent solution the total load is applied all together and only the configuration corresponding to that load is calculated. However, we shall see that for computational

reasons, in practice, even the analysis of such a case frequently requires an incremental solution, performed automatically, with a number of load steps to finally reach the total applied load.

The basic approach in an incremental step-by-step solution is to assume that the solution for the discrete time t is known and that the solution for the discrete time $t + \Delta t$ is required, where Δt is a suitably chosen time increment. Hence, at time $t + \Delta t$ we have

$$R^{t+\Delta t} - F^{t+\Delta t} = 0$$

where the right superscript denotes "at time $t + \Delta t$." Assume that $R^{t+\Delta t}$ is independent of the deformations. Since the solution is known at time t , we can write

$$F^{t+\Delta t} = F^t + F$$

where F is the increment in nodal point forces corresponding to the increment in element displacements and stresses from time t to time $t + \Delta t$. This vector can be approximated using a tangent stiffness matrix K^t which corresponds to the geometric and material conditions at time t ,

$$F \doteq K^t u$$

where u is a vector of incremental nodal point displacements and

$$K^t = \frac{\partial^t F}{\partial^t u}$$

Hence, the tangent stiffness matrix corresponds to the derivative of the internal element nodal point forces F^t with respect to the nodal point displacements u^t .

By substituting, we obtain

$$K^t u = R^{t+\Delta t} - F^t$$

and solving for U , we can calculate an approximation to the displacements at time $t + \Delta t$,

$$u^{t+\Delta t} \doteq u^t + u$$

The exact displacements at time $t + \Delta t$ are those that correspond to the applied loads $F^{t+\Delta t}$.

Having evaluated an approximation to the displacements corresponding to time $t + \Delta t$, we could now solve for an approximation to the stresses and corresponding nodal point forces at time $t + \Delta t$, and then proceed to the next time increment calculations. However, because of the approximation considered for F , such a solution may be subject to very significant errors and, depending on the time or load step sizes used, may indeed be unstable. In practice, it is therefore necessary to iterate until the solution is obtained to sufficient accuracy.

ABAQUS/Standard generally uses Newton's method as a numerical technique for solving the nonlinear equilibrium equations. The motivation for this choice is primarily the convergence rate obtained by using Newton's method compared to the convergence rates exhibited by alternate methods (usually modified Newton or quasi-Newton methods) for the types of nonlinear problems most often studied with ABAQUS.

Implicit solution method vs. Explicit

The finite element method is a popular computational tool used in engineering research and industrial design. In the field of solid mechanics, and specifically non-linear quasi-static problems, finite element equation solution methods can generally be classed as either implicit or explicit and are typically solved incrementally (Harewood et al 2007). In the implicit approach a solution to the set of finite element equations involves iteration until a convergence criterion is satisfied for each increment. The finite element equations

in the explicit approach are reformulated as being dynamic and in this form they can be solved directly to determine the solution at the end of the increment, without iteration.

The word *implicit* in this study refers to the method by which the state of a finite element model is updated from time t to $t + \Delta t$. A fully implicit procedure means that the state at $t + \Delta t$ is determined based on information at time $t + \Delta t$, while the explicit method solves for $t + \Delta t$ based on information at time t .

There are a range of solution procedures used by implicit FE solvers. A form of the Newton–Raphson method is the most common and is presented here. Vectors and matrices are denoted as underlined. When solving a quasi-static boundary value problem, a set of non-linear equations is assembled:

$$G(u) = \int B^T \sigma(u) dV - \int N^T t ds = 0$$

where G is a set of non-linear equations in u , and u is the vector of nodal displacements. B is the matrix relating the strain vector to displacement. The product of B^T and the stress vector, σ , is integrated over a volume, V . N is the matrix of element shape functions and is integrated over a surface, S . The surface traction vector is denoted by t . Above equation is usually solved by incremental methods, where loads/displacements are applied in time steps, Δt , up to an ultimate time, t .

The state of the analysis is updated incrementally from time t to time $t + \Delta t$. An estimation of the roots of equation is made, such that for the i^{th} iteration:

$$\delta u_{i+1} = u_{i+1}^{t+\Delta t} - u_i^{t+\Delta t} = - \left[\frac{\partial G(u_i^{t+\Delta t})}{\partial u} \right]^{-1} G(u_i^{t+\Delta t})$$

where $u_i^{t+\Delta t}$ is the vector of nodal displacements for the i^{th} iteration at time $t + \Delta t$. The partial derivative on the right-hand side of the equation is the Jacobian matrix of the governing equations and can be referred to as the global stiffness matrix, K .

Last equation is manipulated and inverted to produce a system of linear equations:

$$K(u_i^{t+\Delta t})\delta u_{i+1} = -G(u_i^{t+\Delta t})$$

Corresponding equation must be solved, for each iteration, for the change in incremental displacements, δu_{i+1} . In order to solve for δu_{i+1} the global stiffness matrix, K , must be inverted. Although, this is a computationally expensive operation, iteration ensures that a relatively large time increment can be used while maintaining accuracy of solution. Following iteration i , δu_{i+1} has been determined and a better approximation of the solution has been made, $u_{i+1}^{t+\Delta t}$. This in turn is used as the current approximation to the solution for the subsequent iteration ($i + 1$).

The accuracy of the solution is dictated by the convergence criterion where the updated value for G must be less than a tolerance value. Complications can arise in an analysis that has a highly non-linear stress-strain response or where there is contact and sliding between two surfaces. For a complex job it can be difficult to predict how long it will take to solve or even if convergence will occur.

ABAQUS/standard uses a form of the N-R iterative solution method to solve for the incremental set of equations. Formulating and solving the Jacobian matrix is the most computationally expensive process. Several variations on the N-R method exist to improve the solution time. The modified Newton method is the most commonly used alternative and is suitable for non-linear problems. The Jacobian is only recalculated occasionally and in cases where the Jacobian is un-symmetric it is not necessary to calculate an exact value

for it. The modified Newton method converges quite well using a symmetric estimate of the Jacobian.

The *explicit* method was originally developed, and is primarily used, to solve dynamic problems involving deformable bodies. Accelerations and velocities at a particular point in time are assumed to be constant during a time increment and are used to solve for the next point in time. ABAQUS/explicit uses a forward Euler integration scheme as follows:

$$u^{(i+1)} = u^{(i)} + \Delta t^{(i+1)} \dot{u}^{(i+\frac{1}{2})}$$

$$\dot{u}^{(i+\frac{1}{2})} = \dot{u}^{(i-\frac{1}{2})} + \frac{\Delta t^{(i+1)} + \Delta t^{(i)}}{2} \ddot{u}^{(i)}$$

where u is the displacement and the superscripts refer to the time increment. The term *explicit* refers to the fact that the state of the analysis is advanced by assuming constant values for the velocities, \dot{u} , and the accelerations, \ddot{u} , across half time intervals. The accelerations are computed at the start of the increment by

$$\ddot{u}^{(i)} = M^{-1} \cdot (F^{(i)} - R^{(i)})$$

where F is the vector of externally applied forces, R is the vector of internal element forces and M is the lumped mass matrix. As the lumped mass matrix is diagonalised it is a trivial process to invert it, unlike the global stiffness matrix in the implicit solution method. Therefore, each time increment is computationally inexpensive to solve.

A stability limit determines the size of the time increment:

$$\Delta t \leq \frac{2}{\omega_x}$$

Where ω_x is the maximum element eigenvalue. A conservative and practical method of implementing the above inequality is:

$$\Delta t = \min\left(\frac{L^e}{c^d}\right)$$

Where L^e is the characteristic element length and c^d is the dilatational wave speed:

$$c^d = \sqrt{\frac{\lambda + 2\mu}{\rho}}$$

λ and μ are the Lamé' elastic constants and ρ is the material density. A quasi-static problem that is solved using the explicit method would have much smaller time increments than an equivalent problem solved using the implicit method. Although the incremental solution is easy to obtain using the explicit method, it is not unusual for an analysis to take 100,000 increments to solve. In order to maintain efficiency of the analyses it is important to ensure that the sizes of the elements are as regular as possible. This is so that one small element does not reduce the time increment for the whole model.

It is often impractical to run a quasi-static analysis using its true time scale as the runtime would be very large. A number of methods can be used to artificially reduce the runtime of the simulation. The first involves simply speeding up the applied deformation or loading rate and the second involves scaling the density of the material in the model. According to time increment and dilatational wave speed equation, when the density is scaled by a factor, f^2 , the runtime is reduced by a factor f . The latter method is preferable as it does not affect the strain rate dependent response of visco-plastic/rate-dependent materials.

It is important when performing a quasi-static simulation that the inertial forces do not affect the mechanical response and provide unrealistic dynamic results. To reduce the dynamic effects Kutt et al. [16] recommend that the ratio of the duration of the load and

the fundamental natural period of the model be greater than five. It has been shown that by keeping the ratio of kinetic energy to the total internal strain energy at $< 5\%$ dynamic effects in the model are negligible. This is the criterion for quasi-static behavior that is employed in this study.

During implicit analyses where the material gives a nonlinear stress–strain response many iterations are usually needed to solve for an increment. This leads to progressively smaller time steps being used and should the code encounter large non-linearity's convergence may be impossible to achieve in practical terms. As there is no iteration involved in the explicit method, convergence problems are not an issue.

The solution time of the implicit solver is proportional to the square of the wavefront size in the global stiffness matrix. This has implications when increasing the size of the model and when running 3D simulations. In the case of the explicit solver there is a linear relationship between the size of the model and the solution time, as dictated by the characteristic element length and the number of elements in the model.

Virtual Simulation of Seat Comfort

The strong competition in the automotive market requires from the OEM new model types in continuously reduced time intervals. Thereby the customer demands for more economical and safer solutions including a higher driving and seating comfort. The fact of the current financial crisis rises this challenge for the OEM, as the cost for the development of new products must be reduced constantly (Siefert et al. 2009).

Thereby the application of digital prototypes is of great benefit, since by numerical simulations it allows for the layout design and thus reduces the number of required hardware tests. Due to the high quality of prognosis compared to crash tests, numerical

simulations with digital prototypes already are a standard element in the R & D departments of OEM and Tier1 seat-suppliers (Siefert et al. 2008).

Within previous approaches, simulations for the assessment of the static and dynamic seating comfort have been carried out as methodical investigations only, due to their complexity. Thereby especially the representation of the human body with its static and dynamic properties by a finite-element (FE) model has been a great challenge, (Verver, 2004; Cakmak et al., 2006). Therefore, compared with requirements of mechanical systems, a seating comfort simulation is overlaid with the definition and the mapping of the human body and its behavior.

In the field of mapping the human body and its properties with a finite-element (FE) model, different approaches have been published for seat comfort simulation within the last years. Thereby, only parts of the human body or the whole body have been modelled. Particular works to build the human thigh with pelvis and femur have been published by Moes and Horva'th (2002), Verver (2004) and Mergl (2006). The presented models have been used for static comfort simulations.

For whole-body human FE models, publications of Choi et al. (2006) and Pankoke (2003) exist. Pankoke presented the human model CASIMIR, which is used in the simulation method of this study.

Compared to experimental testing, the application of a simulation method with a validated human model provides the possibility of investigating the loads on the driver and evaluating his performance.

Based on the set-up of the complete model, the simulation of seating comfort can be divided into three steps:

- Seat structure
- Non-occupied seat
- Occupied seat

These steps correspond to the procedure of the experimental testing. In the first step, the seat structure itself is modelled and validated to its nonlinear behavior in joints, adjusting mechanism and damping behavior. The non-occupied seat model thus is an expansion of the foam cushions and the seat cover and includes the interaction of these parts to the seat structure. Finally, the occupied seat defines the whole system. Because of the influence on resulting quantities, e.g. the seat pressure distribution, the interaction definition between the human model and foam cushions is very important.

Seat modelling

The task always starts with the FE modelling of the seat structure. Generally speaking, the seat framework is usually constructed of normal steel that has been formed into tubular configurations or of stamped or rolled sheet metal except the part most affected by dynamic stresses, such as the side uprights of the backrest, in which high resistance steel is used. Historically, the function of structural backbone has been limited to providing shape for the cushioning members and support for its own weight and that of its occupant. Redesign and strengthening of seat framework in conjunction with its anchorages can provide the force resistance necessary for occupant restraint during moderate and severe front, side and rear-end collisions.

The design definition of the structure represents a fundamental step of the seat development, not only for the functions that it has to perform but also, the structure will be an invisible component of the seat which can use for different cars.

The studied seat structure of the specific automobile is shown here (Figure 7).

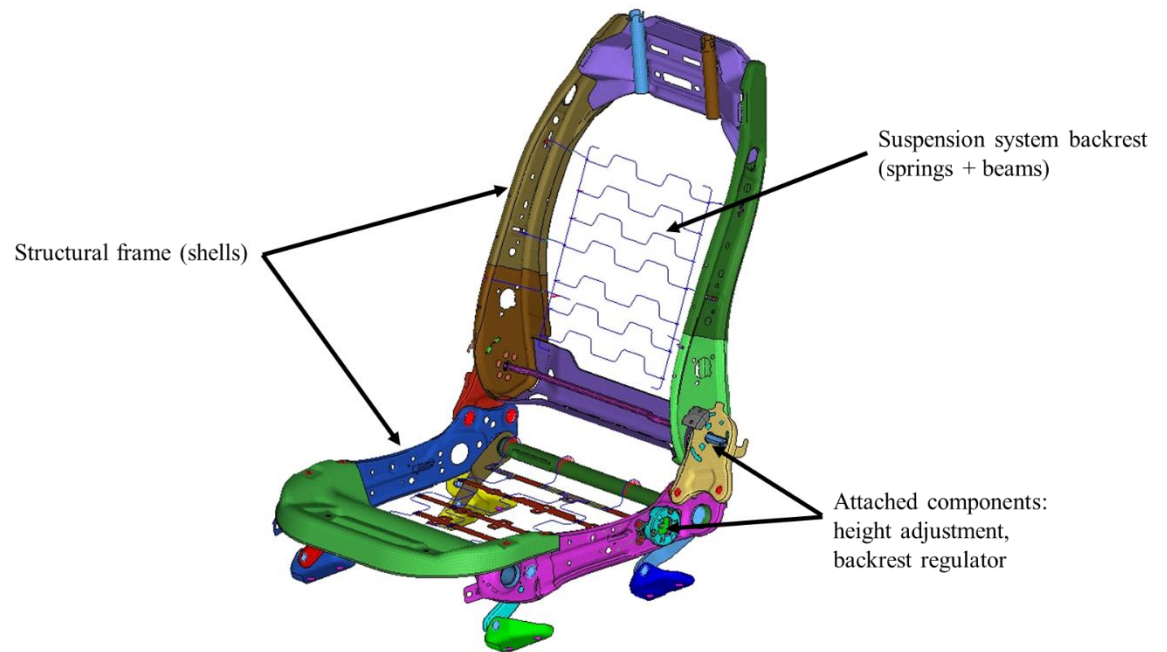


Figure 7. Model of seat structure

The model must always contain all components with a strong influence on the resulting values. Therefore, an expansion of the structure by the armrest or operation elements such as the steering wheel and gear lever is required.

The structural model is generated and validated within the scope of the usual development process. Especially in the automotive area the application of improved crash models is economically efficient. The set-up of the structural model can be subdivided into the following parts:

- Structural components

- Attached assemblies (e.g. height adjustment mechanism, backrest regulator)
- Coupling elements there between (e.g. joints)
- Compliant interfaces for foam cushions (suspension systems)

The supporting components as well as the supplements are usually modelled based on CAD data with shell elements, beams and springs. Realization of volumetric components is carried out with continuum element (ABAQUS element type: C3D8) such as height adjustment mechanism shown by figure 8. Furthermore, for an adequate application of this digital prototype the seat adjustment must be considered. Only by inclusion of the variation of e.g. the seat rail or the recliner all required real settings can be investigated.

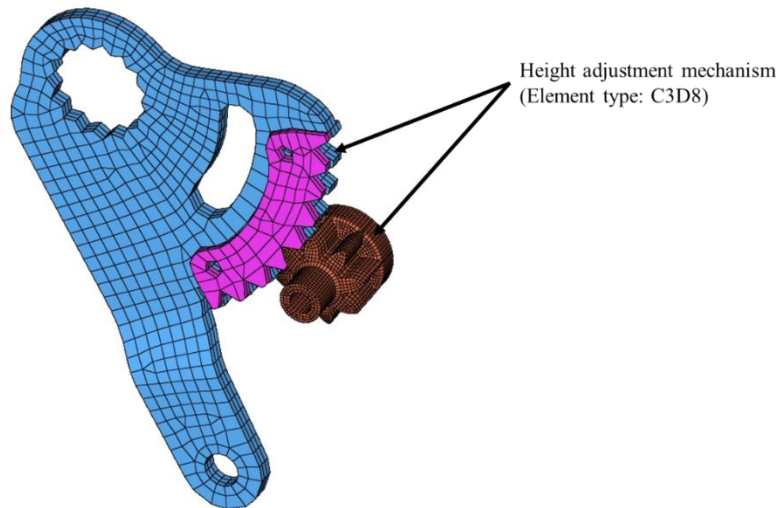


Figure 8. FE model of height adjustment mechanism

Connections between the structural part e.g. spot welds are modeled using kinematic couplings (Figure 9). Moreover, the coupling between structural parts is defined by connectors that represent the kinematics of the seat. Besides the influence on dynamic

behavior, the connector elements enable different seat settings, which define the practical operation mode.

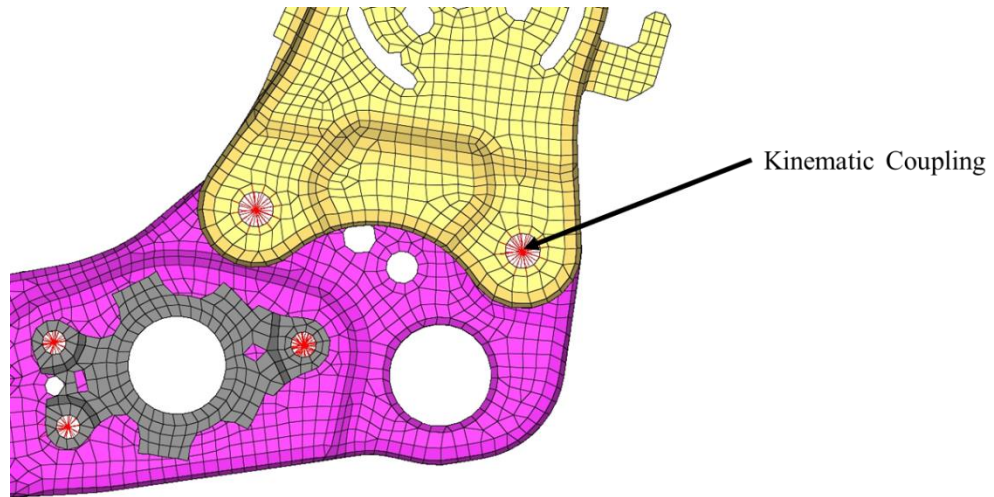


Figure 9. Kinematic coupling of structural parts

If the seat simulation is carried out after a hardware prototype has been built, the structural model should be validated by the results of an experimental modal analysis (EMA). The evaluation is carried out by natural frequencies, mode shapes and damping ratios. The differences between simulation and experimental testing should be only a few percent (Pankoke et al., 2005).

According to the simulation of the static and dynamic seating comforts, the impact of the suspension systems (rear and base) is very high. This is based on their compliance compared to other parts and the direct interaction with the cushions.

The modelling of the foam cushions can be done on the basis of the CAD geometry of the out-of-tool parts. Within the modelling of the foam cushion (Fig. 10), the option of

morphing the shape should be considered. Besides the material choice, this provides a second possibility to optimize the seating comfort.

The foam cushions are modelled with solid elements. Investigations of different element types have shown that the application of second-order tetrahedron elements meets the requirements of computation. This has the advantage of an automatic meshing being possible and the needed modelling time is dramatically reduced. However, in order to guarantee the right contact nodal forces, and especially for contact problems, a modified element approach must be applied.



Figure 10. Model of cushion and backrest foam with tetrahedron elements

The seat cover can be modelled with a shell layer, defined by the contact faces of the foam cushions. As the nodes of the foam and the cover are merged a shear force transmission between these parts is possible, which does not definitely reflect the real

behavior. This approach can represent the stiffening effects of the trimming process, though simplified. Compared to an alternative modelling method, including the trimming process (Cakmak et al., 2006), this procedure is very time efficient.

Material properties

The foam material of a commercial vehicle seats has great influence on the static and dynamic seating comfort. Due to the fact that mechanical properties of the foam has a direct physical effect on the driver, this study is dedicated to identify the material parameters using the finite-element-solver ABAQUS based on experimental data. In another words, the material parameters are validated by simulating the experiments and evaluating the corresponding results.

Usually, several different PUR-foam materials are applied in a modern passenger car seat. For example, in the cushion and backrest flank areas, the application of a stiffer mixture is preferred in order to guarantee more lateral hold during rolling turn and durability. Thereafter, two different types of foams have been considered for cushion and backrest.

Considering the fact that numerical simulation is carried out for a foam specimen whose dimensions are defined to 100*100*50 mm, geometrical modeling is a 3D solid foam. Moreover, in the numerical test which follows the ISO 3386-1 standard test, the foam specimen is compressed up to 70%. Hence, discretization of geometry was done by C3D8H solid element which is 8-node linear brick hybrid incompressible solid element.

Hybrid elements are intended primarily for use with incompressible and almost incompressible material behavior; these elements are available only in ABAQUS/Standard. When the material response is incompressible, the solution to a problem cannot be obtained

in terms of the displacement history only, since a purely hydrostatic pressure can be added without changing the displacements.

Near-incompressible behavior occurs when the bulk modulus is very much larger than the shear modulus (for example, in linear elastic materials where the Poisson's ratio is greater than .48) and exhibits behavior approaching the incompressible limit: a very small change in displacement produces extremely large changes in pressure. Therefore, a purely displacement-based solution is too sensitive to be useful numerically (for example, computer round-off may cause the method to fail).

This singular behavior is removed from the system by treating the pressure stress as an independently interpolated basic solution variable, coupled to the displacement solution through the constitutive theory and the compatibility condition. This independent interpolation of pressure stress is the basis of the hybrid elements. Hybrid elements have more internal variables than their non-hybrid counterparts and are slightly more expensive.

For present study firstly, free meshing algorithm was used to create surface quad mesh then, brick elements were created in presence of cuboid surfaces using subpanel of solid map as it is shown in figure 11.

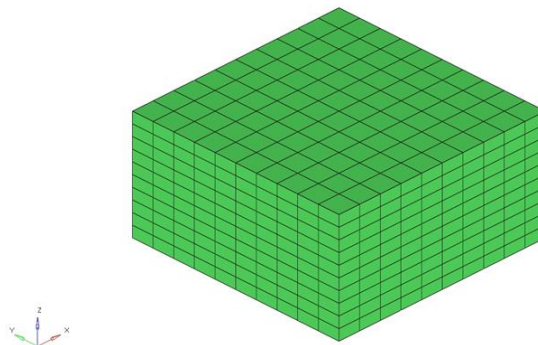


Figure 11. Discretization of foam specimen

It is worth to say that rigid plate which used to apply compressive force on foam specimen was discretized by R3D4 element. R3D4 is a three-dimensional rigid element which can be used to define the surfaces of rigid bodies for contact.

Elastomeric foam material model in following case must be isotropic, nonlinear and be validated for cellular solids whose porosity permits very large volumetric changes. Moreover, it can deform elastically to large strains, up to 90% strain in compression; and requires that geometric nonlinearity be accounted for during the analysis step. Based on aforementioned reasons, HYPERFOAM property was selected to be used as the material model. Material model is obtained by a nonlinear least-squares fit of the uni-axial compression test data (i.e. nominal stress and nominal strain values).

The boundary condition is the application of a force and/or constraint. In HyperMesh, boundary conditions are stored within what are called load collectors. Quite often especially at the beginning a load collector is needed for the constraints (also called SPC – Single Point Constraints). Therefore, in our case study all translational degrees of freedom except the third one (translation in Z-direction) for rigid plate and foam specimen considered as Homogeneous Dirichlet Boundary Conditions i.e. $u_x = u_y = 0$.

A contact pair is defined between the rigid plate, which is modeled by a rigid surface, and a slave surface composed of the faces of the elements in the contact region. The friction coefficient between the rigid plate and the foam is 0.8.

The numerical simulation of uni-axial compression test of PUR-foam is Nonlinear Static Analysis because of material nonlinearity, large displacement and also presence of contact. Furthermore, simulated experiment is static uni-axial compression test of foam

and inertia effects can be neglected. Because of nonlinearity, NLGEOM and UNSYMM options which are referred to geometry nonlinearity and un-symmetric stiffness matrix respectively, are invoked in *STEP definition.

In ABAQUS/Standard the rigid plate is displaced downward by a prescribed displacement boundary condition in the first step, indenting the foam specimen by a distance of 35 mm. Geometric nonlinearity should be accounted for in this step, since the response involves large deformation. In the second step the rigid plate is displaced back to its original position. Static analysis is performed for both steps. During a static step the material behaves purely elastically, using the properties specified with the HYPERFOAM model. In appendix, INPUT file which included steps, analysis procedure, prescribing boundary conditions and output requests for each steps, was presented.

For determining the material properties of foams static measurement has to be performed. Thereby the static test procedure is based on the ISO 3386-1 standard. For the testing cuboid foam specimens of two different materials are used. Eliminating the tolerances out of the production process, three samples are tested for each material. According to the ISO standard the foam specimen is compressed uni-axially between two rigid plates. Taking into account a conditioning of the material, only the fourth cycle of the load-deflection curve is used for the evaluation.

In the static tests the foam specimen are compressed up to 70 %. The measurement is carried out with a controlled deformation speed of 2 mm/s. The dimensions of the specimen are defined to 100 x100 x 50 mm.

Altogether two foam materials are tested within this investigation. As can be observed the seat-cushion-foam is stiffer than the seat-backrest-foam to guarantee more compressive load which applied by buttock.

Elastic materials in compression and tension can store usually up to 100% of energy due to deformation. Whereas viscoelastic materials don't store 100% of energy under deformation; but actually lose or dissipate some of this energy as heat. This dissipation energy is also known as hysteresis loss. The importance of the hysteresis measurement is that it gives a strong indicator about the material capacity to absorb energy and/or relief pressure. The area under the loading curve can be called as the total mechanical energy input. The area under the return curve can be considered as the return of stored energy and the area between the two curves is the energy which cannot be returned but rather is dissipated and converted to heat as shown in figure 12. This dissipated heat loss can be called also hysteresis loss.

It is well understood that the deformation of open-cell foams shows three main regions. These regions can be divided into an initial linear elastic region where strain energy is stored in the reversible bending of the struts; a plateau region where struts begin to impinge upon each other and finally the third region which is the densification area.

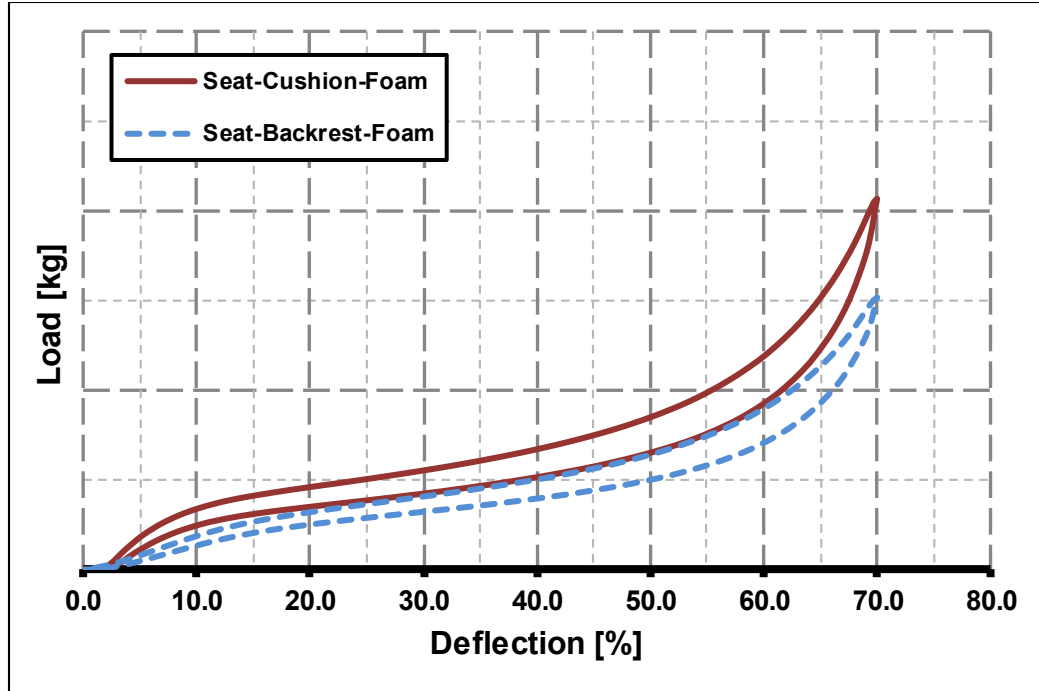


Figure 12. Comparison of stress-strain-curve for tested foam materials

As a material approach for the description of foams, a hyper-elastic law, following equation, similar to Ogden's strain energy potential formulation is used in ABAQUS. The difference between the two formulation is based on the consideration of high compressibility, being a main property of the investigated polyurethane foams.

$$U = \sum_{i=1}^N \frac{2\mu_i}{\alpha_i^2} \left[\lambda_1^{\alpha_i} + \lambda_2^{\alpha_i} + \lambda_3^{\alpha_i} - 3 + \frac{1}{\beta_i} ((J^{el})^{-\alpha_i\beta_i} - 1) \right]$$

Description: Strain energy potential formulation for static foam behavior

In the finite-element-solver ABAQUS, this material model is described by the option *HYPERFOAM with the included variables describing the following materials parameters:

- N – Order of formulation
- μ_i – Part of initial shear modulus
- λ_i – Principal stretches
- J^{el} – Elastic volume ratio
- β_i – Degree of compressibility
- α_i – Material dependency

Figure 13 and figure 14 show the comparison for the static stress-strain curve of a standard seat-cushion-foam and standard seat-backrest-foam respectively, under uni-axial load. The identification is carried out on the average value between loading and unloading. It is worth to say that initial part of experimental results has not been taken into account to achieve more good correlation. The comparison of the simulation results for the stress-strain curve with the executed tests, perform for validation, shows excellent correlation. The slight difference at larger strain result from defining the Poisson's ratio equal to zero.

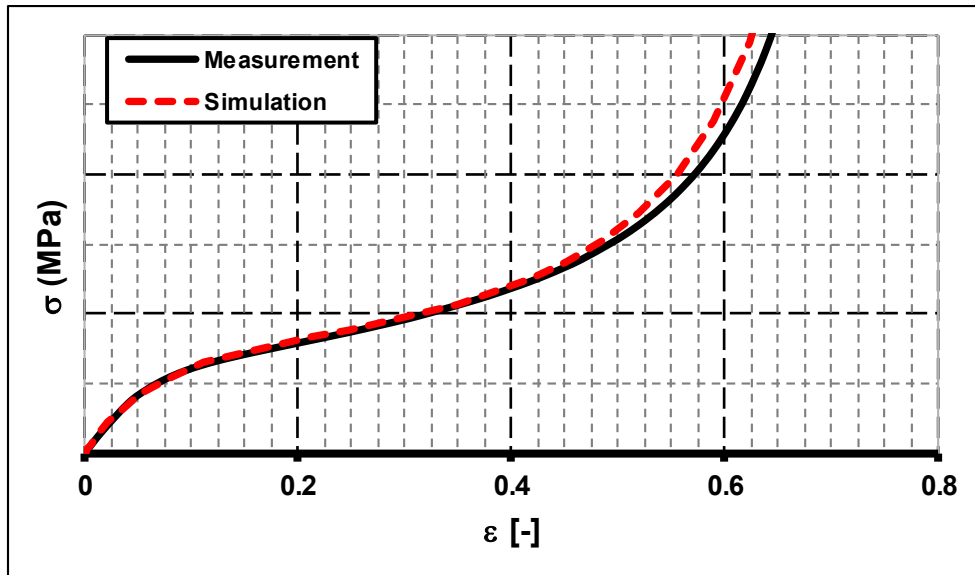


Figure 13. Comparison of Experimental and Numerical results for seat-cushion-foam

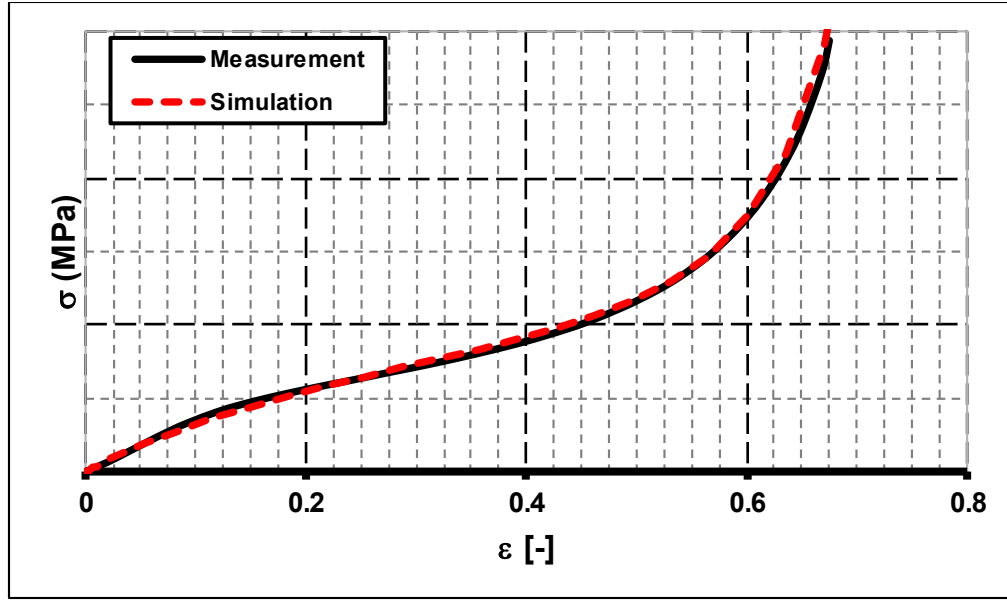


Figure 14. Comparison of Experimental and Numerical results for seat-backrest-foam

Since the free material parameters are determined by using a mathematical optimization procedure, different values of order of formulation, N , have been investigated. Selection of order of formulation is based on the balance between accuracy, stability, and cost of simulation. Figure 15 and figure 16 display the numerical results for different values of order of strain energy potential formulation. Although The uniaxial compression results for both values of $N=2$ and $N=3$ match the test data extremely well, the order of series expansion is chosen to be $N=2$ since this fits the test data with sufficient accuracy. It also provides less simulation cost and a more stable model than the $N=3$ case.

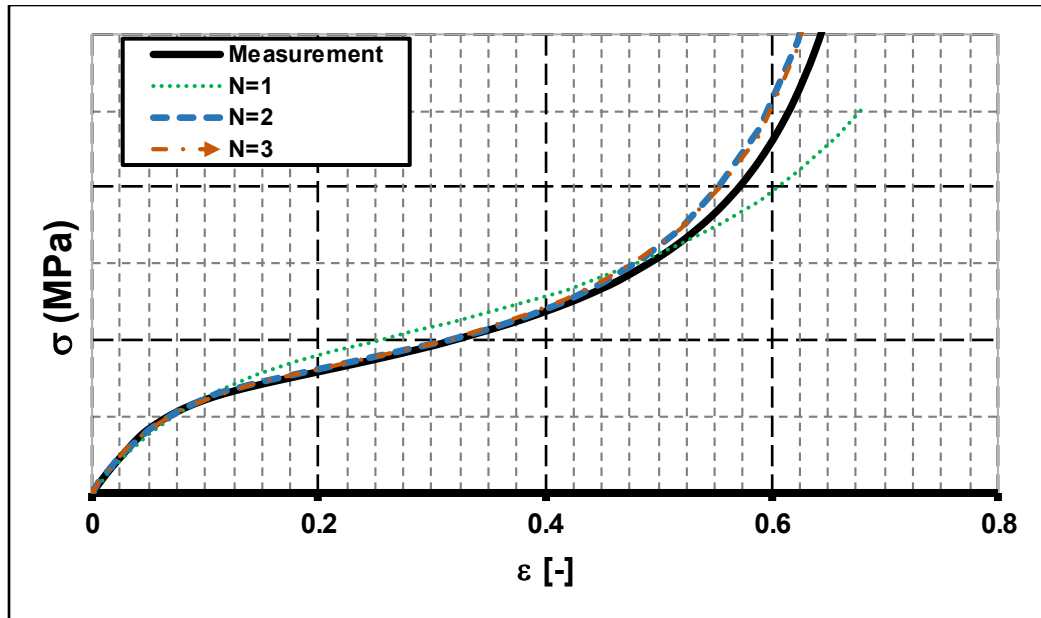


Figure 15. Effect of order of formulation on numerical simulation for seat-cushion-foam

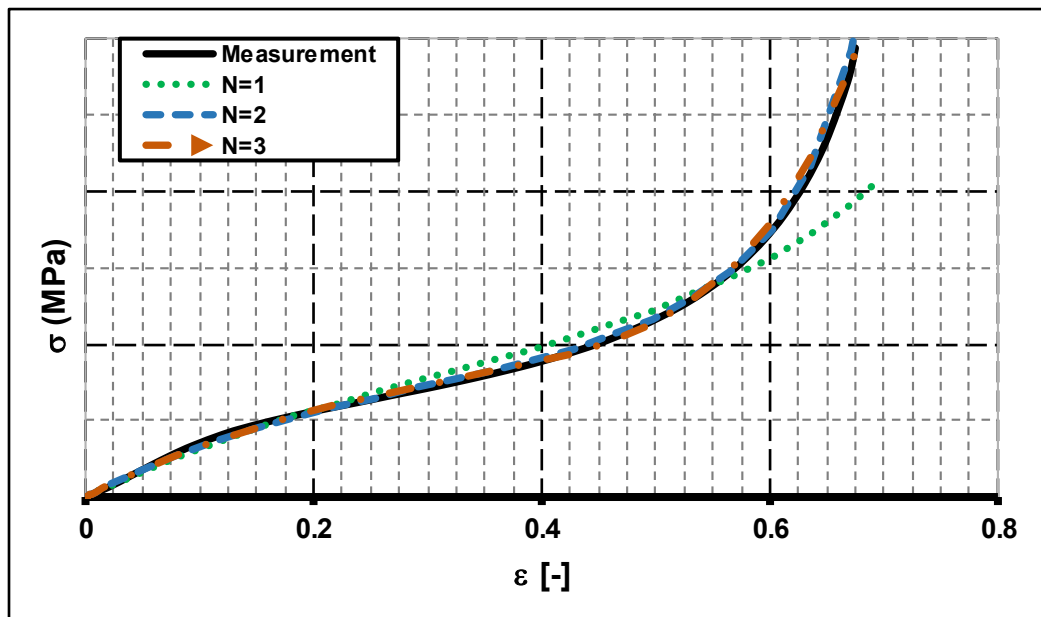


Figure 16. Effect of order of formulation on numerical simulation for seat-backrest-foam

Human FE model CASIMIR

Today, in many fields various human models are used in distinct applications (Digital Human Modeling Conference, 2002; Wolfel et al., 2004). Most common is the use of CAD based human models such as RAMSIS (Human Solutions) or UGS Classical Jack, which are applied for the design of the interior package. Within the application of these models, the mechanical properties of the package and the human, beside the kinematics, are not considered. Accordingly, distinctions from the real conditions can occur. Especially the influence of compliant materials as foam of the seat and soft tissue of the human body, which cause great deformations under static loads, is not considered. The procedure to support these geometric methods with measure quantities, such as the H-Point, is not possible within a complete virtual development process.

Consequently, for this procedure the application of human models, considering the mechanical behavior, represents an improvement. This effect comes along with the advantage of carrying out simulations to evaluate static and dynamic seating comforts.

Within the group of models including the mechanical properties, one must differentiate between *phenomenological* and *anatomical* set-ups. Phenomenological models serve to reproduce one single characteristic of man precisely described (a “phenomenon”). The advantage of a simple model configuration is limited to the fact that these models are not applicable for the simulation of properties beyond this phenomenon. Most of these phenomenological models represent the whole body in the standing or in a sitting posture. Figure 17 shows models from Fairley and Griffin (2003), Knoblauch (1992) and DIN 45676 (2003).

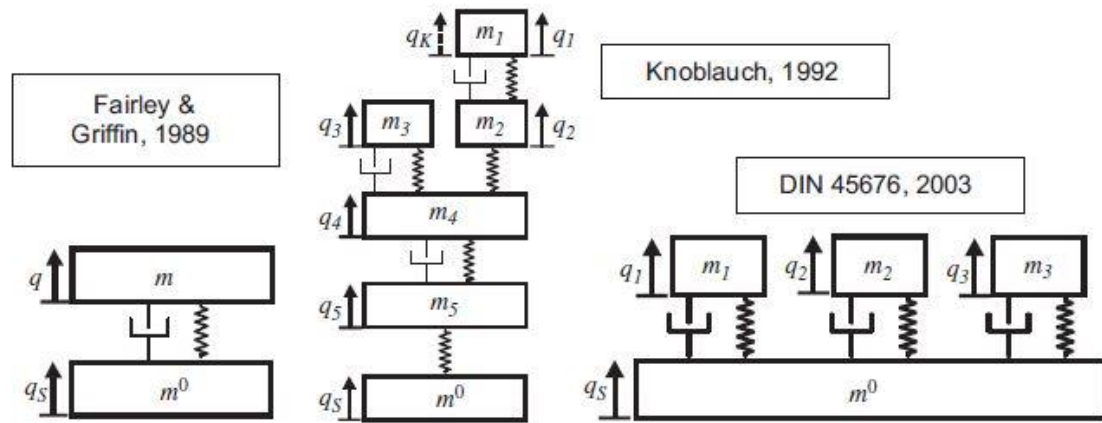


Figure 17. Phenomenological models of a man in the sitting posture

On the contrary, anatomical models represent man on the basis of his physiological characteristics. Depending on the desired results, these models can describe the whole body or a part of it. Figure 18 displays models of Moes and Horvath (2002), Verver (2004) and Mergl (2006), which represent a compliant thigh including pelvis and femur and have been applied for seat comfort simulations.

If appropriately modelled and validated, anatomical models have the capability of predicting the mechanical behavior of physical quantities that are not part of the input data for set-up generation.

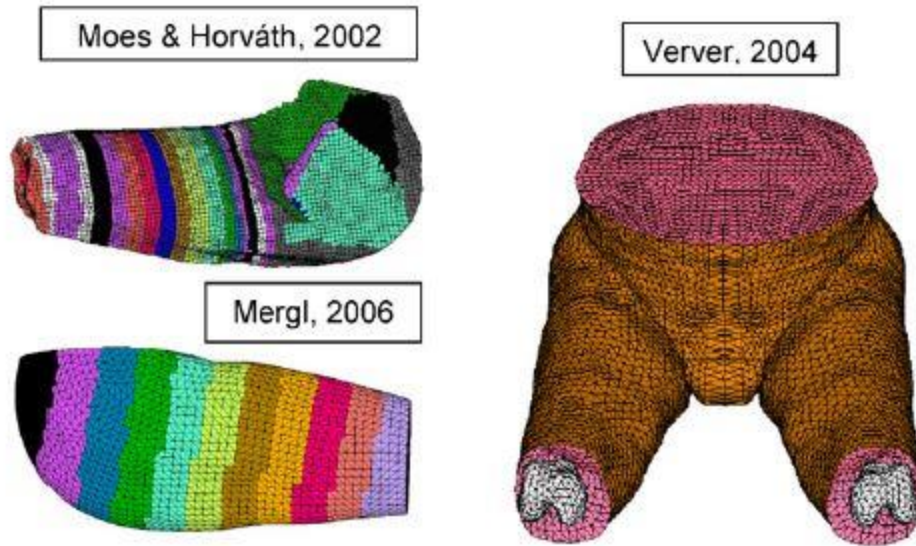


Figure 18. Anatomical models of the compliant thigh with pelvis and femur

Thus, these models provide the possibility of evaluating especially the dynamic seating comfort via vibration parameters sensed by man. Furthermore, the results can be taken into account with subjective assessment (e.g. forces in the lumbar spine, accelerations of different abdominal parts).

The following preconditions must be fulfilled by an anatomical model to allow a numerical evaluation of static and dynamic seating comforts according to whole-body behavior:

- Model geometry derived from human anatomy
- Masses, stiffness and damping properties defined via physiological data
- Detailed model of the lumbar spine

- Consideration of static muscle activation for the static equilibrium of the upper part of the body under gravity load
- Consideration of dynamic muscle effect representing frequency-dependent stiffness and damping properties

The requirement for a detailed model of the lumbar spine is based on the fact that this part of the body is the most important for the whole-body vibrations of man. After the model generation, the set-up and its properties must be validated with test person measurements. The most important parameters for static and dynamic seating comforts are as follows:

- Static seating pressure distribution
- Dynamic mass with excitation of the seating man at the buttocks
- Transfer functions of the excitation from the buttocks to the head
- Transfer functions of the excitation from the buttocks to further parts, particularly to measuring points at shoulder and lumbar spine

CASIMIR represents a dynamic, anatomical predictive FE model of a man in a sitting posture (Siefert et al., 2006). Currently, it is available for the FE code ABAQUS. In the course of its application for seating comfort, the following components have been developed recently:

- Detailed model of the lumbar spine including frequency-dependent damping properties of the intervertebral discs
- Detailed model of the relevant abdominal and dorsal musculature
- Dynamic model of the abdominal cavity
- Detailed skeletal model of pelvis, femur, tibia, cervical spine, head and arms

- Model of the body soft tissue in the relevant contact regions to the seat, including static and dynamic tissue properties

Whereas Fig. 20 shows the detailed parts of the abdominal musculature and the lumbar spine with intervertebral discs, Fig. 19 displays a view of the complete model. The presented 50th percentile reflects a man with averaged anthropometric values which is the percentile used in current study.

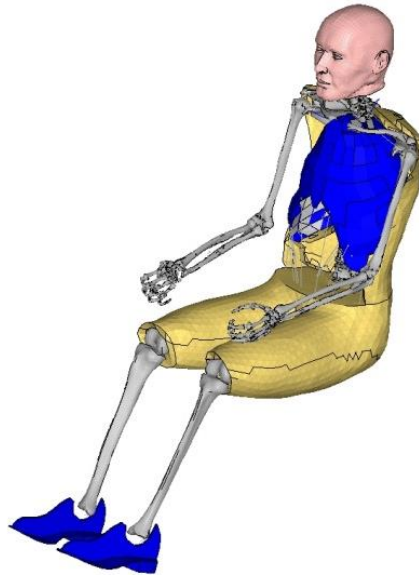


Figure 19. CASIMIR model for man of the 50th percentile

Within the detailed model of the abdominal musculature, all relevant muscles are considered with nonlinear and frequency-dependent spring and dashpot elements. The muscle activation for the posture under gravity is computed by an optimization routine following the principle of minimizing the required energy. The determined values correspond to electromyographic measurements.

The material behavior of the different components of the lumbar spine as annulus and nucleus are defined over literature values. All bone components are modelled as rigid bodies, as their stiffness, compared to the compliant parts as muscles and tissue, is very high. The set-up of the whole model and its components are described in detail by Buck (1997) and Pankoke (2003).

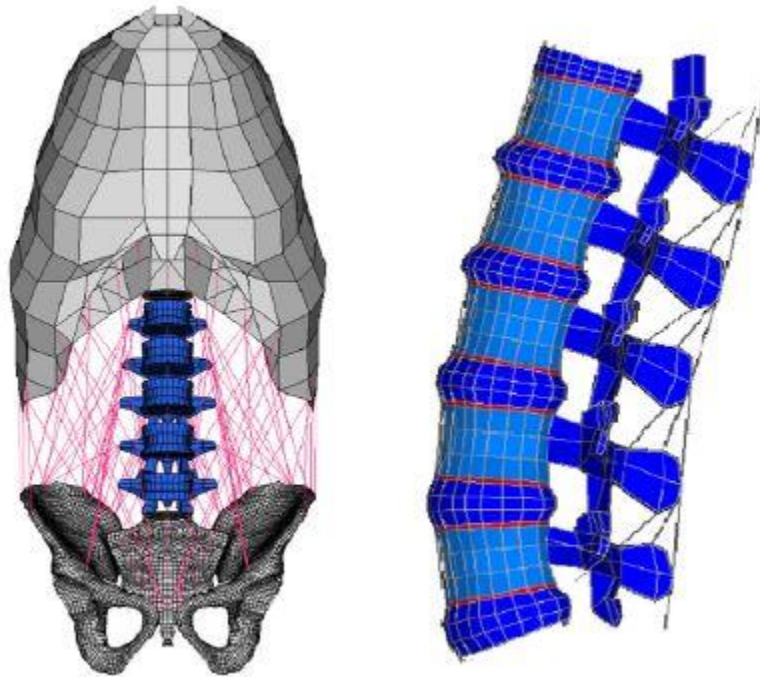


Figure 20. Detailed model of abdominal muscles (left) and lumbar spine (right)

For the widespread application of a human model in the evaluation of the static and dynamic seating comforts, a modulation of the set-up must be possible. Thereby, percentile, body height and mass on the one hand, which have been described statistically, and the posture on the other hand must be considered. Both parameters have significant

influence on the interaction with the seat and the static pressure distribution hereupon as well as on the dynamic whole-body-vibration behavior.

The range of required percentiles depends on the desired customer clientele. While for the seating comfort of luxury cars the overall spectrum—starting with the 5%-female (percentile f05) via the 50%-male (m50) until the 95%-male (m95)—is significant, the range decreases for small cars to the lower percentiles.

According to such specifications and by means of an individualization algorithm, covering a choice of seven anthropometric values, as described in Pankoke et al. (1998), CASIMIR can be adapted to the value combination of percentiles or even individuals. Figure 21 shows the CASIMIR family with the average definition m50 and the limits f05 and m95.

While the decision for the percentile is related to the customer, the global adaptation of the posture is primarily defined by the seat and its possible adjustment ranges, which are given by the package design. The adjustment of the CASIMIR posture is effected via the definition of relative joint angles and a related adaptation of the model parameters (Pankoke, 2003).

Additionally, it is possible to define posture variations that depend on the driver himself or that can vary during long driving distances. CASIMIR has the potential to consider a lordotic or kyphotic bearing of the lumbar spine. Thereby, it is possible to model a concentrated or a more relaxed posture of the driver on the one hand and investigate the influence of common lumbar support systems of seats on the other.

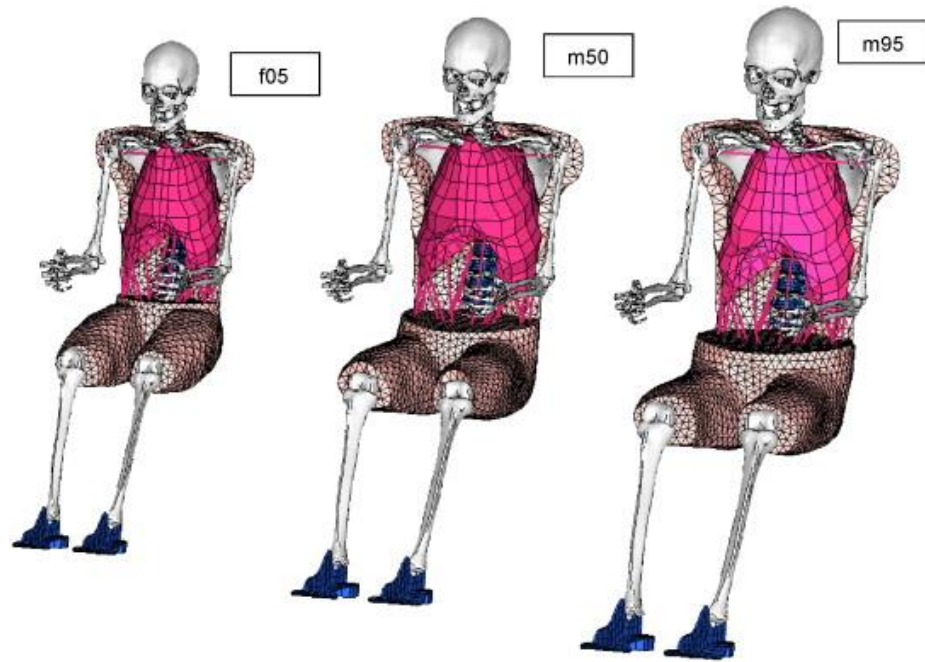


Figure 21. CASIMIR family—f05—m50—m95 (left to right)

Chapter 4.

Numerical vs. Experimental Study

Seating comfort is becoming increasingly important. Higher demands on the performance of vehicles and the comfort-related physical complaints by professional drivers have led to an increasing demand for more comfortable cars. Car manufacturers use comfort as an item to distinguish themselves from their competitors. However, the development and introduction of a new, more comfortable car seat or interior is time consuming and costly. The use of computer models of human and seat could facilitate this process.

In the early stages of the design process a new design can be tested for its degree of comfort by computer simulations with models of the human and the seat. This allows manufacturers to speed up the design process of a new (car) seat or interior and reduce costs. To bridge the gap between the subjective feeling of comfort and the prediction of the comfort level of new designs by virtual testing, a relation has to be defined between that subjective feeling and objective parameters. Pressure distribution was proposed as an objective measure for (dis)comfort prediction.

Pressure distribution represents a measure of the load pattern in the contact interaction between human and seat. Several studies showed the relation between a subject's personal sensation of comfort and seat pressure distributions. Mean pressure, maximum pressure, the size and symmetry of the contact area are parameters most widely reported in the investigation of seating (dis)comfort.

A combination of measurements of seat pressure distributions with virtual testing tools can be very useful and any established relation between (dis)comfort and pressure distribution can be used as a basis for prediction of (dis)comfort by virtual testing. A finite element model of the human body i.e. CASIMIR can be used to predict the interface pressure. Measurements of seat pressure distributions can be used for verification of the model for interface pressures. In combination with a finite element model of a seat, both models could provide insight into changes in contact interaction between human and seat due to variations seat properties.

The objective of the present chapter is the simulation of driver sitting to evaluate the seat pressure distribution. Furthermore, a validation study is performed based on seat pressure distributions measured in volunteer experiments.

Numerical Study

For a realistic reproduction of static seating under gravity loading, an appropriate contact definition between the seat and the driver is essential, whereby the effects of friction must be considered.

The interaction between the CASIMIR and the foam surface is defined by two independent contact pairs, backrest and back on the one hand and cushion and buttocks on the other hand. The chosen algorithm is a so called “master–slave contact”, where internal variables are created for each node of the slave surface. The applied Lagrange multipliers are discontinuous, as a “hard” contact formulation is chosen. The computation of the contact problem is carried out by considering the friction by a coefficient of 0.2.

The pre-analysis positioning of CASIMIR, i.e. in the pre-processor, is carried out in two steps: First, the posture of CASIMIR is synchronized with the posture of the seat.

This is defined by the opening angle between the backrest and seat cushions (correlation angle of cushion/angle of backrest inclination). In order to define the posture of CASIMIR, two kinds of information are required. The first set of positioning data is come from experimental instruction which are called posture definition (Figure 22), and the last one is called seat characteristics coming from seat cushion and backrest inclinations.

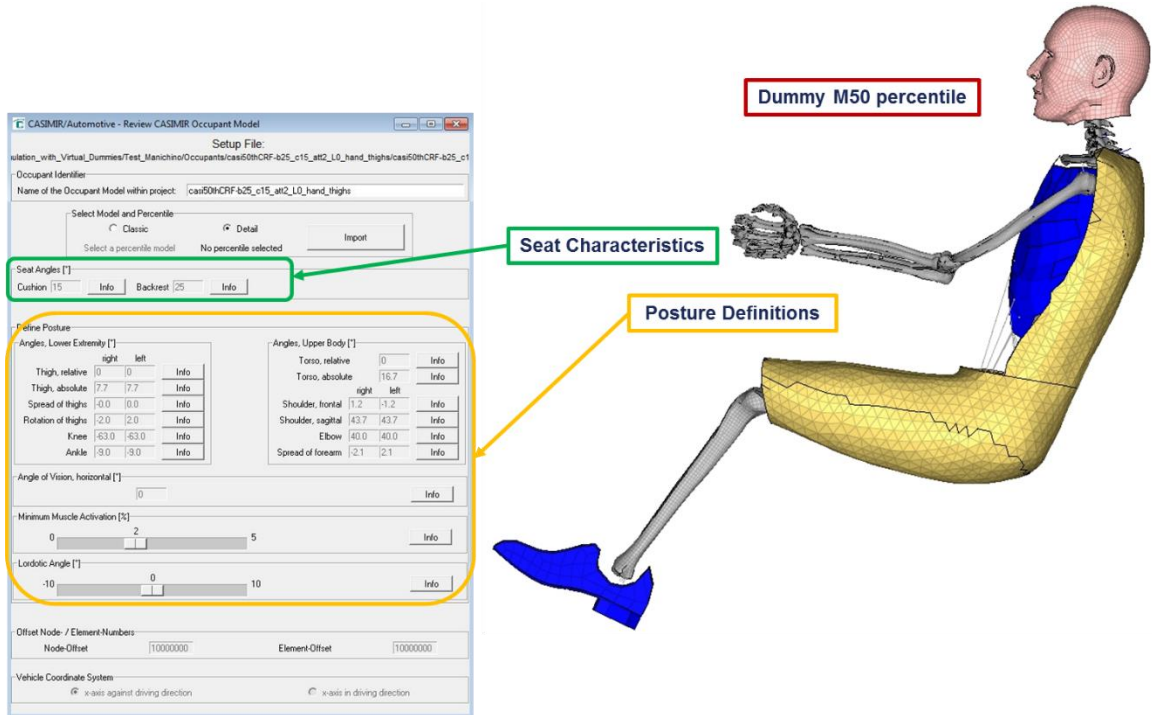


Figure 22. CASIMIR posture definition

Second, considering the fact that seat is usually generated in the vehicle coordinate system, the occupant position must be adjusted. The CASIMIR model is positioned levitating above the seat with disappearing interspaces to the cushion or backrest (Figure 23).

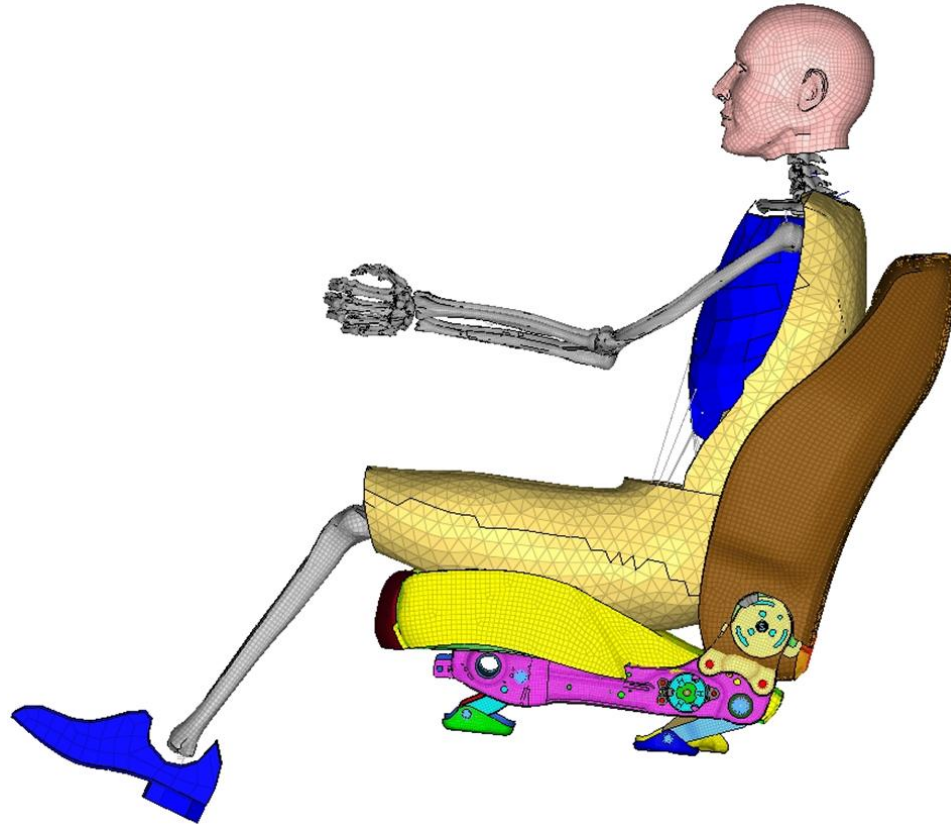


Figure 23. Positioning of CASIMIR with respect to seat

The computation of the seating process is carried out under gravity loading in the negative z-direction. Due to the fact that static sitting procedure could be considered as the quasi-static problem, *Implicit solution* is used. STEP definition for static simulation combines the load out of gravity with the horizontal positioning load on the backrest. The horizontal load is used only to make convergence more probable in the first 0.1 second of virtual time. Therefore, as the positioning is carried out at the beginning, the positioning load F_{hor} is increased up to 100% at the virtual step time of 0,1 and decreased to 0 at 0,4. It is observed in figure 24 that gravity load is increasing linearly over the step.

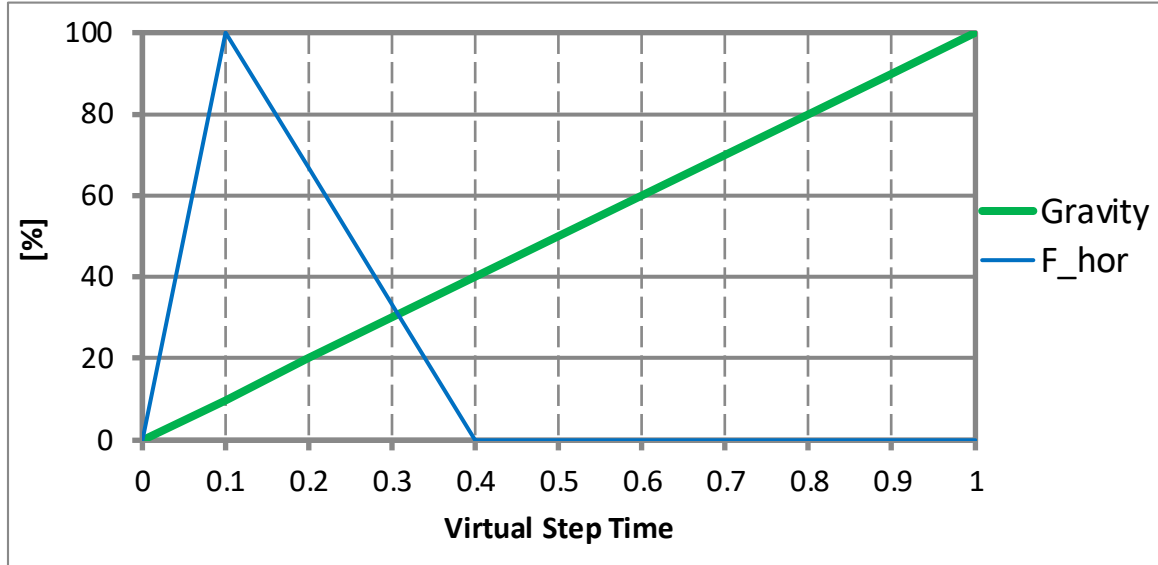


Figure 24. STEP definition

As a result of the large displacements caused by the compliance of the foam cushions, the simulation is geometrically nonlinear. The seat structure is fixed at the restraint points of the seat rail. The boundary conditions of the occupant model reproduce real possible movements. Accordingly, feet and hand movements are defined by the operation environment, that is, e.g. a translation of the feet in the x-direction (movements footwell) as well as a rotation of the hands around the y-axis (hold steering wheel) is possible. Furthermore, position of heels with respect to the footboard (a plate which simulates the position of pedals) is adjusted by CONNECTOR MOTION keyword in ABAQUS.

The main results of the static simulation are:

- Displacement in the z-direction on the seat cushion

- Displacement in the x-direction on the backrest
- Location of the hip joint
- Contact pressure on the seat cushion
- Contact pressure on the backrest

The pressure distributions of the cushion and the backrest are the most important evaluation values in static seating comfort. Recently, they have increasingly become part of more development specifications for seats the Tier-1 suppliers have to meet. Early-phase prediction is possible with static seating simulations.

Figure 25 shows contact pressure results with CASIMIR, m50 percentile of a car driver seat.

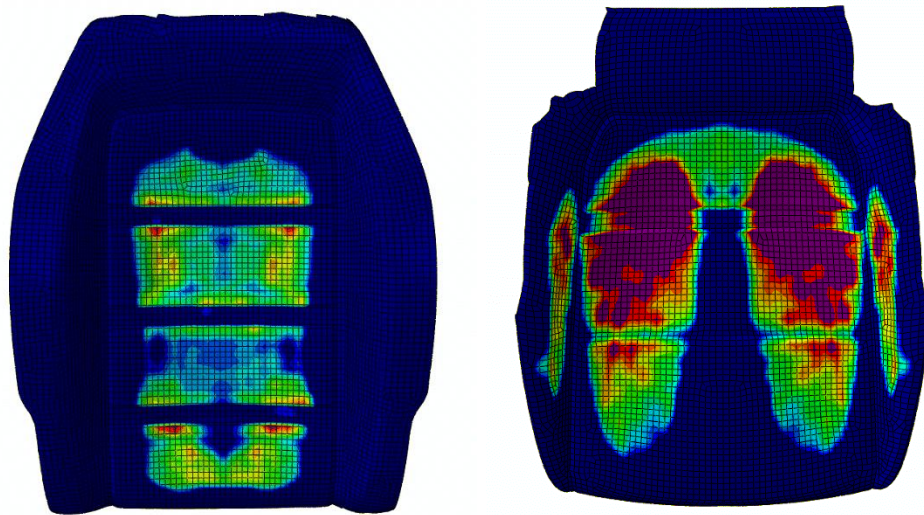


Figure 25. Pressure distributions of backrest (left) and cushion (right)

Numerical results displayed that maximum contact pressure is placed under the seating bones.

Experimental study

The pressure distribution is achieved by means of short term experiments. These experiments focus on the seat cushion and backrest. The test collective consists of six subjects. The average height of the subjects is 175 cm (standard deviation 2.3 cm). The weight is in average 76.5 kg with a standard deviation of 6 kg. The body heights and weights of the test subjects are visible in table 2.

Table 2. Experimental test subjects

50%ile	Weight [Kg]	Height [cm]
1	71	176
2	74	178
3	84	173
4	74	177
5	74	171
6	88	177

It is worth to say that subjects have conventional anthropometric data close to m50 percentiles as well as numerical dummy.

During subjects sitting on the seat the pressure distribution is taken by a pressure mat. The sensor which was used in order to measure experimental interface pressure is PX100 series of Xsensor products. The X3 PX100 series of sensors are designed as a conformable and durable sensor for measuring interface pressures. These capacitive sensors were initially designed for medical applications in rehabilitation seating and have since been more widely used in automotive seating, aerospace, research, and product

design. The PX100 series of sensors are known for accuracy, durability, and repeatability.

Table 3 displays the physical and sensing characteristics of PX100:36.36.02 sensor which is used to measure experimental pressure distributions.

Table 3. PX100:36.36.02 characteristics

Sensing & Physical Characteristics	
Sensor Technology	Capacitive Pressure Imaging
Pressure Range	0.14-2.7N/cm ²
Spatial Resolution	12.7mm
Accuracy	±10% full scale
Sampling Frame Rate	45frames/s
Total Area	62.2cm×62.2cm
Sensing Area	45.7cm×45.7cm
Thickness	0.08cm

The most key features of PX100:36.36.02 pressure mat are as follows:

- High-resolution sensors with a 12.7 mm pitch (resolution) and 1,296 sensing points (i.e. 36*36 cells)
- Very good repeatability
- Low hysteresis and consistent data
- Designed for comfort and healthcare pressure seating applications
- Durable sensor that conforms well to surfaces with a proven track record

Figure 26 shows the pressure mat which is used for experimental measurements.

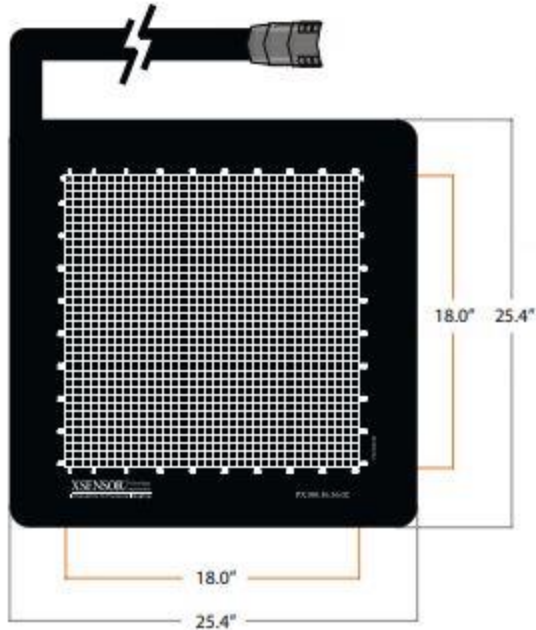


Figure 26. PX100:36.36.02 pressure mat

The subjects were asked to adjusted the seat so that it would be possible for them to drive a car in this setting. After this the subjects stood up and the pressure mat for the seat pan was placed on the seat. The subjects sat down on the mat again and resumed the standard posture based on experimental procedure. Then, the pressure was recorded with the PX100 sensor. Figure 27 shows Body Pressure Distribution (BPD) comes from experimental measures for six different subjects. Pressure values are presented in a graphic form using Excel program; the “warmer” the color is, the bigger the pressure.

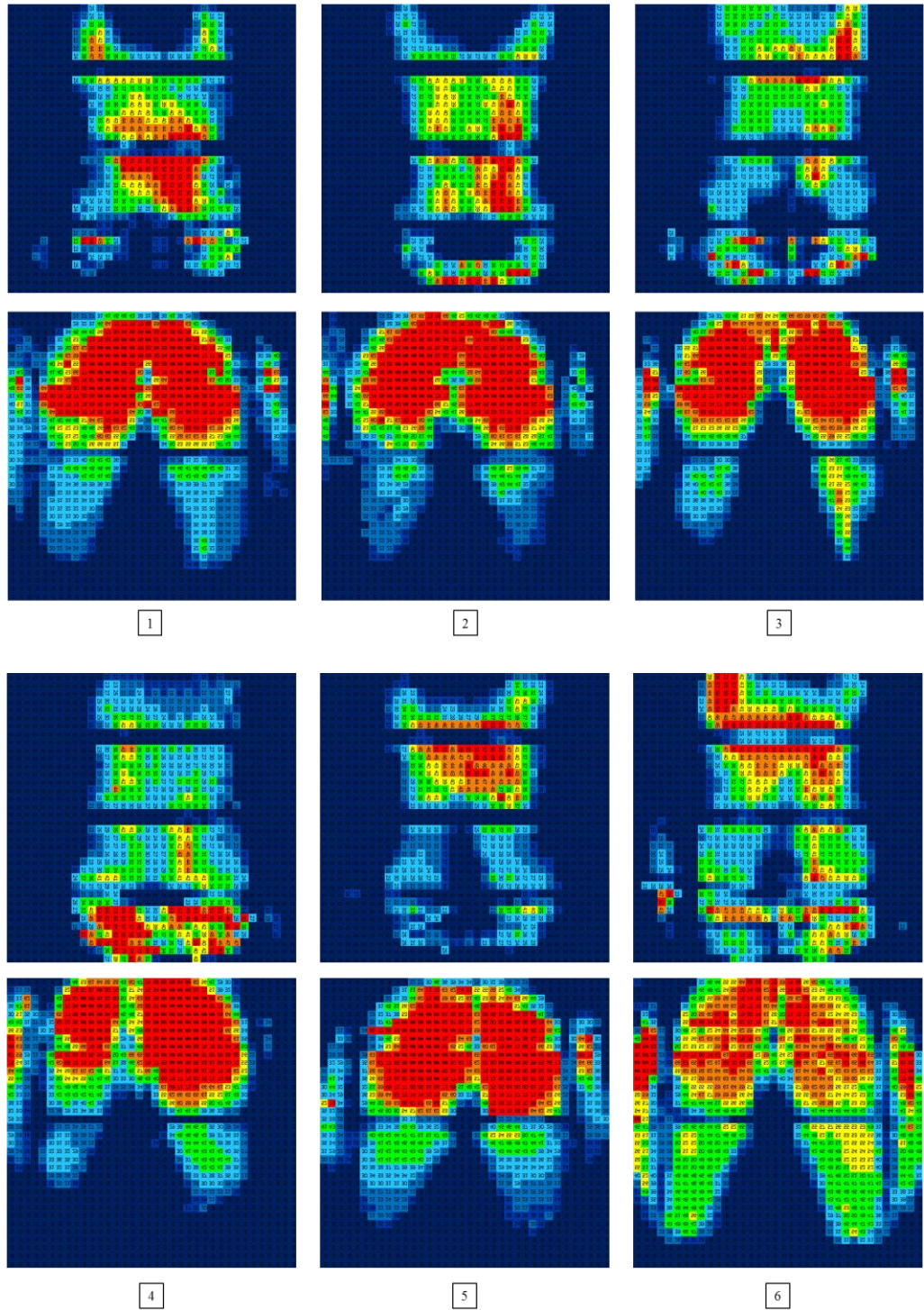


Figure 27. Experimental body pressure distribution (BPD)

The body parts are arranged symmetrically to the spine. Therefore, it can be assumed that the pressures are also symmetrically and the same for corresponding body parts (for example left and right buttock). In reality the pressures vary in some case considerable for instance pressure distribution in the cushion corresponding to subject number four. This can be caused by:

- Test subjects are leaning on one side
- The left and the right leg is bent differently caused by accelerator or clutch pedal

Furthermore, as it is observed in figure 27, the lateral part of backrest for most subjects shows the contact pressure which suddenly reduced to zero which is not reasonable. To cancel out the effect of mentioned unacceptable contact pressure a small correction has been carried out for body pressure maps.

However, based on table 2 subjects number two and four have the conventional anthropometric data so close to each other, mean pressure values for cells greater than zero in cushion are equal to 52.92 [gr/cm²] and 57.09 [gr/cm²] respectively. Corresponding differences could result from subjects' posture.

While degree of freedom in posture of subjects are constrained based on experiment procedure, still there are significant differences in leaning of subjects. Hence, in order to relieve those effects, body pressure distributions have been symmetrized as displayed in figure 28. It is worth to say that symmetrizing of the body pressure distribution (BPD) has been done by other literature (Mergl et al. 2006, Siefert et al. 2008) as well.

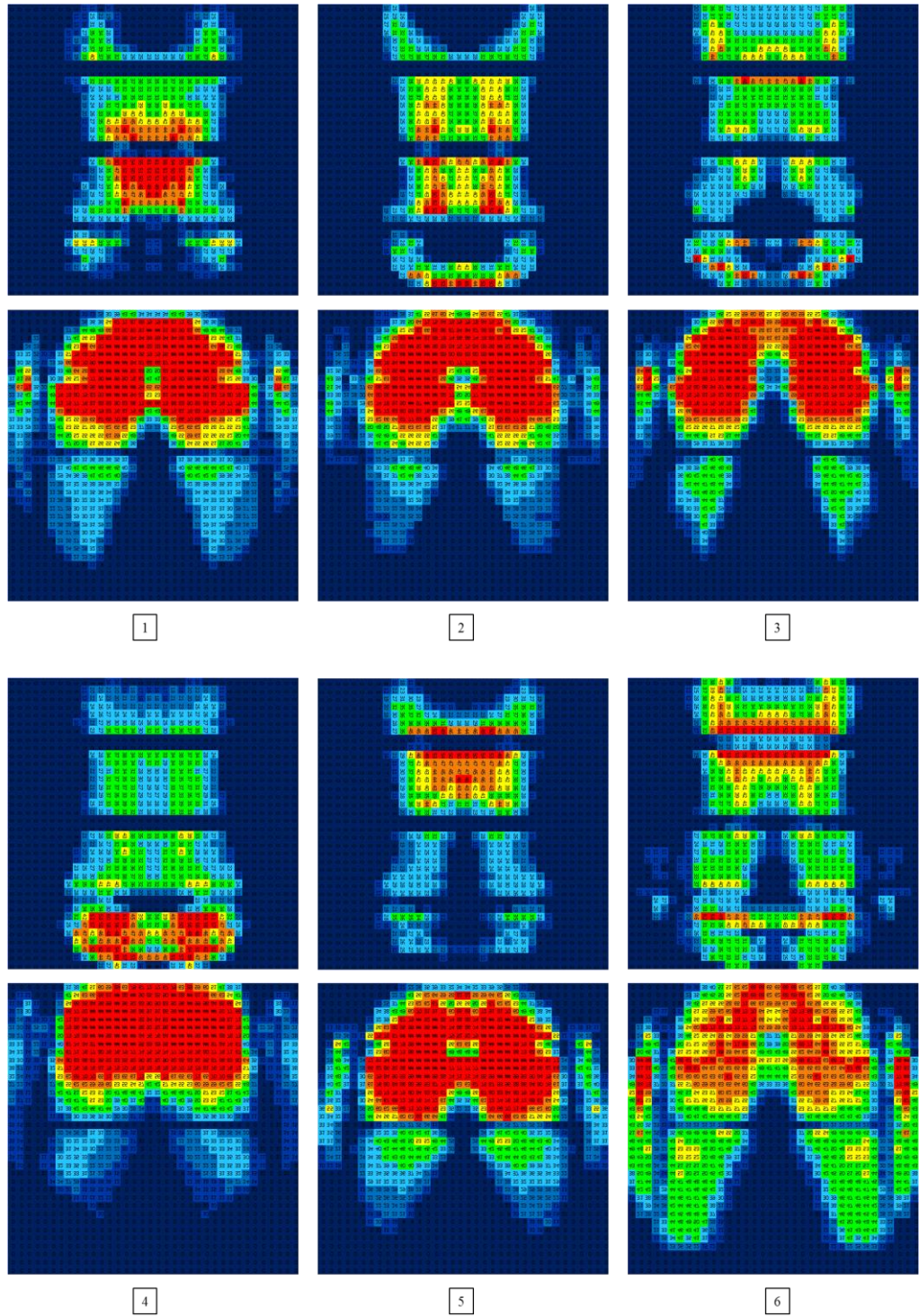


Figure 28. Symmetric body pressure distribution (BPD)

Correlation

In this section, the correlation study for numerical and experimental body pressure distributions is carried out. The pressure data is analyzed in relation to the body map used by Mergl 2006 (figure 29). The seat pan is divided into eight body parts: buttocks left and right, middle of thighs left and right, front of thighs left and right and side support left and right. The zoning plan is shown in Table 4. Here “BP” represents body part, “V” vertical direction and “H” horizontal direction. An example on how to read the table is given by body part ten (buttock left side): The size of this body part is 34% of the length of the thigh and 40% of the width of the hip.

Table 4. Zoning of the body map

BP	10	11	12	13	14	15	16	17
V	34	34	100	33	33	100	33	33
H	40	40	10	40	40	10	40	40

In order to analyze the experimental pressure data according to body parts, a grid is placed over the matrix of the pressure with the classification of the body map. Then the body map is adapted in length and width to the size of the test subject. Afterwards the grid is aligned to the pressure distribution: the maximum pressure under the ischial tuberosities has to be in the body parts ten and eleven and the grid has to be centered laterally over the pressure distribution. This analysis is implemented within an Excel program.

After the correct superposition of the grid over the pressure distribution the program computes automatically several parameters out of the pressure distribution. In each body part the following parameters based on the work done by Mergl (2006) were computed:

- Percentage of load: the total load in the body part divided through the total load on the whole seat pan.
- Maximum pressure: this is the peak pressure in the concerning body part.
- Mean pressure: this is the mean value of all sensors in the concerning body part.

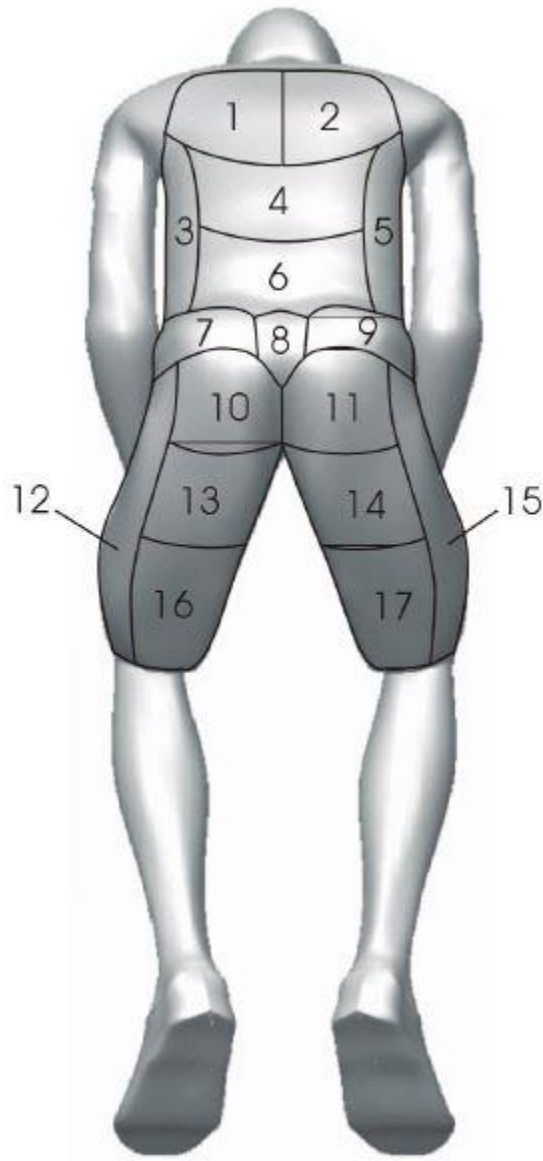


Figure 29. Body map (Hartung 2006)

In order to correlate numerical results with experimental ones, the same language must be used. It means that same objective parameters corresponding to each body parts must be extracted from the numerical results. Hence, The Virtual X-sensor which is a virtual grid with 36 by 36 cells is used. Virtual Xsensor is a mathematical matrix whose arrays are implemented by the values of numerical contact pressure at different nodes (figure 30). The position of the reference point for cushion and backrest is determined according to experimental procedure. The pathway of translating data from ABAQUS output file to consistent way like real pressure mat is shown by figure 31. The right image shown in figure 31 is the translated numerical BPD (Body Pressure Distribution).

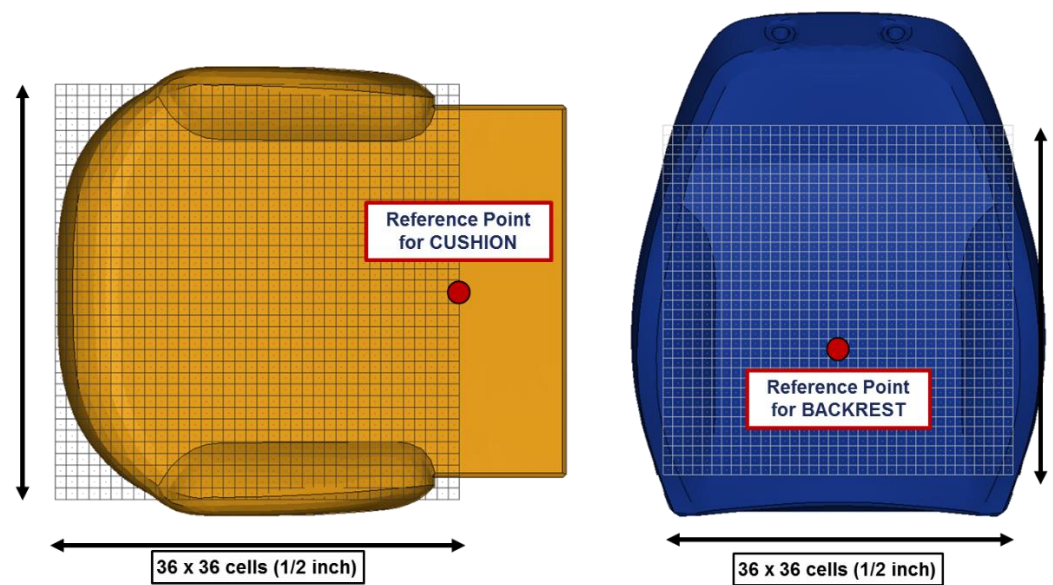


Figure 30. Virtual Xsensor

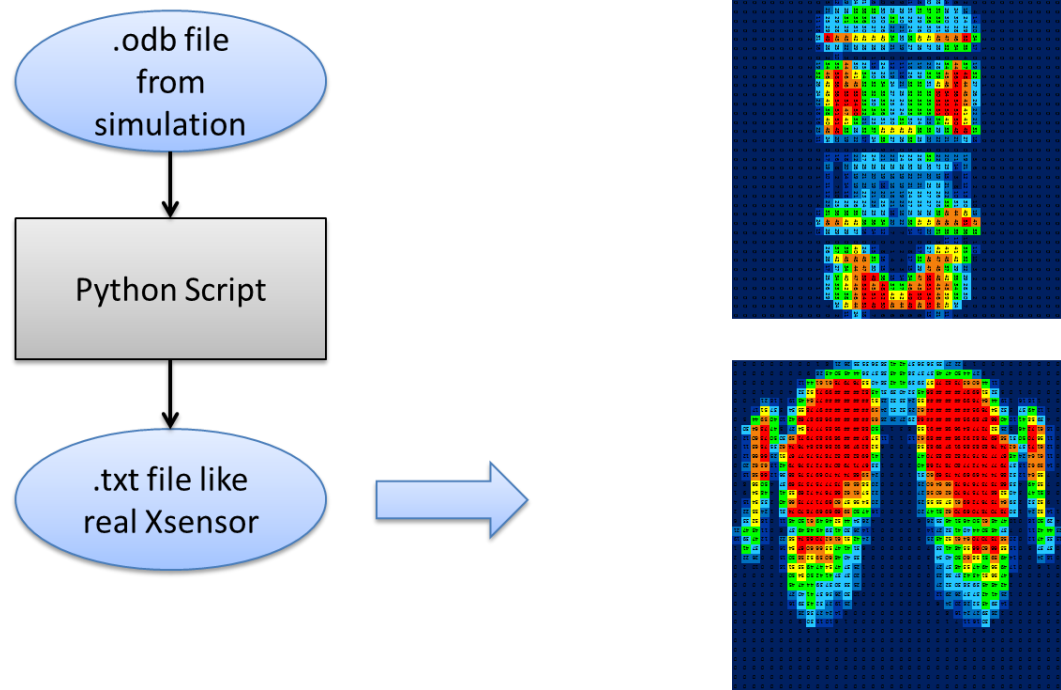


Figure 31. Flow-chart of virtual Xsensor creation (left) and numerical BPD (right)

Thereafter, the definition of the rule for correlation is required. As it is observed in figure 32, the experimental mean BPD has a significant difference specially in backrest with respect to each subject itself. In another word, using of the experimental mean BPD as a tool for correlation is not a wise strategy. The defined rule in this study expresses that if the value of objective parameters is between the corresponding maximum and minimum values, it would be correlated. Hence, the spider graph is used in which value of the objective parameter for each subject is displayed on the principle lines. Then the lines passed through the experimental maximum, experimental minimum and numerical one are drawn. If the numerical closed loop is inside the range between experimental maximum and minimum, the objective parameter is correlated (Figure 33-38).

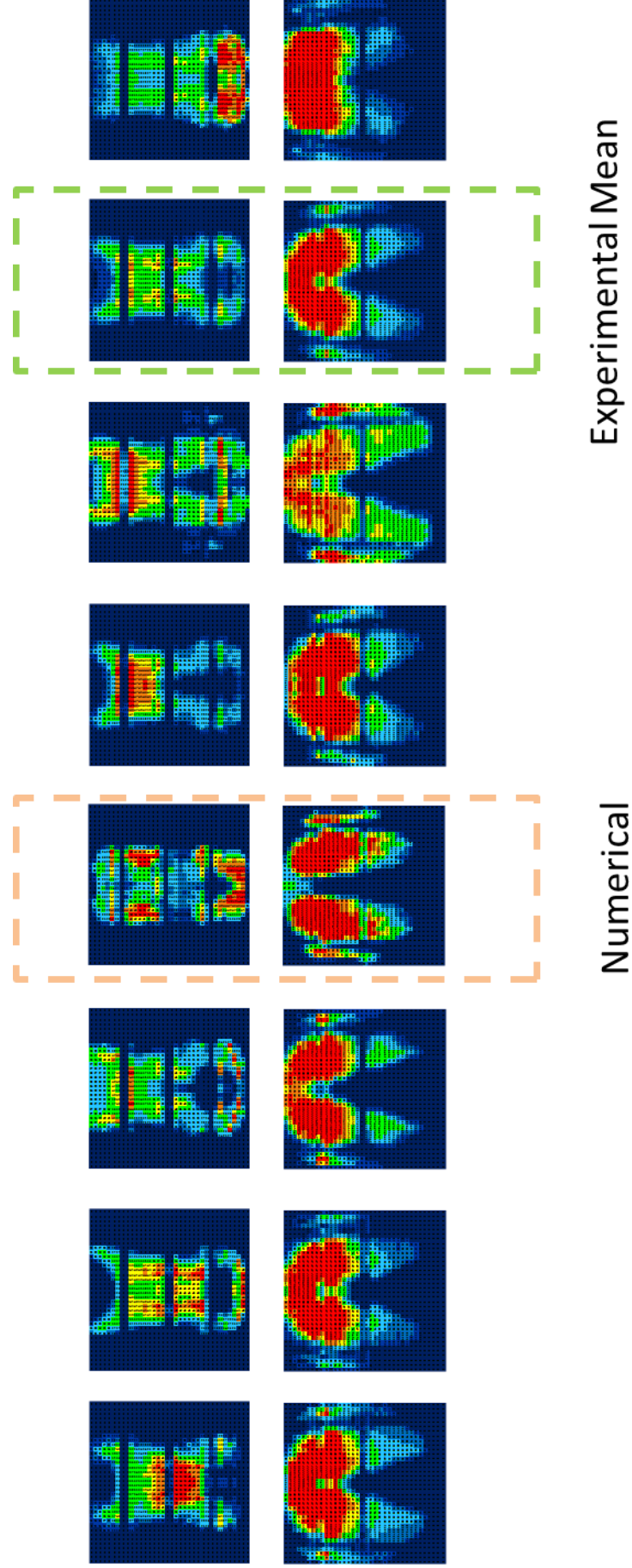


Figure 32. Comparison of experimental mean BPD and subjects' BPD

Figure 33-35 show the spider graphs for Maximum Pressure, Mean Pressure and Load Percentage in the cushion respectively, as the objective parameters used in different body part. It is observed that the maximum pressure and mean pressure for different body zones in the cushion are completely inside the range which means that numerical results are correlated with experimental ones in different body zones for those objective parameters (Figures 33-34). The load percentage variable is correlated for six different body parts in the cushion and only thigh zone (i.e. zones 13 and 14) is slightly larger than the corresponding experimental maximum value. As the summation, 22 parameters out of 24 are correlated which means the level of correlation is around 91%.

Same objective parameters are considered for the backrest. Figures 36-38 display that the percentage of correlation is around 88. The out of range parameters in the backrest are so close to the experimental maximum values. As it is displayed by figure 36, maximum pressure in the shoulder zone (i.e. zones 1 and 2) is larger than the corresponding experimental maximum value. It must be highlighted the degree of freedom of subjects for backrest posture is higher than the cushion due to the fact that the buttock pressure mostly is derived by gravity and it is less effective regarding to the posture. In contrary, the contact pressure in the backrest is more affected by posture. Therefore, the small difference in numerical contact pressure of shoulder zone with respect to experimental BPD could come from the posture influence.

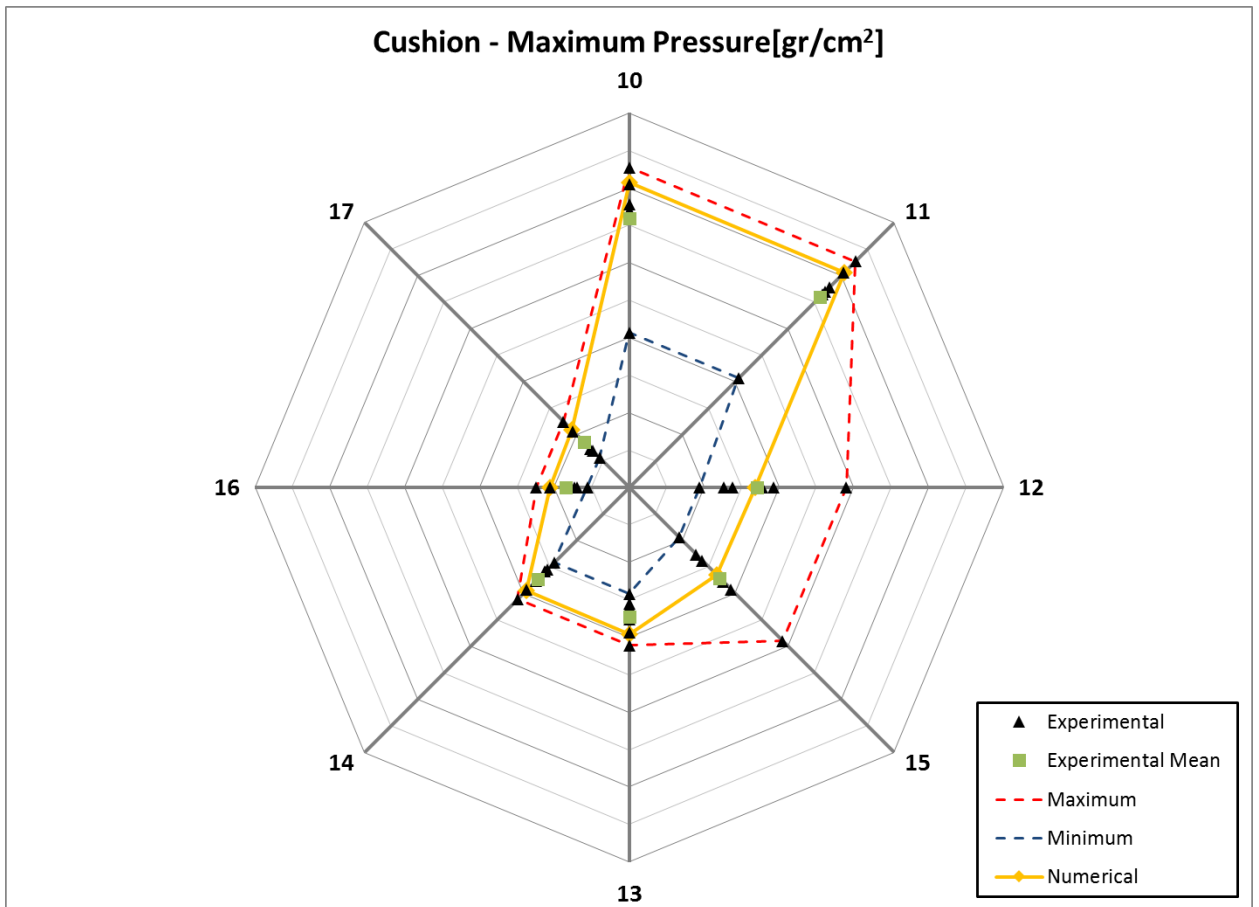


Figure 33. Maximum pressure spider graph for the cushion

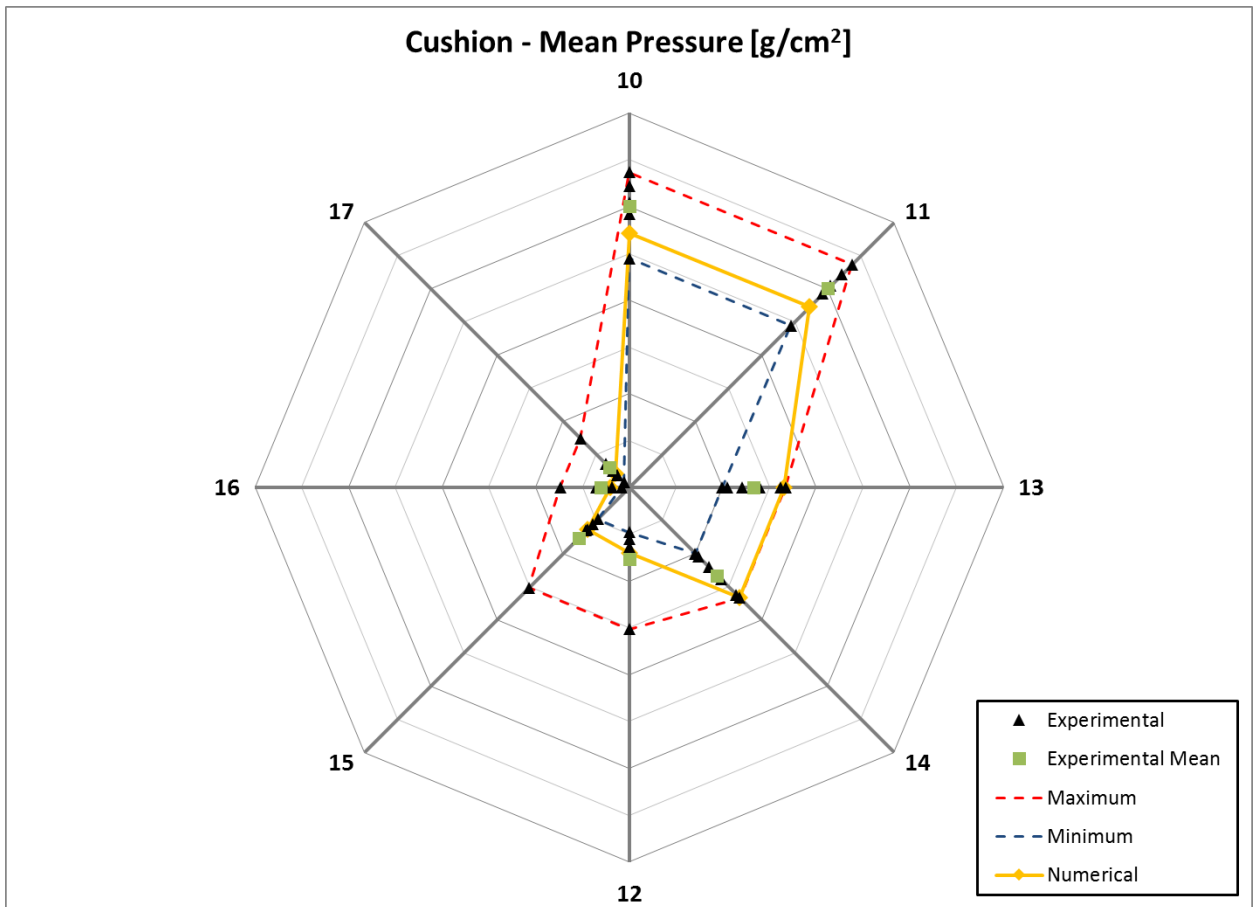


Figure 34. Mean pressure spider graph for the cushion

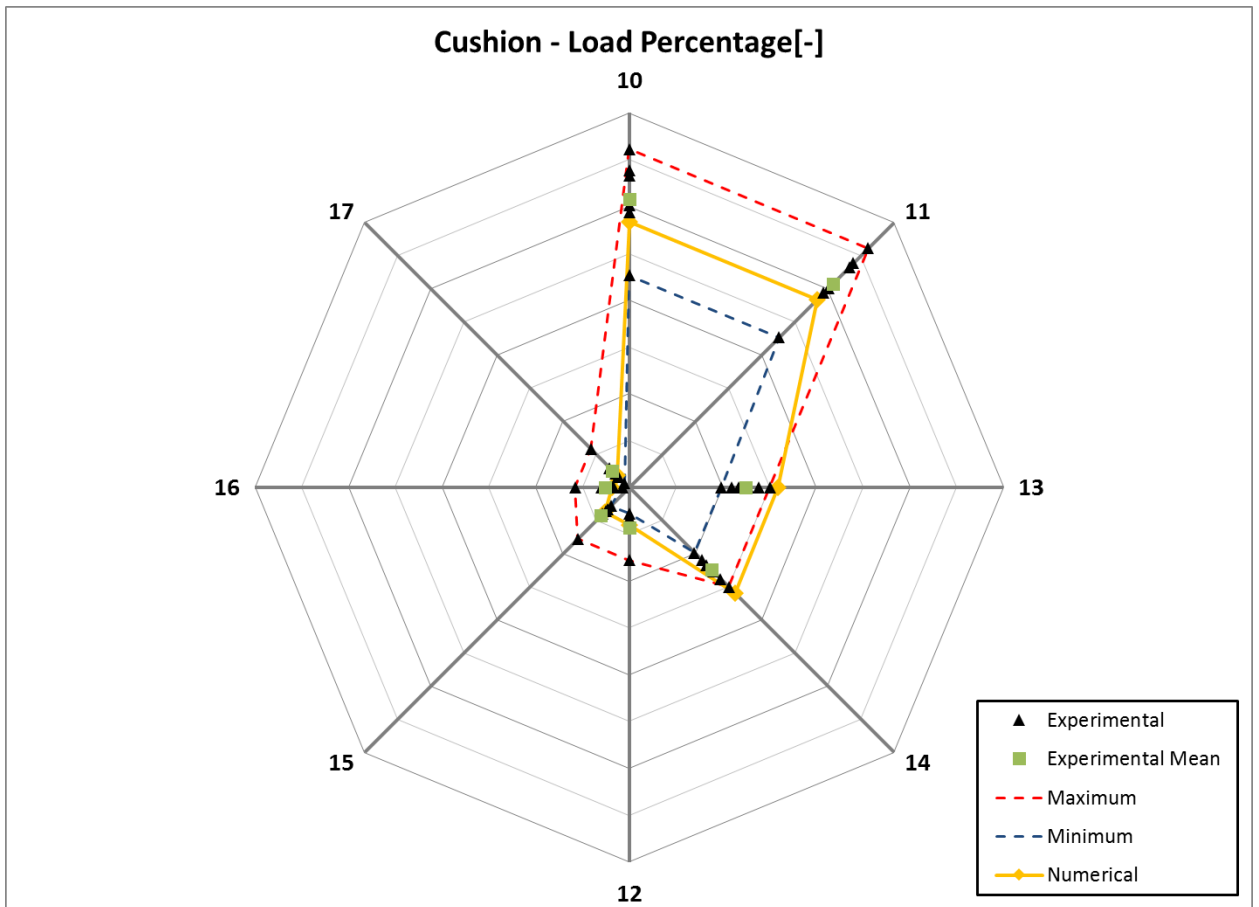


Figure 35. Load percentage spider graph for the cushion

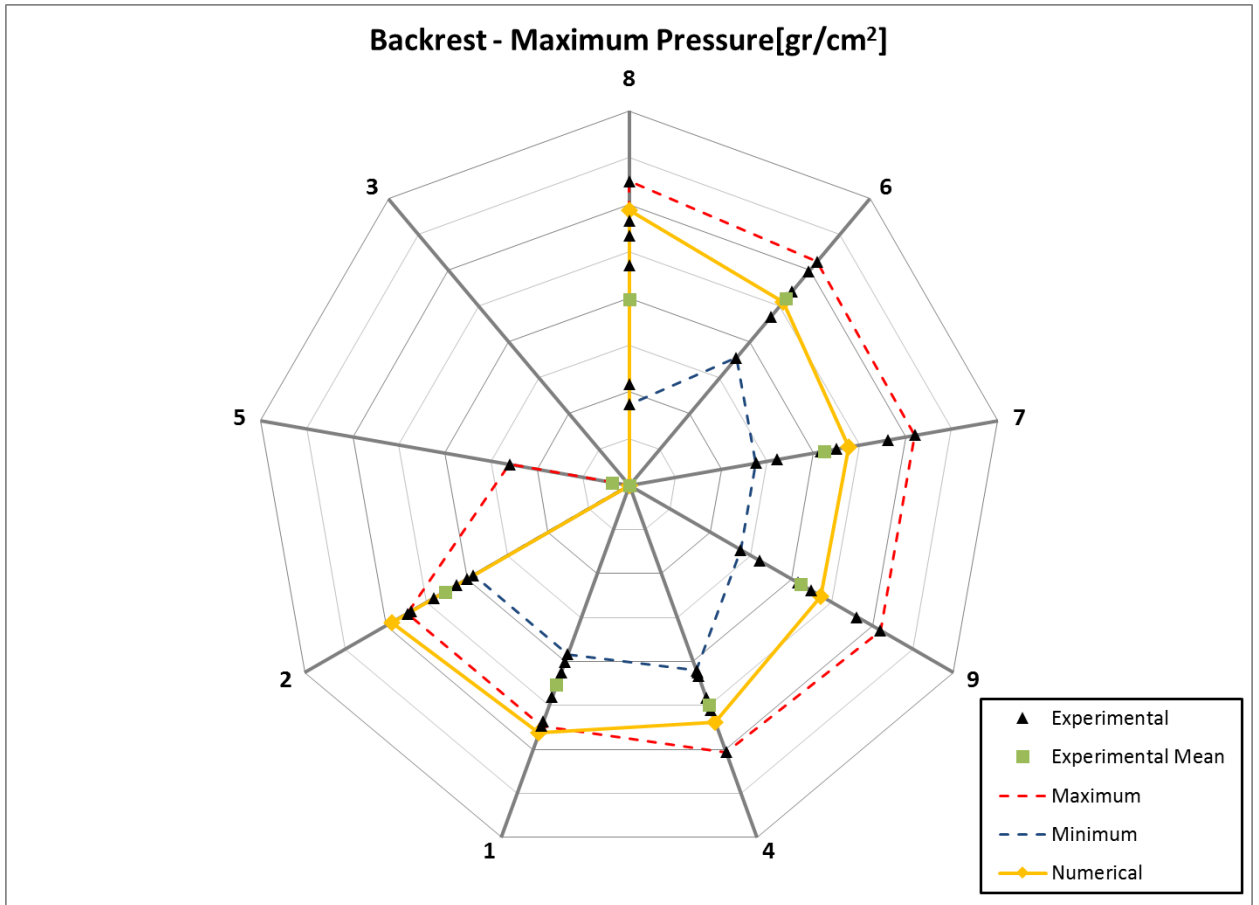


Figure 36. Maximum pressure spider graph for the backrest

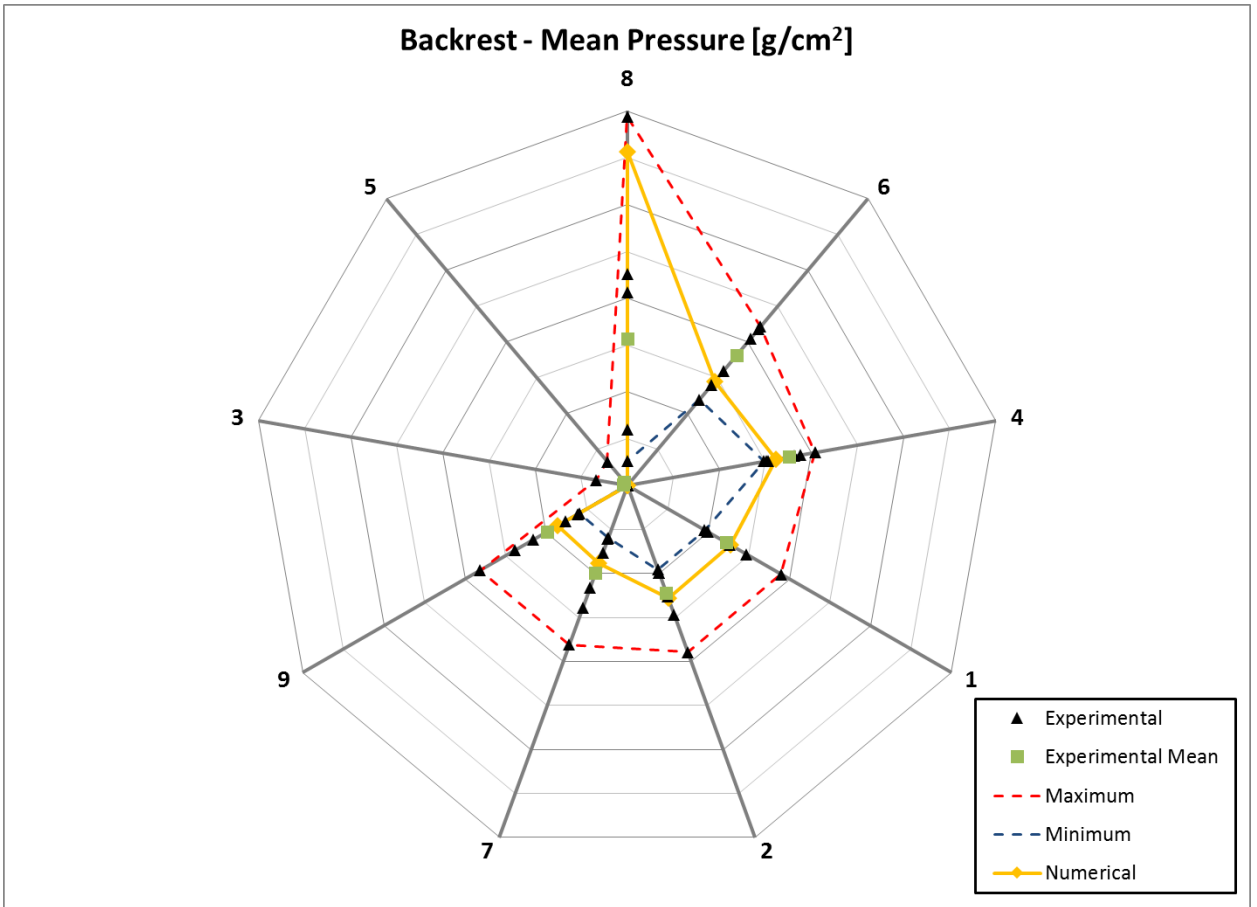


Figure 37. Mean pressure spider graph for the backrest

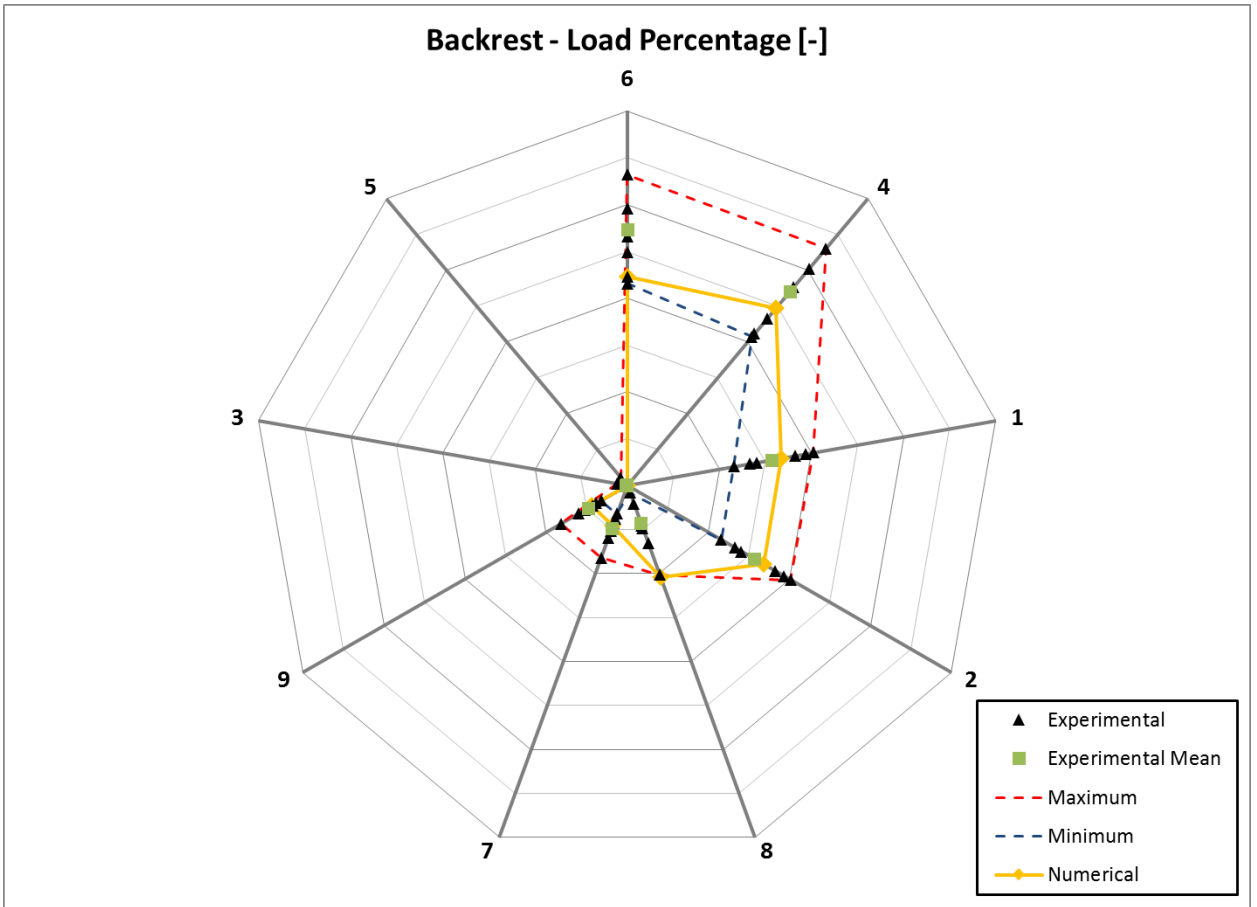


Figure 38. Load percentage spider graph for the backrest

Chapter 5.

Virtual Optimization

The term comfort has been used several times in current thesis. The meaning of comfort as described in literature is very broad with very diverse definitions. It is often not difficult for a person to describe whether a seat sits fine or not. However, it is hard to define how or why something is comfortable. Hertzberg (1972) and Shen & Vértiz (1997) defined comfort by the absence of discomfort. Slater (1985) defined comfort by the state of pleasure influenced by psychological, physiological and physical factors. Some researchers go further: they state that comfort can be divided into levels and introduced comfort scales. Others state that comfort and discomfort may concern two sides of one scale, having various levels, not only for discomfort, but also for comfort.

On the other hand, Zhang et al. (1996) and de Looze et al. (2003) state that comfort and discomfort may be associated with different factors and should be expressed on different scales. According to this definition, discomfort is underlined by physical factors. Exposure, dose and response are main factors. On the other hand, comfort concerns feelings of relaxation, pleasure and well-being. From this point of view, it can be expected that the relationships between objective parameters with discomfort would be stronger than for comfort (first step Figure 4), as the link between discomfort and objective measures is more direct.

Therefore, there seems to be a diversity of views on comfort expressed in literature. One common view, however, is that comfort is a subjective parameter influenced by psychological, physiological and physical impressions of the environment on a person. In the present thesis, this has been the basic assumption when the term comfort is used. This definition of comfort suggests a number of contributory physical aspects like vision, noise, thermal factors, vibration, seating, and posture. In the current thesis, the focus is on mechanical parameters. Since these mechanical parameters are more related to discomfort than to comfort (Zhang et al., 1996; de Looze et al., 2003), it basically means that in this thesis the application of virtual simulation for investigation of *discomfort* is described.

The previous chapter described the validation of numerical results and showed that the virtual simulation via objective parameters can predict the discomfort perception. In this chapter, firstly the effect of the seat characteristics on the objective parameters presented by Mergl 2006 is studied. Thereafter, the Response Surface Model based on input variables is extracted. Finally, Virtual Optimization of output variables is carried out in order to optimize the pressure distribution based on multi-objective optimization approach.

The discomfort criteria presented by Mergl 2006 are summarized in table 5. As it is expressed by table 5, he found the strong relation between the discomfort feeling and objective parameters in the middle of thigh (i.e. zone 13/14) and the acceptable relation for the maximum pressure and mean pressure in the buttocks (i.e. zone 10/11). Based on Mergl discomfort criteria, all parameters show relevance for the prediction of discomfort. Not a single parameter can predict the discomfort but the combination of all is needed to interpret pressure distributions. This fact can be illustrated by the example of sitting on a needle. If

one has a seat on which the distribution of load is according to above mentioned results but he is sitting on a needle the subject will of course feel discomfort.

Table 5. Discomfort guidelines (“green” strong relation, “blue” acceptable relation, “orange” weak relation, “-“ no relation); (10/11 buttocks, 13/14 middle of thigh, 16/17 front of thigh, 12/15 sideways, 1/2 shoulder, 4 upper back, 6 lower back, 8 coccyx, 7/9 lateral iliac crest)

	Body parts	% of Load [%]	Max. Pressure [kPa]	Mean Pressure [kPa]
Cushion	10/11	24.5-28.5	< 20	5.5 - 6.5
	13/14	< 14	<7	< 4
	16/17	< 3	-	< 0.2
	12/15	-	-	-
Backrest	1/2	-	2-7	-
	4	20-50	2-7	-
	6	20-30	2-7	-
	8	-	> 0	-
	7/9	> 0	2-7	-

As discussed in Chapter 2, various seat characteristics can affect pressure distribution whilst sitting. Different shapes of cushions lead to different pressure distributions. Not much studies investigated the effect of cushion material on comfort and discomfort of seats.

Kyung and Nussbaum (2008) found significant effects of different seats on pressure variables, such as average pressure on buttock and thigh, peak pressure on buttock and

thigh, and contact area on buttock and thigh. This may be due to the different dimensions of the tested seats, but may also be caused by different shapes and cushion materials. According to Reed et al. (2000), cushion length is an important determinant of thigh support. A cushion that is too long can put pressure on the posterior portion of the occupant's legs near the knee. Pressure in this area will lead to local discomfort and restrict blood flow to the legs. This is supported by Mergl (2006), who defined the ideal pressure distribution for car driver's seats. He showed that comfort is rated high when there is an ideal pressure distribution under the legs and buttocks. Additionally, Hostens et al. (2001) found that a smaller backrest inclination angle leads to higher sub-maximum pressures on the seat pan and smaller sub-maximum pressures on the backrest. However, Park et al. (2013) did not find significant effects of car driver's seat height (determined by occupant package layout) on pressure distribution of lower-body parts (i.e. buttock and thighs).

However, some studies have been carried out regarding the influence of seat characteristics on the interface pressure, still there exist no clear correlation between them. In order to clarify the correlation between interface pressure and seat characteristics, *input variables* and *output variables* should be defined. The output variables are the objective parameters defined by Mergl 2006 for different body zones as expressed in table 5. Regarding the input variables in the current thesis, cushions' material, convexity and concavity of cushions' surface, length of the cushion and angle of seats' bolster are taken into account.

Design of Experiment – DOE

The aim of the DOE is to establish an experiment to study a process. The process could be interpreted as a physical test or numerical modeling. As a general approach, the mentioned processes are designed and conducted so that the planned and targeted variation applied to the input parameter(s) lead to extract desired information for analysis of output parameter(s).

The main principles of DOE are randomization, replication and blocking. These three principles act in a supportive manner. They complete each other to increase the precision of the experiment. Precision of experiment is threatened by either extraneous errors or systematic error due to nature of the experiment.

By randomization, in fact one tries to be sure that the entire input parameter domain is surveyed. The goal of randomization is to guarantee that the entire domain has the same chance of being examined.

By replication, one tries to be sure that the entire possible scenario between all input parameters is covered. In other words, repeating the experiment with planned decision and controlled condition. Replication with randomization allows the experimenter to predict the error variance. Without randomization, a large number of replication to predict the error variance would be useless. More replication leads to more precise results from the experiment. Blocking means treatment of all desired input parameters by excluding undesired parameters (noises).

It's worth mentioning that since this thesis deals with a computer experiment, there would be no random error, which is very common in physical experiments.

Since one expect to draw a meaningful conclusion from the results, having a proper statistical approach is necessary. Answers to questions such as what is to be studied, how the data are to be collected, how these data are to be analyzed, are essential.

By considering what came before, to establish a DOE with the proper statistical approach, the following guideline is required.

Recognition of the problem. The Experimenter needs to consider all aspect of the experiment as well as goals and possible ideas, which could arise during the experiment. Another aspect is interaction of experiment with other departments, which is considerable, simultaneously.

All possible problems or studies that can be addressed by the experiment should be reflected. Possible problems or studies are about stability and robustness, finding unknown areas of problem, verifying if the system has a similar performance under varied circumstances, optimization and factor screening.

Selection of input parameters (Factors) ranges and levels. Experimenter needs to identify the important input parameters, which has an influence on response parameters. The input identification leads to selection of factors that planned to be varied during the experiment. Design factors are selected, to be studied during the experiment and Constant factors are example of typical classification of parameters.

Hereafter, *factor(s)* identifies the input parameters, over which the experimenter can exercise control and intends to change. It's notable that since one deals with simulation experiments, all the factors are controllable and so noise factors are negligible.

The next step would be selecting the range of the factors. This range should be selected according to specification of the variable. Also the number of levels that each

factor can take to vary needs to be determined. The range and the levels comes from process knowledge. Process knowledge is a combination of awareness regarding theory and the previous practical experience.

Selection of proper design (sampling method). In this step, experimenter decides on sample size (number of experiments) and also selection of proper run order. Also in this step randomization and blocking will be applied on the run methods, if be required. Generally, the sampling method determines how the design points spread out through the domain. Since the sampling method defines the possible combination of input parameters which can occur, it would affect both quality of results and the required time for DOE.

Statistical analysis. Statistical analysis methods are crucial to interpret the data. Furthermore, statistical analysis is used to ascertain the reliability and validity of results.

Generally speaking, in order to perform a DOE, it is necessary to define the problem and choose the variables, which are called factors or parameters by the experimental designer. A design space, or region of interest, must be defined, that is, a range of variability must be set for each variable. The number of values the variables can assume in DOE is restricted and generally small. Therefore, we can deal either with qualitative discrete variables, or quantitative discrete variables. Quantitative continuous variables are discretized within their range. At first there is no knowledge on the solution space, and it may happen that the region of interest excludes the optimum design. If this is compatible with design requirements, the region of interest can be adjusted later on, as soon as the wrongness of the choice is perceived. The DOE technique and the number of levels are to be selected according to the number of experiments which can be afforded. By the term levels we mean the number of different values a variable can assume according to its

discretization. The number of levels usually is the same for all variables, however some DOE techniques allow the differentiation of the number of levels for each variable. In experimental design, the objective function and the set of the experiments to be performed are called response variable and sample space respectively.

In this study, *modeFRONTIER* is used as a tool to implement sensitivity analysis by design of experiment (DOE). The sensitivity analysis is done by workflow showed in figure 39.

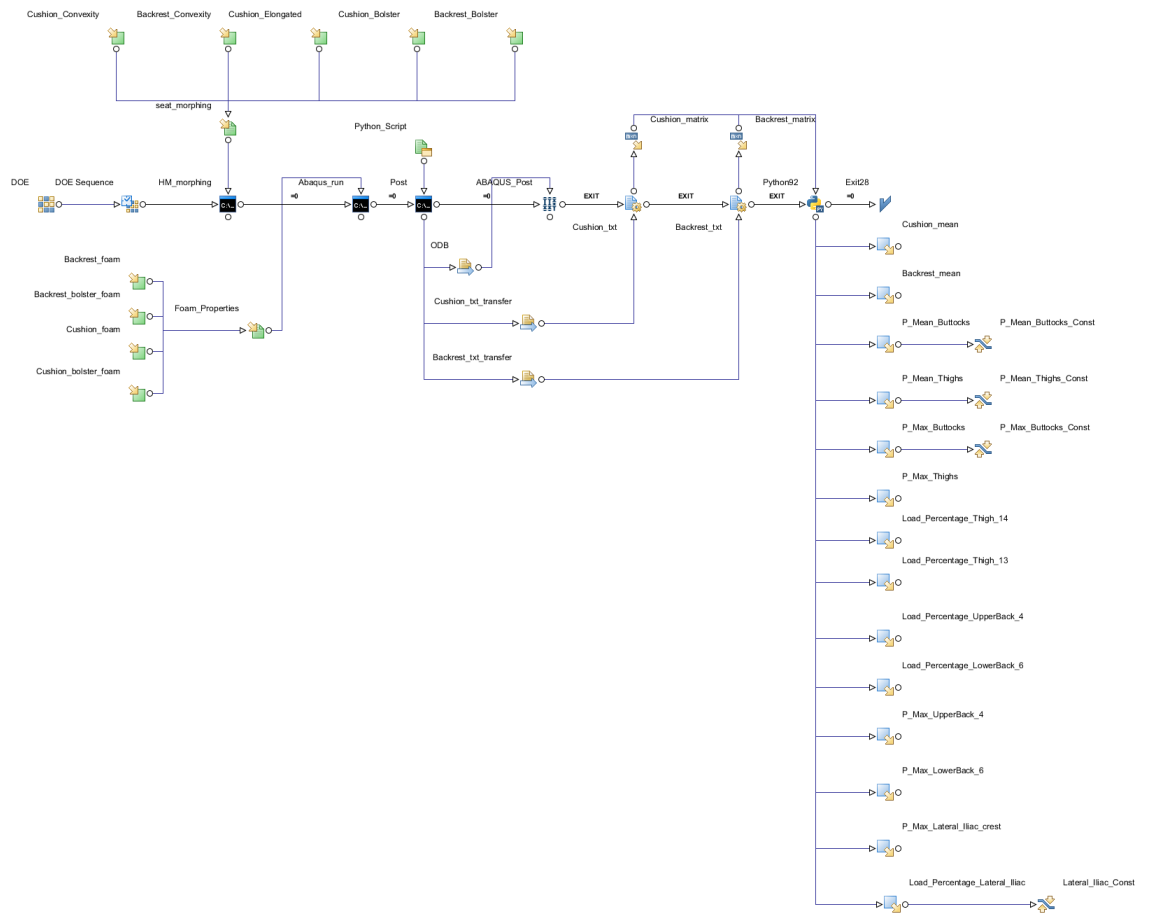


Figure 39. workflow at modeFRONTIER for sensitivity analysis

As it is observed in figure 39, the seat characteristics (i.e. cushions' material, seat shape and seat dimension) are considered as the input variables, and the objective parameters presented in table 5 as the output variables. The characteristics of DOE used for sensitivity analysis are summarized by Table 6.

Table 6. DOE characteristics

DOE Algorithm	Reduced Factorial
Number of levels	2
Number of experiments	64
Input variables	Cushion insert foam Backrest insert foam Cushion lateral foam Backrest lateral foam Cushion length Cushion surface profile Cushion bolster angle Backrest surface profile Backrest bolster angle

The main advantage of factorial DOE algorithm is the giving quantitative estimation of the influence the factors, or the interaction of the factors, upon the response variable. As the number of parameters increases, a full factorial design may become very onerous to be completed. The idea of the *Reduced Factorial* design is to run only a subset of the full factorial experiments. Doing so, it is still possible to provide quite good information on the main effects and some information about interaction effects.

It is worth to say that the range of variation in the bolster angle is $\pm 10^\circ$, in the cushion length is ± 20 mm. For the surface profile of backrest and cushion, the maximum

value of convex profile in the backrest and cushion are 10 mm and the minimum value of concaved surface profile in backrest is 10 mm as well. The concaved surface profile for cushion is not considered because of design limitations which causes some problem in the durability of seat cover.

The material database which could be used was consisted of 17 different Polyurethane foams. In order to reduce the computational efforts, the foam which had more or less same stress-strain curve, one of them have been considered. By this means, the range of variation in the materials is from 1 to 12 in which the ascending order means increase of foam stiffness (Figure 40). Hence, foam ID01 is the softest foam and foam ID12 the hardest one.

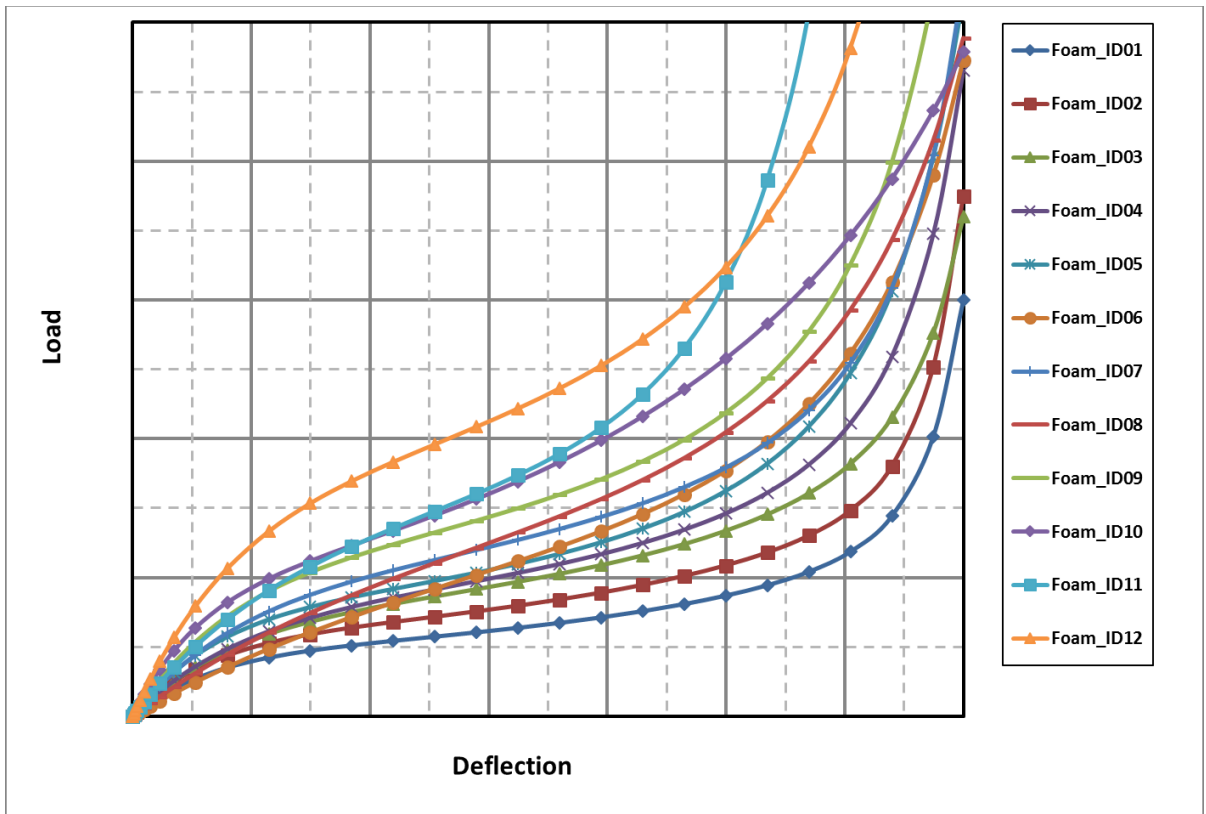


Figure 40. Different cushions' material used for DOE analysis and virtual optimization

Results

Correlation matrix is the advantageous classical statistical tool, which evaluates the correlation coefficient between a pair of variables. The range of correlation is from +1 to -1, which reveals the strength of correlation. Zero value means lack of correlation. In another word, a correlation coefficient close to -1 means that the variables in a pair are inversely correlated; a correlation coefficient close to 1 means that the variables in a pair are directly correlated, while a correlation coefficient close to 0 means the two variables are not correlated. Figure 41 shows the correlation matrix obtained by DOE analysis. The absolute correlation coefficient higher than 0.3 are filtered to make more visible the strong correlation between input and output variables. The red color in correlation matrix is showing the direct relation and the blue one is inverse relation between a pair of variable.

It is observed that increase in cushion foam stiffness will result in increasing of maximum pressure in buttocks. Moreover, increasing of backrest convexity will reduce the contact of lateral iliac crest and consequently a reduction in maximum pressure and load percentage.

Increase in backrest foam stiffness will cause a rotation of dummy somehow, so that a reduction of mean pressure in buttocks and an increase in the load percentage in thighs observed.

Based on correlation matrix showed in figure 41, elongation of the cushion doesn't show any significant effect on the output, since our dummy is the M50 percentile. But it is most likely to observe its influence on other percentiles i.e. f05 and m95 percentiles.

Values of cushion convexity coefficient is showing that this parameter is not correlated with output, it might be due to the number of level that we considered for

Reduced Factorial method. It may have a parabolic effect on outputs, since we got two levels for input variables, we are restricting the correlation to a linear correlation. For this reason, a study on the number of levels has been conducted but same result was obtained. Hence, the convexity of cushion surface profile has no significant effect on the corresponding objective parameters.

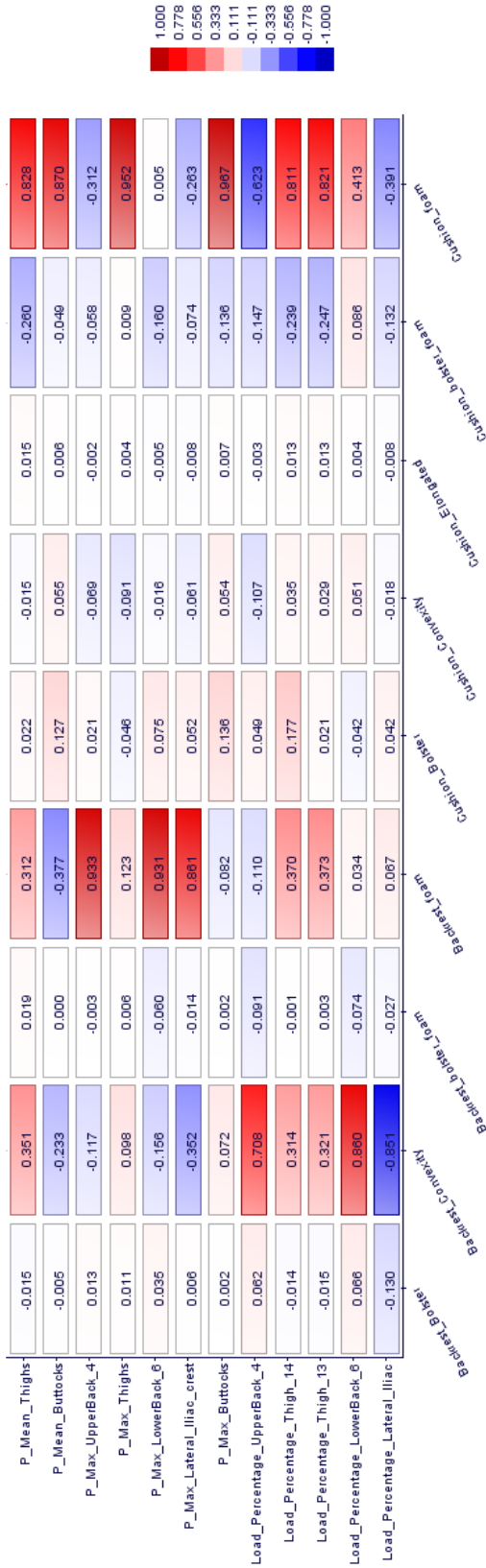


Figure 41. Correlation matrix obtained by DOE analysis

Response Surface Model - RSM

Response surface modelling, or response surface methodology, is strictly related to DOE. The main idea is to use the results of a DOE run in order to create an approximation of the response variable over the design space. The approximation is called response surface or meta-model and can be built for any output parameter. The reason for building a response surface is that, although it is just an approximation, it can be used to estimate the set of input parameters yielding an optimal response. The response surface is an analytical function, thus an optimization based on such a model is very fast and does not require additional experiments or simulations to be performed. Therefore, the use of meta-models can be very advantageous, and can be applied even when little is known about the problem, although it must be kept in mind that if the design space exploration (made with the DOE or the RSM model adopted) is poor, and the response variable is particularly irregular, the result of the meta-model-assisted optimization can be far from the truth because of the bad estimation of the model coefficients or the choice of an unsuitable model.

The DOE is generally followed by the Response Surface Modelling (RSM). We call RSM all those techniques employed in order to interpolate or approximate the information coming from a DOE. Different interpolation or approximation methods (linear, nonlinear, polynomial, stochastic, ...) give different RSM techniques. The idea is to create an interpolating or approximating n -dimensional hypersurface in the $(n + 1)$ -dimensional space given by the n variables plus the objective function.

In current thesis, the objective parameters with the strong and acceptable correlations come from Mergl criteria (i.e. table 5) are considered as the objective function

for creation of Response Surface Model (RSM). Therefore, *Load Percentage*, *Max. Pressure*, *Mean Pressure in Thigh zone* and *Max. Pressure of Buttocks* are defined as the objective functions. All the other values of objective parameters in table 5 are considered as the *Constraints* in the modeFRONTIER workflow. Figure 42 shows the modeFRONTIER workflow which was used to create Response Surface Model or meta-model.

To increase the accuracy of the RSM, the number of samples must be sufficient. In order to interpolate the information coming from the DOE by a polynomial of degree two, the minimum required samples is $\frac{(9+2)!}{9!2!} = 55$. The number of samples coming from reduced factorial algorithm used for sensitivity analysis was equal to 64. Therefore, in order to increase the dimension of design space, the Uniform Latin Hypercube (ULH) DoE algorithm is used.

ULH is a particular case of Latin Hypercube Sampling. ULH is an advanced Random (Monte Carlo) Sampling: more precisely it is a constrained Monte Carlo (i.e. random) sampling scheme. The constraint refers to the way each variable is sampled: the uniform statistical distribution is split in n intervals with the same probability, and then a random value is selected within each interval. In this way the points are relatively uniformly distributed over the variable range. On the contrary, with the Monte Carlo scheme, n values are chosen independently, according to the global uniform density function.

Compared to Random DoE (Monte Carlo), ULH maps better the marginal probability distributions (i.e. the statistical distribution of each single variable), especially

in case of small number of generated designs. ULH algorithm is useful for generating a uniform distribution of points in the input space.

Finally, 100 designs produced by ULH algorithm are added to 64 designs come from reduced factorial algorithm to build the total design space. Training of Response Surface is implemented by 154 samples and the rest is used to validate the accuracy of the meta-model.

Three different RSM techniques; Polynomial SVD, Kriging and Neural Network; are used to interpolate the response variable over the design space. Table 7 summarizes the DOE characteristics to produce design space and the RSM techniques as well.

Table 7. RSM and DOE characteristics

	Algorithm	Number of Designs
DOE	Reduced Factorial	64
	Uniform Latin Hypercube (ULH)	100
RSM Training	Polynomial SVD (degree 2)	154
	Kriging	
	Neural Network	
RSM Validation	Polynomial SVD (degree 2)	10
	Kriging	
	Neural Network	

In order to evaluate the accuracy of the RSM produced by different techniques, two most common parameters i.e. Mean Absolute Error and R-Squared (coefficient of determination) are used. Hence, the RSM produced by a technique which has the lowest value of Mean Absolute Error, and value of R-Squared close to one is considered as the default RSM for virtual optimization.

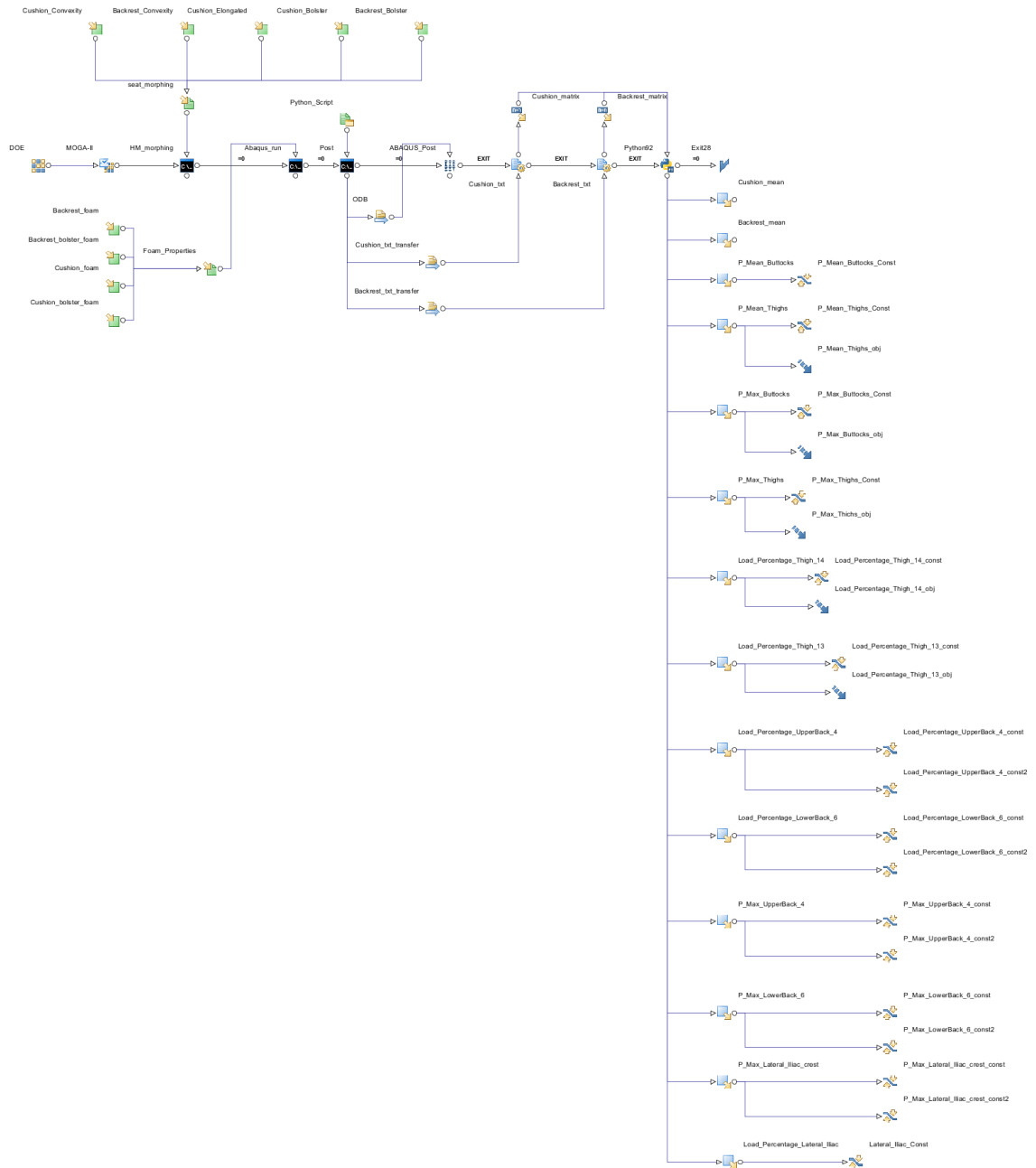


Figure 42. modeFRONTIER workflow used for RSM implementation

It is observed in table 8 that all the Response Surface Model created by Polynomial SVD technique with quadratic polynomial has more accuracy except Maximum Pressure in thigh zone whose approximation by Kriging technique is more precise with respect to other techniques. Then, based on the precise technique for each objective function (showed by green color in table 8), the default RSM for each objective function is defined.

Table 8. Mean absolute error and R-squared comparison for different RSM techniques

Objective Function	RSM Technique	Mean Absolute Error	R-Squared
Load Percentage - zone 13	Polynomial SVD	0.145	0.868
	Kriging	0.177	0.803
	Neural Network	0.209	0.685
Load Percentage - zone 14	Polynomial SVD	0.142	0.898
	Kriging	0.226	0.734
	Neural Network	0.246	0.607
Max. Pressure - thigh	Polynomial SVD	1.1	0.96
	Kriging	0.994	0.949
	Neural Network	1.6	0.899
Mean Pressure - thigh	Polynomial SVD	0.294	0.846
	Kriging	0.404	0.698
	Neural Network	0.49	0.589
Max. Pressure - buttock	Polynomial SVD	1.89	0.964
	Kriging	2.05	0.937
	Neural Network	2.85	0.908

Virtual Optimization

The Multi-Objective Genetic Algorithm (MOGA-II) with characteristics summarized in table 9 is used as the optimization algorithm. Using ULH algorithm a design space contains of 100 experiments is created. Then, 100 generations defined by Genetic Algorithm results in 10000 samples which are evaluated to find the optimum solution.

Table 9. Characteristics of Multi-Objective Genetic Algorithm

Optimization Algorithm	Multi-Objective Genetic Algorithm (MOGA-II)
Number of Generations	100
Probability of Directional Cross-Over	0.5
Probability of Selection	0.05
Probability of Mutation	0.1
DNA String Mutation Ratio	0.05

Due to the nature of multi-objective problems, ranking and selecting between alternatives is a relatively common, yet often difficult task. In order to make ranking and selecting between optimum solutions, Linear Multi Criteria Decision Making (MCDM) is used. The Linear MCDM algorithm calculates the utility function, which is used as the basis for the ranking of available alternatives. The utility function takes into account the weight and the alpha value of the attributes. These parameters can be set by the user, giving them complete control over the definition of the decision-making process.

The weight of each attribute, i.e. its relative importance with respect to other attributes, and the alpha value (in a 0.1-10 range), which reflects the linearity or non-

linearity of the corresponding function are adjusted to 0.2 and 1 (indicates a linear function) respectively (Figure 43).

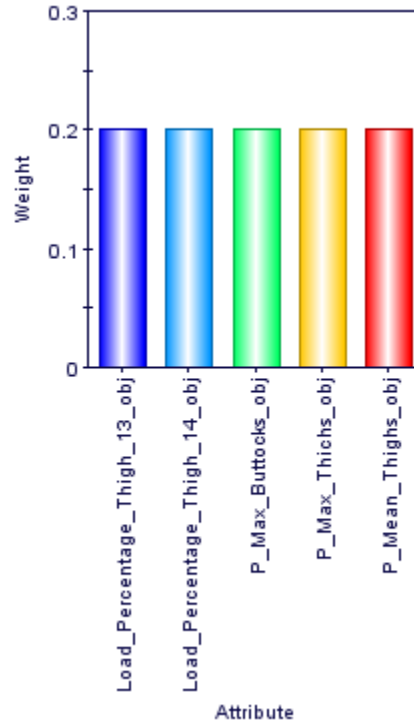
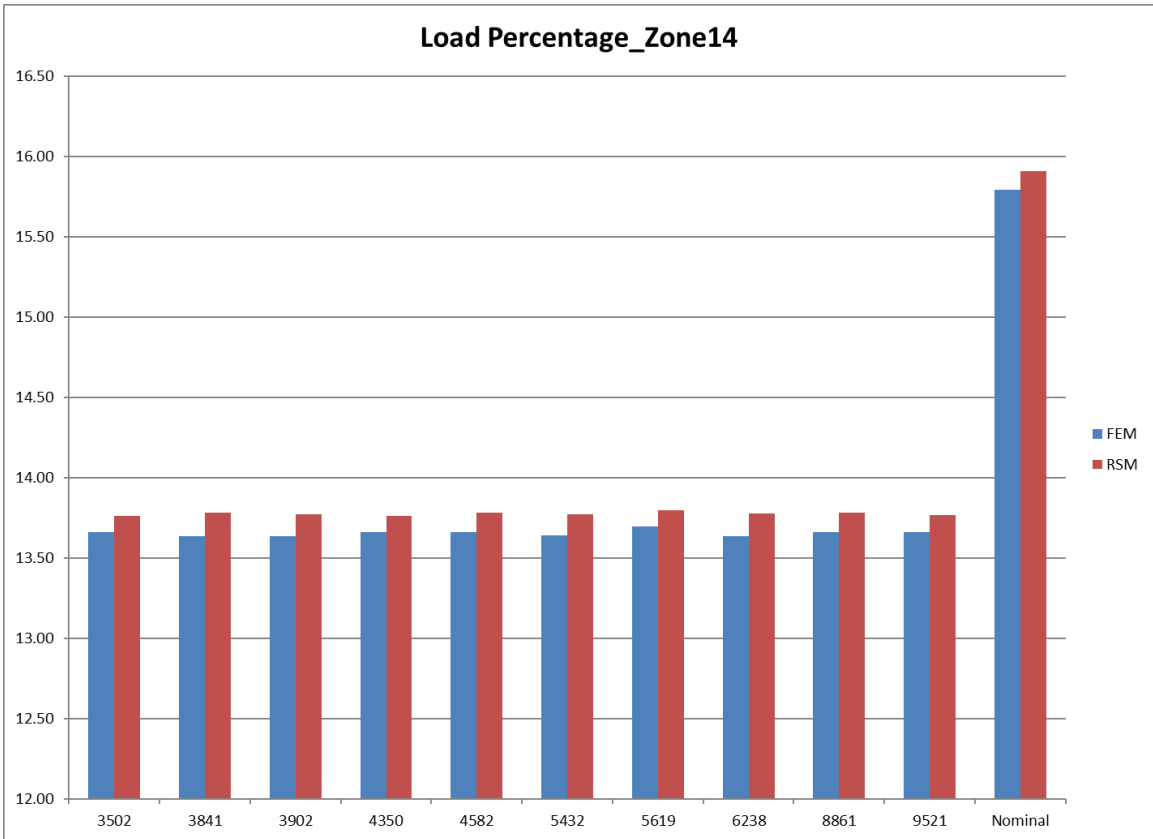
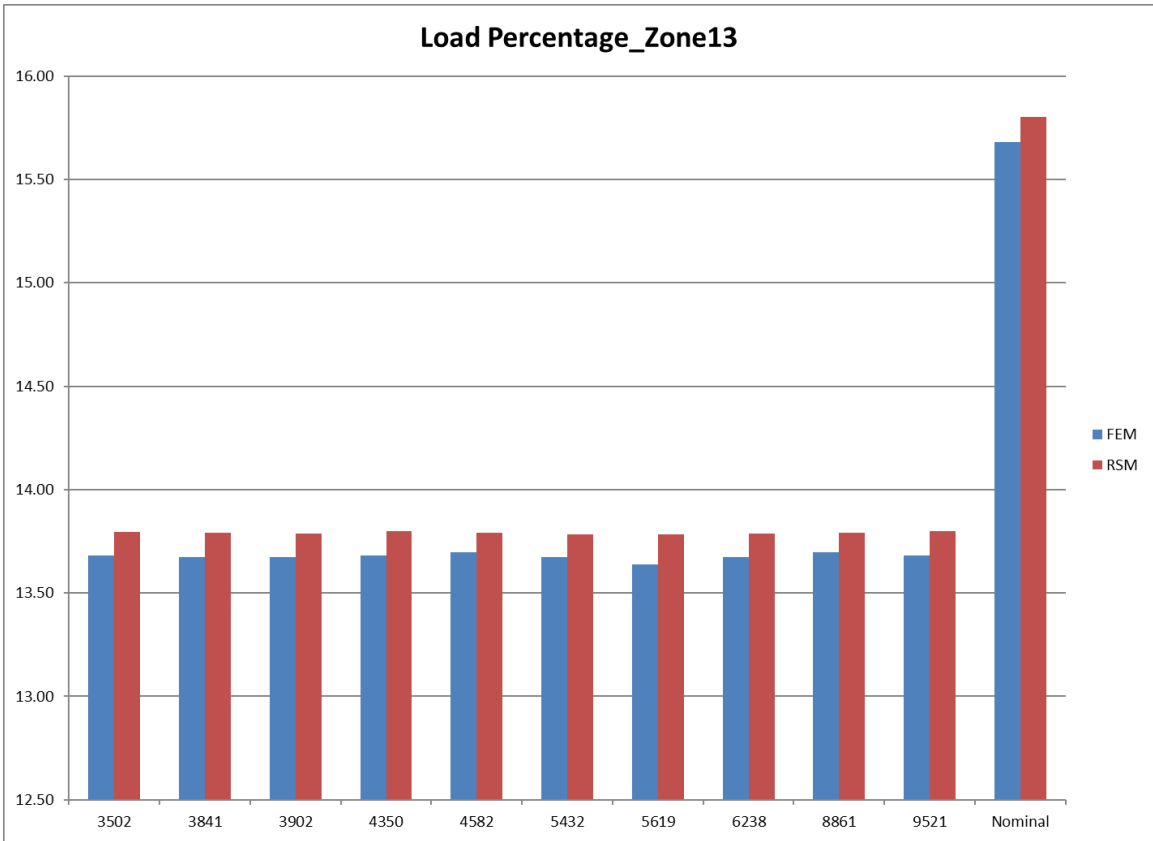
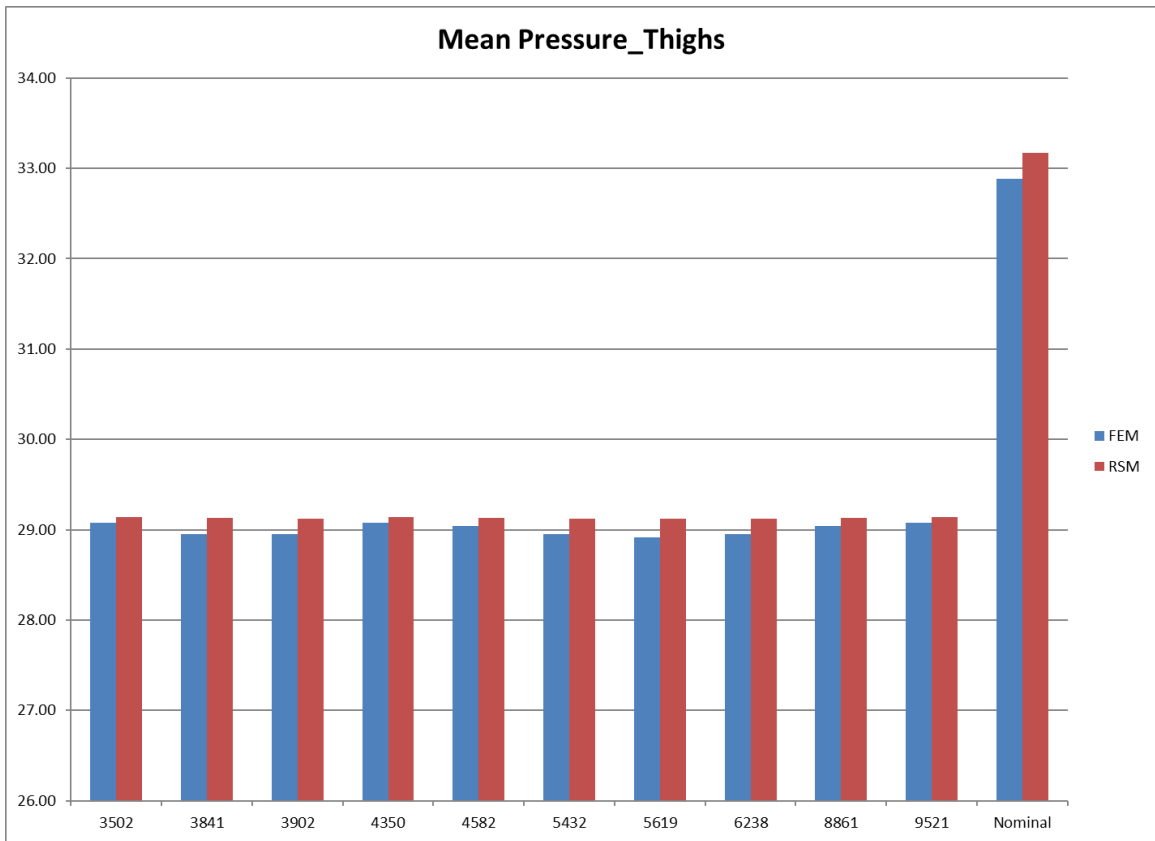
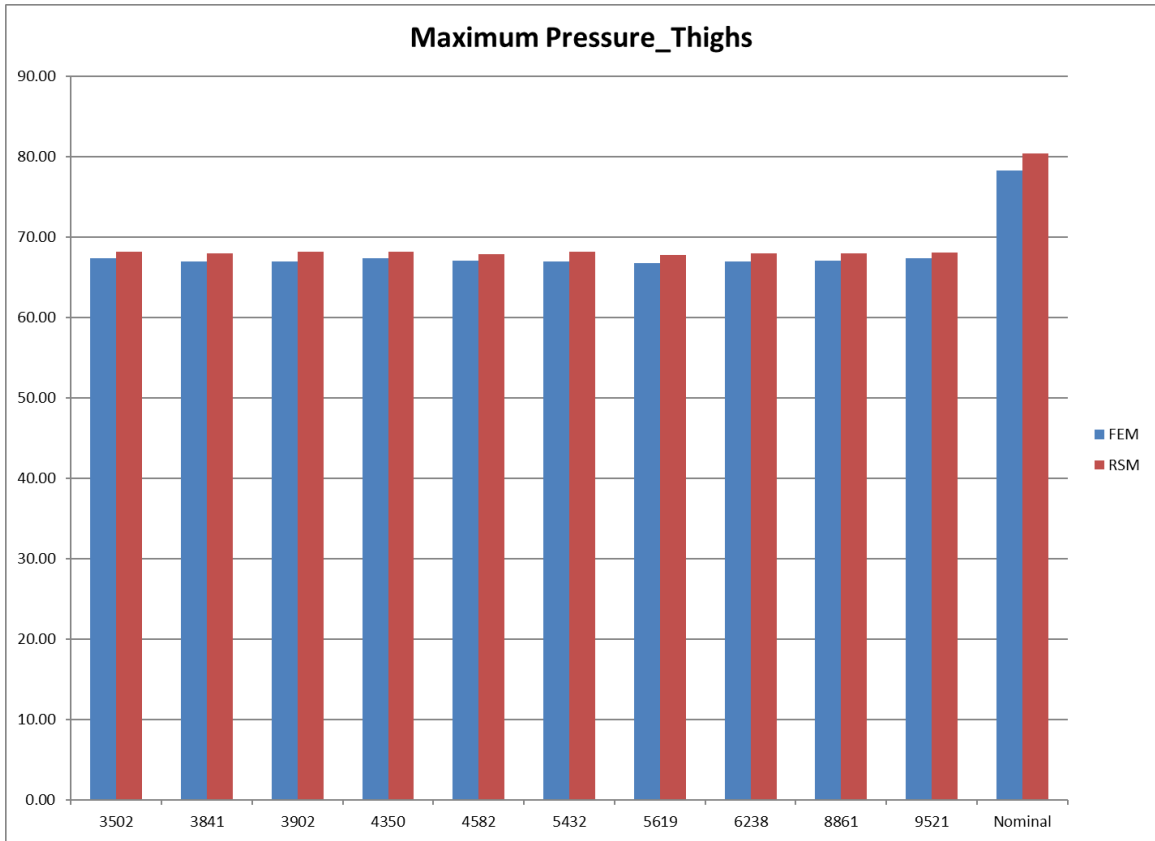


Figure 43. Weight of each objective function

By performing the virtual optimization and Linear MCDM, 10 first optimum results were extracted and the Finite Element Model with corresponding input variables simulated in order to evaluate the level of accuracy. Figure 44 compare the objective parameters resulted from virtual optimization and the FEM which is real one. As it is displayed, the maximum difference between virtual optimum cases and the real one is 1.73% for the Max. Pressure parameter in thigh zone which shows by design ID 5432.





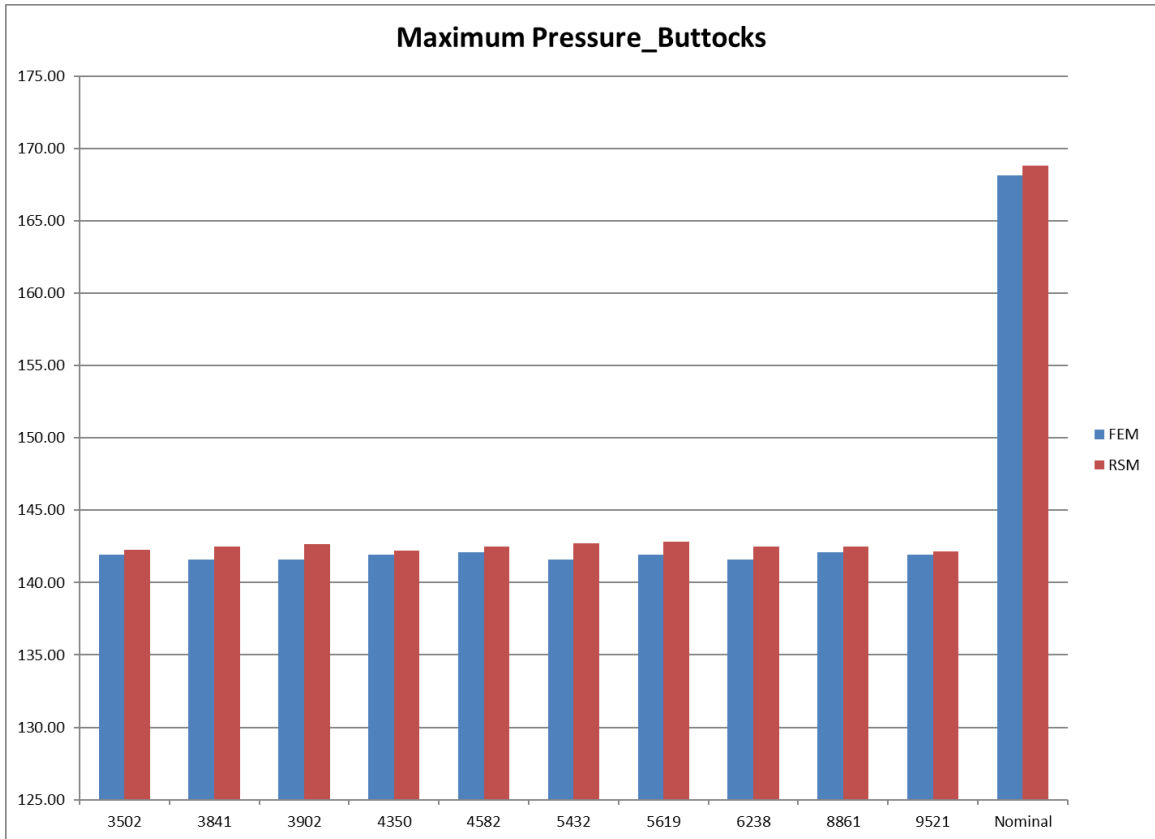
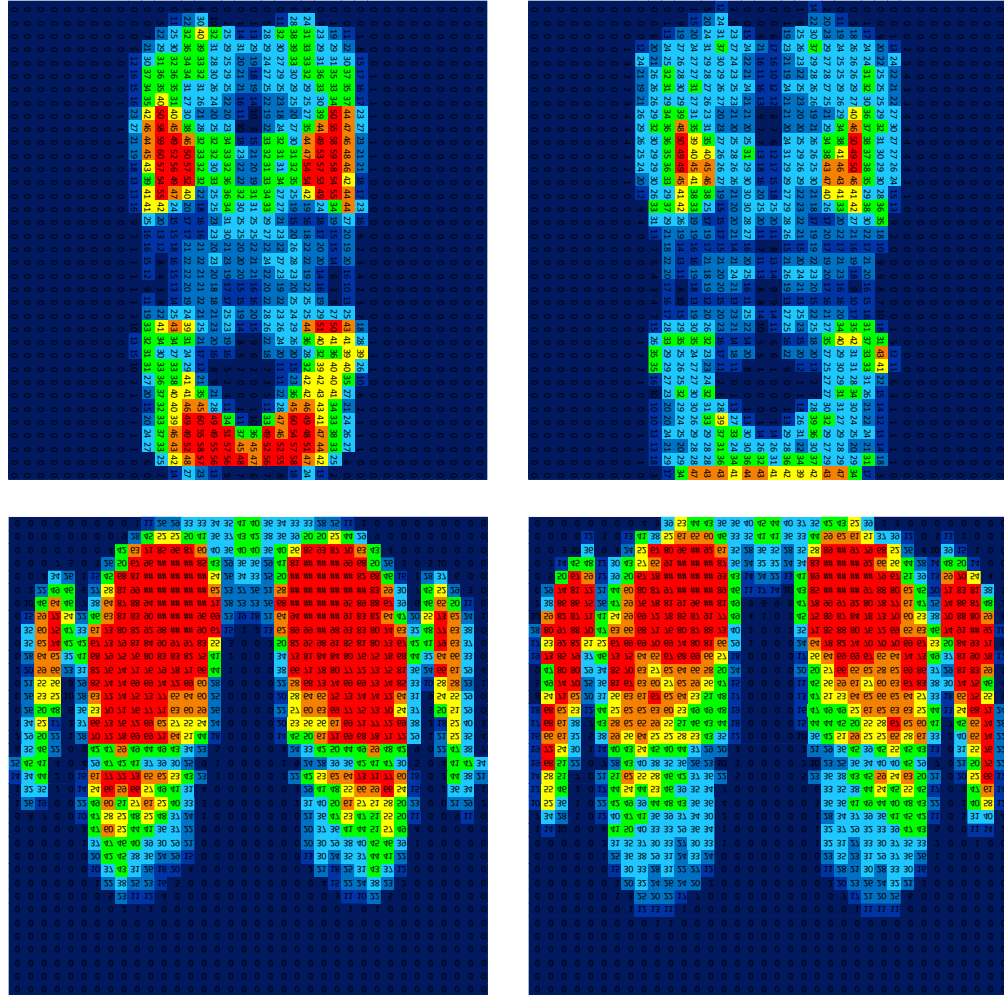


Figure 44. Comparison between virtual optimal cases and corresponding FEM

It is worth to highlight that the objective function as it is observed in figure 44 were minimized since all the optimal cases have lower value in terms of objective function with respect to the nominal case. Moreover, figure 45 shows the Body Pressure Distribution (BPD) of the optimal case (1st rank) compared to the nominal one. Investigation of BPD shows a significant of reduction in term of contact pressure for the backrest and cushion.



(a)

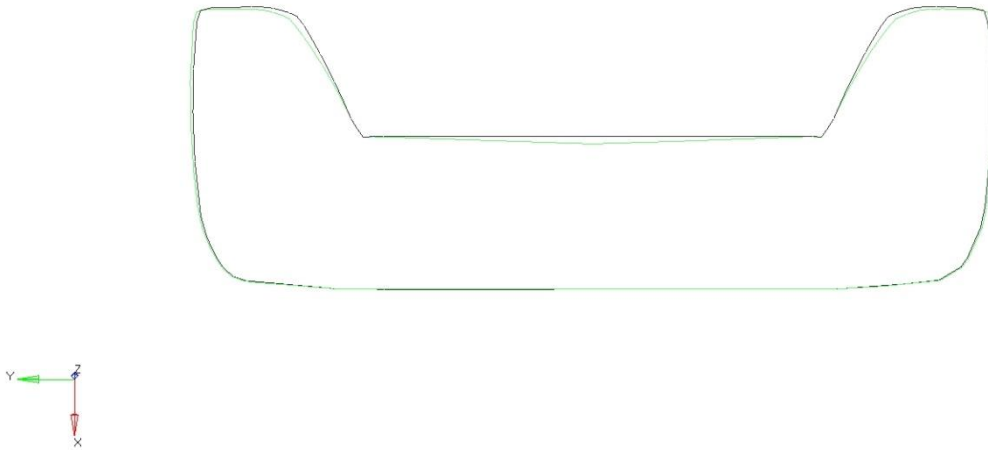
(b)

Figure 45. Optimal seat (b) compared to the nominal seat (a)

Taking into account the characteristics of the optimal seat, figure 46 displays the cushion and backrest cross-section for the optimal seat and nominal one in order to visualize the differences in terms of the seat shape. It must be noticed that the foam ID's for the backrest bolster and insert are Foam-ID05 and Foam-ID01 respectively. The cushion bolster and insert foams are Foam-ID12 and Foam-ID01 showed in figure 40.



(a)



(b)

Figure 46. Cushion (a) and backrest (b) cross-sections of optimal seat

Conclusion and Recommendations

The aim of this thesis was to present a virtual optimization and design guide on how to design comfortable passenger seat. Not only the numbers of passenger transport are increasing, the (cultural) diversity of passengers is increasing as well. Furthermore, a revolution in ICT devices, applications and networks, development of autonomous driving cars also introduce a larger variation in activities that passengers are able to perform while traveling. Although the first studies on passenger seat comfort appeared already 50 years ago, the knowledge regarding the influence of the seat properties, on the comfort and discomfort perception of passengers is not well considered.

Simulation of the occupied seat has strategic relevance for all vehicle manufacturers and Tier-1 suppliers. In particular, a consequent integration of the simulation of the static seat comfort in the digital development process shows the advantages such as Avoidance of expensive late modifications at the seat or construction vehicle and Noticeable reduction of the test expenditure.

Therefore, the influence of seat characteristics on the discomfort perception of passengers was studied through the virtual simulation. The human body model CASIMIR was used as the sophisticated human model in seating posture to evaluate the contact pressure on the cushions as the objective parameters. Before implementing of virtual optimization, the correlation of experimental study and numerical one was performed in which objective parameters showed a good level of correlation.

Thereafter, a design space contains 64 samples; extracted by Reduced Factorial DOE technique; was created to study the sensitivity of objective parameters into the seat characteristics.

Finally, the most correlated objective parameters come from Mergl study were considered as the objective functions to implement the virtual optimization. The result of virtual optimization showed that changing in the concavity of the backrest and using the softer foam result in getting far from discomfort criteria in a positive direction.

For the correlation between pressure and discomfort, the following recommendations have resulted from this thesis.

First, the postures obtained by the participant have a large influence on the obtained results. For example, when measuring pressure distribution, this is strongly dependent on the performed task and the corresponding sitting position.

Furthermore, perceived discomfort increases in time, and the more comfortable the seat, the longer it takes before discomfort occurs. Consequently, it is important to implement a model which could be used to predict the issues come from prolonged contact pressure resulted from this study.

A deviation from the ideal pressure distribution in the seat pan can lead to back complaints. At the same time, the postures obtained by passengers affect the pressure distribution significantly. The active seating system can lead to idealized pressure distribution .

Kinetosis, i.e. travel sickness in cars is another important issue, whose occurrence may hamper the successful introduction of vehicle automation, stopping people from doing

other things like working, reading and writing as they are transferred to their destination. Vibrating and moving seats are seen as promising anti-motion sickness solutions, as they could stimulate the vehicle occupants while the self-driving car makes turn, brakes or accelerates thus avoiding the uncorrelated vestibular/balance vs. visual perception that is at the basis of motion sickness.

Finally, considering the fact that the body pressure distribution is more sensitive to the foam characteristics, a consideration should be which age of the seat should be used in evaluating comfort. The hardness of the cushions reduces in time, influencing the comfort experience of passengers. Hence, in order to evaluate showroom cushions, new cushions should be used, but in order to evaluate the actual lifetime comfort, a representative deterioration should be applied to the cushions, to simulate the state in which they will be in use the longest.

Appendix 1.

STEP definition in foam characterization

```
*****  
*STEP, NLGEOM, INC=200, AMPLITUDE=RAMP, UNSYMM=YES  
  
Displace punch 35 mm downwards.  
  
*STATIC  
  
.0015, 1.00, , .05  
  
*BOUNDARY  
  
PUNCH, 3, 3, -35.  
  
*PRINT, CONTACT=YES, solve=yes  
  
*CONTACT PRINT, SLAVE=FOAM  
  
**CONTACT FILE, SLAVE=FOAM, FREQUENCY=10  
  
*ENERGY PRINT, FREQUENCY=5  
  
*ENERGY PRINT, ELSET=FOAM, FREQ=5  
  
*ENERGY PRINT, ELSET=ETOP, FREQ=5  
  
*EL PRINT, FREQUENCY=50, ELSET=ETOP  
  
S,  
  
E,  
  
*NODE PRINT, FREQUENCY=25  
  
U,  
  
RF,  
  
*OUTPUT, FIELD, FREQUENCY=4  
  
*NODE OUTPUT  
  
U, V, A, RF
```

```

*ELEMENT OUTPUT

S, LE, NE

*CONTACT OUTPUT, VARIABLE=PRESELECT, NSET=TOP

*OUTPUT, HISTORY, FREQUENCY=1

*NODE OUTPUT, NSET=PUNCH

U, V, A, RF

*ELEMENT OUTPUT, ELSET=ETOP

S, LE, NE

*ENERGY OUTPUT, VARIABLE=PRESELECT

*END STEP

*****

*STEP, NLGEOM, INC=200, AMPLITUDE=RAMP, UNSYMM=YES

Return punch to original position.

*STATIC

.0015, 1.00, , .05

*BOUNDARY, OP=MOD

PUNCH,3,3,0.0

*OUTPUT, FIELD, FREQUENCY=4

*NODE OUTPUT

U, V, A, RF

*ELEMENT OUTPUT

S, LE, NE

*CONTACT OUTPUT, VARIABLE=PRESELECT, NSET=TOP

*OUTPUT, HISTORY, FREQUENCY=1

*NODE OUTPUT, NSET=PUNCH

U, V, A, RF

*ELEMENT OUTPUT, ELSET=ETOP

S, LE, NE

```



```
*ENERGY OUTPUT, VARIABLE=PRESELECT
```

```
*print, solve=yes
```

```
*END STEP
```

[Bibliography/References/Works Cited.]

- Ali, I., Arslan, N., 2009. Estimated anthropometric measurements of Turkish adults and effects of age and geographical regions. *International Journal of Industrial Ergonomics* 39(5): 860–865.
- Andreoni, G., Santambrogio, G.C., Rabuffetti, M., Pedotti, A., 2002. Method for the analysis of posture and interface pressure of car drivers. *Applied Ergonomics* 33 (6): 511–522.
- Bazley, C., Nugent, R., Vink, P., 2015. Patterns of Discomfort During Work. *Journal of Ergonomics*, in press.
- Buck, B., 1997. Ein Modell für das Schwingungsverhalten des sitzenden Menschen mit detaillierter Abbildung der Wirbelsäule und Muskulatur im Lendenbereich. Shaker Verlag, Aachen, Germany.
- Cakmak, M., Delavoie, C., Fuhrlinger, L., 2006. Sitzkomfortsimulation: eine neue methode in der pilotanwendung (A seating comfort simulation: a new method in pilot application). *Numerical Analysis and Simulation in Vehicle Engineering*. VDI-Berichte 1967, VDI-Verlag, Dusseldorf, Germany.
- Chen, J., Hong, J., Zhang, E., Liang, J., Bingheng, L.U., 2007. Body pressure distribution of automobile driving human machine contact interface. *Chinese Journal of Mechanical Engineering* 20(4), 66–70.
- De Looze, M.P., Kuijt-Evers, L.F.M., Van Dieën, J.H., 2003. Sitting comfort and discomfort and the relationships with objective measures. *Ergonomics* 46: 985–997.
- De Looze, M.P., Kuijt-Evers, L.F.M., Van Dieën, J.H., 2003. Sitting comfort and discomfort and the relationships with objective measures. *Ergonomics* 46: 985–997.
- Desmet, P.M.A., Hekkert, P., 2007. Framework of product experience. *International Journal of Design* 1(1): 57-66.
- DIN 45676, 2003. Mechanical impedances at the driving point and transfer functions of the human body, DIN.
- Ebe, K., Griffin, M.J., 2001. Factors affecting static seat cushion comfort. *Ergonomics* 44(10): 901–921.

- Eklund, J.A.E. and Corlett, E.N., "Evaluation of Spinal Loads and Chair Design in Seated Work Tasks", *Clinical Biomechanics*, Vol. 2, 1987, pp. 27-33.
- Fairley, T.E., Griffin, M.J., 2003. The apparent mass of the seated human body: vertical vibration. *Journal of Biomechanics* 22, 81–94.
- Genta, G., 2009, *Vibration Dynamics and Control*, Springer
- Gyi, D.E., Porter, J.M., 1999. Interface pressure and the prediction of car seat discomfort. *Applied Ergonomics* 30(2): 99–107.
- Hamberg-van Reenen, H.H., A.J. van der Beek, B.M. Blatter M.P. van der Grinten, W. van Mechelen, P.M. Bongers, 2008. Does musculoskeletal discomfort at work predict future musculoskeletal pain? *Ergonomics* 51: 637-648
- Harewood, F.J., McHugh, P.E., 2007, Comparison of the implicit and explicit finite element methods using crystal plasticity, *Computational Materials Science* 39: 481-494
- Hekkert, P., Schifferstein, H.N.J., 2011. Introducing product experience. In: H.N.J. Schifferstein and P. Hekkert (Eds.) *Product experience*. Amsterdam: Elsevier.
- Helander, M. G. and Zhang, L., "Field Studies of Comfort and Discomfort in Sitting", *Ergonomics*, Vo. 20, No. 9, 1997, pp. 865-915.
- Helander, M.G., Quance, L.A., 1990. Effect of work-rest schedules on spinal shrinkage in the sedentary worker. *Applied Ergonomics* 21: 279-284.
- Hertzberg, H.T.E. 1972, "The Human Buttocks in Sitting: Pressures, Patterns, and Palliatives", Society of Automotive Engineers, Inc., New York, NY, USA, 1972, SAE Technical Paper no. 72005.
- Hiemstra-van Mastrigt, S., Kamp, I., Van Veen, S.A.T., Vink, P., Bosch, T., 2015. The influence of active seating on car passengers' perceived comfort and activity levels. *Applied Ergonomics* 47(2015): 211–219.
- Hostens, I., Papaioannou, G., Spaepen, A., Ramon, H., 2001. Buttock and back pressure distribution tests on seats of mobile agricultural machinery. *Applied Ergonomics* 32(4): 347–356.
- Hozeski, K. W. and Rohles, R. H., 1987. Subjective evaluation of chair comfort and influence on productivity, in: Knave, B. and Wideback, P.G.. (eds) *Work with Display Units*, Amsterdam: Elsevier Science Publishers B.V. (the Netherlands).
- Jackson, C., Emck, A.J., Hunston, M.J., Jarvis, P.C., 2009. Pressure Measurements and Comfort of Foam Safety Cushions for Confined Seating. *Aviation, Space, and Environmental Medicine* 80(6): 6.

- Jackson, C., Emck, A.J., Hunston, M.J., Jarvis, P.C., 2009. Pressure Measurements and Comfort of Foam Safety Cushions for Confined Seating. *Aviation, Space, and Environmental Medicine* 80(6): 6.
- Jürgens, H.W., Aune, I.A., Pieper, U., 1990. *International Data on Anthropometry (Occupational and Health Series no.65)*. International Labor Office: Geneva, Switzerland.
- Kennedy, K.W. *International Anthropometric Variability and Its Effects on Aircraft Cockpit Design*. P. 47-66.
- Knoblauch, J., 1992. *Entwicklung und Bau eines physikalischen Schwingungsmodells des sitzenden Menschen*. Dissertation, Shaker Verlag, Aachen, Germany
- Kolich, M., 2003. Automobile seat comfort: occupant preferences vs. anthropometric accommodation. *Applied Ergonomics* 34(2): 177–184.
- Komlos, J., Baur, M. (2004). From the tallest to (one of) the fattest: the enigmatic fate of the American population in the 20th century. *Econ. Hum. Biol.*, 2: 57-74.
- Kroemer, K.H.E., 1989. Engineering anthropometry. *Ergonomics* 32: 767-784.
- Kyung, G., Nussbaum, M.A., 2008. Driver sitting comfort and discomfort (part II): Relationships with and prediction from interface pressure. *International Journal of Industrial Ergonomics* 38 (5–6): 526–538.
- Kyung, G., Nussbaum, M.A., 2008. Driver sitting comfort and discomfort (part II): Relationships with and prediction from interface pressure. *International Journal of Industrial Ergonomics* 38 (5–6): 526–538.
- Le, P., Rose, J., Knapik, G., Marras, W.S., 2014. Objective classification of vehicle seat discomfort. *Ergonomics* 57(4): 536–544.
- Lijmbach, W., Miehke, P., Vink, P., 2014. Aircraft Seat in-and Egress Differences between Elderly and Young Adults. In: *Proceedings of the Human Factors and Ergonomics Society Annual Meeting 2014*: 58 page 520-524, SAGE Publications: Thousand Oaks.
- Litman, T.A., 2015. *Autonomous Vehicle Implementation Predictions: Implications for Transport Planning*. Transportation Research Board 94th Annual Meeting, January 11-15, 2015, Washington, D.C., USA. Paper no. 15-3326.
- Matton L, Duvigneaud N, Wijndaele K, Philippaerts R, Duquet W, Beunen G, Claessens AL, Thomis M, Lefevre J., 2007. Secular trends in anthropometric characteristics, physical fitness, physical activity, and biological maturation in Flemish adolescents between 1969 and 2005. *Am J Hum Biol.* 19(3):345-357.

- Mergl, C., 2006. Entwicklung eines Verfahrens zur Objektivierung des Sitzkomforts auf Automobilsitzen. PhD thesis, Lehrstuhl für Ergonomie, Technische Universität München.
- Mergl, C., 2006. Entwicklung eines Verfahrens zur Objektivierung des Sitzkomforts auf Automobilsitzen. PhD thesis, Technische Universität München.
- Mergl, C., Klendauer, M., Mangan, C., Bubb, H., 2005. Predicting Long Term Riding Comfort in Cars by Contact Forces Between Human and Seat, SAE international conference, Iowa
- Moes, C.C.M., 2007. Variation in Sitting Pressure Distribution and Location of the Points of Maximum Pressure with Rotation of the Pelvis, Gender and Body Characteristics. *Ergonomics* 50(4): 536–561.
- Moes, C.C.M., 2007. Variation in Sitting Pressure Distribution and Location of the Points of Maximum Pressure with Rotation of the Pelvis, Gender and Body Characteristics. *Ergonomics* 50(4): 536–561.
- Moes, N.C.C.M., Horva' th, I., 2002. Using finite elements model of the human body for Shape optimization of seats: optimization material properties. In: International Design Conference—Design 2002, Dubrovnik.
- Molenbroek, J.F.M. (1994). Op Maat Gemaakt: Menselijke Maten voor het Ontwerpen en Beoordelen van Gebruiksgoederen. PhD Thesis, Delft University of Technology, Delft, the Netherlands.
- Na, S., Lim, S., Choi, H.-S., Chung, M.K., 2005. Evaluation of driver's discomfort and postural change using dynamic body pressure distribution. *International Journal of Industrial Ergonomics* 35(12): 1085–1096.
- Noro, K., Fujimaki, G., Kishi, S., 2005. A Theory on Pressure Distribution and Seat Discomfort. In: *Comfort and Design: Principles and Good Practice*, P. Vink (ed.). Boca Rotan: CRC Press, 33–39.
- Noro, K., Naruse, T., Lueder, R., Nao-i, N., Kozawa, M., 2012. Application of Zen sitting principles to microscopic surgery seating. *Applied Ergonomics* 43(2): 308–319.
- Ortman, J.M., Velkoff, V.A., Hogan, H., 2014. An Aging Nation: The Older Population in the United States, Current Population Reports. U.S. Census Bureau: Washington, DC.
- Pankoke, S., 2003. Numerische simulation des raumlichen Ganzkorperschwingungsverhaltens des sitzenden Menschen unter Berücksichtigung der individuellen Anthropometrie und Haltung. Fortschritt-Berichte VDI No. 522, VDI-Verlag, Dusseldorf, Germany.

- Pankoke, S., Siefert, A., Breitfeld, Th., 2005. Numerische simulation von schwingungen in oberklasse-pkw: einsetz des finite-elementemensch-modells CASIMIR (Numerical simulation of seat vibrations in luxury-class automobiles: application of the finite-element-manmodel CASIMIR). Reifen-Fahrwerk-Fahrbahn, VDI-Berichte 1912, VDI-Verlag, Dusseldorf, Germany.
- Park J., Lee, H., Choi, Y., Park, K., Kim, M., You, H., 2014. Development of an ergonomic bus seat profile design protocol. Proceedings of the Human Factors and Ergonomics Society Annual Meeting 2014 58:1825-1828.
- Paul, G., Daniell, N., Fraysse, F., 2012. Patterns of correlation between vehicle occupant seat pressure and anthropometry. Work 41: 2226–2231.
- Paul, G., Daniell, N., Fraysse, F., 2012. Patterns of correlation between vehicle occupant seat pressure and anthropometry. Work 41: 2226–2231.
- Perissinotto, E., Pisent, C., Sergi, G., Grigoletto, F., Enzi, G., 2002. Anthropometric measurements in the elderly: age and gender differences. British Journal of Nutrition 87: 177-186.
- Pheasant, S., Haslegrave, C.M., 2006. Bodyspace: Anthropometry, Ergonomics and the Design of Work, Third Edition. CRC Press: Boca Raton.
- Porter, J.M., Gyi, D.E., Tait, H.A., 2003. Interface pressure data and the prediction of driver discomfort in road trials. Applied Ergonomics 34 (3): 207–214.
- Reed, M.P., Manary, M.A., Flannagan, C.A.C., Schneider, L.W., 2000. Effects of Vehicle Interior Geometry and Anthropometric Variables on Automobile Driving Posture. Human Factors: The Journal of the Human Factors and Ergonomics Society 42(4): 541–552.
- Runkle, V.A., “Benchmarking Seat Comfort”, Society of Automotive Engineers, Inc., Warrendale, PA, USA, 1994, SAE Technical Paper No. 940217.
- Sember, J.A., 1994. The biomechanical relationship of seat design to the human anatomy. In: Lueder, R., Noro, K. (Eds.), Hard Facts about Soft Machines: the Ergonomics of Seating (pp. 221–230). Taylor & Francis: London.
- Siefert, A., Pankoke, S., Wölfel, H.-P., 2008, Virtual optimisation of car passenger seats: Simulation of static and dynamic effects on drivers’ seating comfort, International Journal of Industrial Ergonomics, Vol. 38: 410-424.
- Siefert, A., Pankoke, S., Hofmann, J., 2009, CASIMIR/Automotive: A Software for the virtual Assessment of static and dynamic Seating Comfort, SAE International
- Verver, M.M., 2004. Numerical tools for comfort analyses of automotive seating. Dissertation, Technische Universiteit Eindhoven, Eindhoven

- Vincent, A., Bhise, V.D., Mallick, P. (2012). Seat comfort as a function of occupant characteristics and pressure measurements at the occupant-seat interface. SAE Technical Paper 2012- 01-0071, 2012, doi:10.4271/2012-01-0071.
- Vos, G.A., Congleton, J.J., Moore, J.S., Amendola, A.A., Ringer, L., 2006. Postural versus chair design impacts upon interface pressure. *Applied Ergonomics* 37(5): 619–628.
- Wolfel, H.P., Rutzel, S., Mischke, Ch., 2004. *Biodynamische Modelle des Menschen*. In: VDI-Conference on Human Vibrations; Darmstadt, Germany.
- Zhang, L., Helander, M. G., Drury, C. G., “Identifying factors of comfort and discomfort in sitting”, *Human Factors*, Vol. 38, No. 3, 1996, pp. 377–389.